5. Sidewall adit heading

5.1 Road tunnel "Hahnerberger Straße" in Wuppertal, Germany

5.1.1 Introduction

To create a high-capacity and therefore non-intersecting east-west connection between the freeways A46 and A1, it was planned to newly construct and improve the state highway L418 running through the city of Wuppertal, Germany, as a four-lane road. Within the scope of this construction project, the Hahnerberger Straße, a street running approximately in north-south direction, was to be undercrossed in the city district of Hahnerberg at an angle of 60° by underground construction (Fig. 5.1). This task proved to be quite difficult, since the tunnel has a low overburden and a large excavated cross-section. Also, a limitation to the tunneling-induced ground surface subsidence had to be kept due to the buildings at the ground surface in the area of the tunnel alignment.

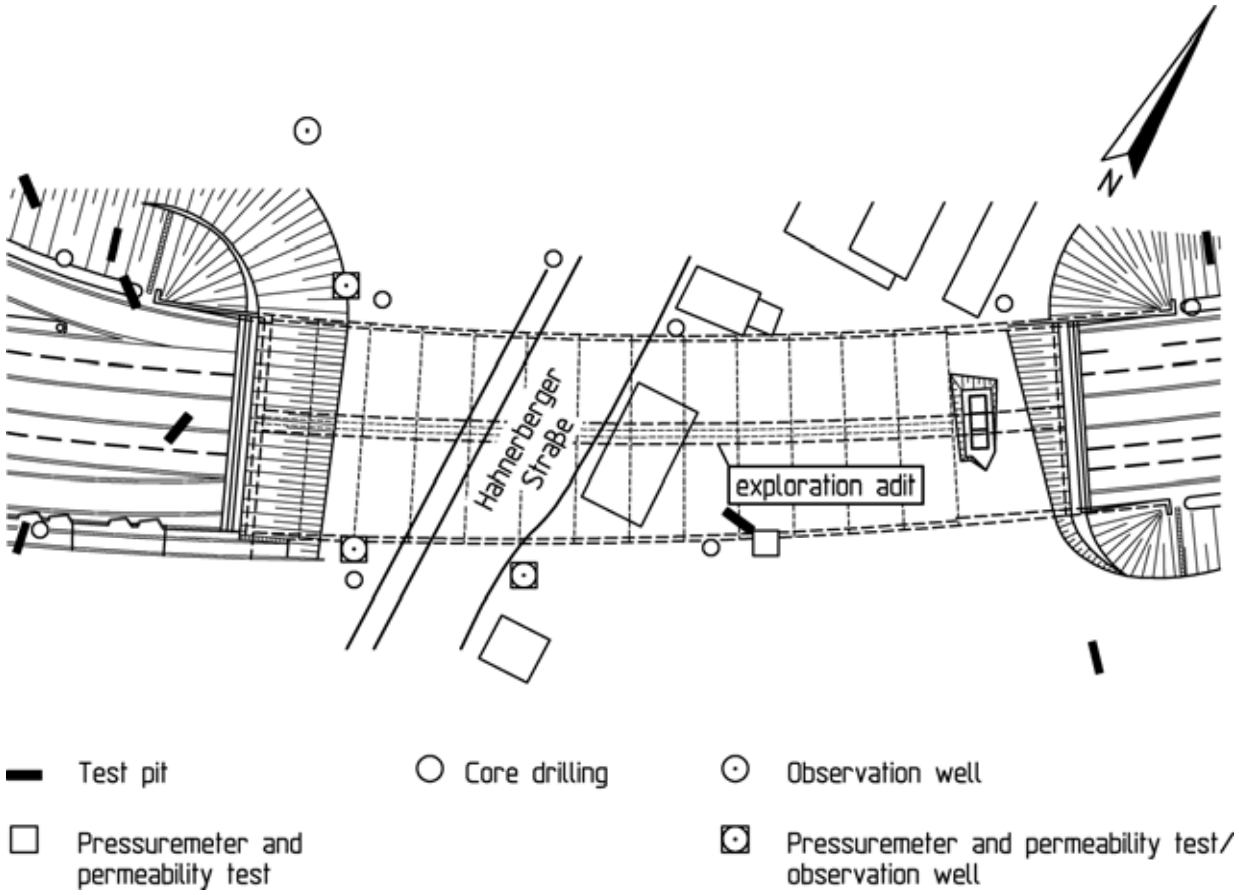

Fig. 5.1: Road tunnel Hahnerberger Straße, site plan and exploration

5.1.2 Structure

The approx. 130 m long tunnel must provide room in each direction for two main driving lanes and one exit or approach lane, respectively (Fig. 5.2 and 5.3). The widths of the required clearances range between 13.5 m and 16.2 m. The height of the clearances amounts to 4.90 m. The tunnel has a total width of approx. 37 m and a total height of approx. 12 m (Fig. 5.3). To illustrate these very large dimensions, the cross-section of a double-tracked tunnel for the new high-speed railway lines of German Rail (Deutsche Bahn AG) is shown in Fig. 5.3.

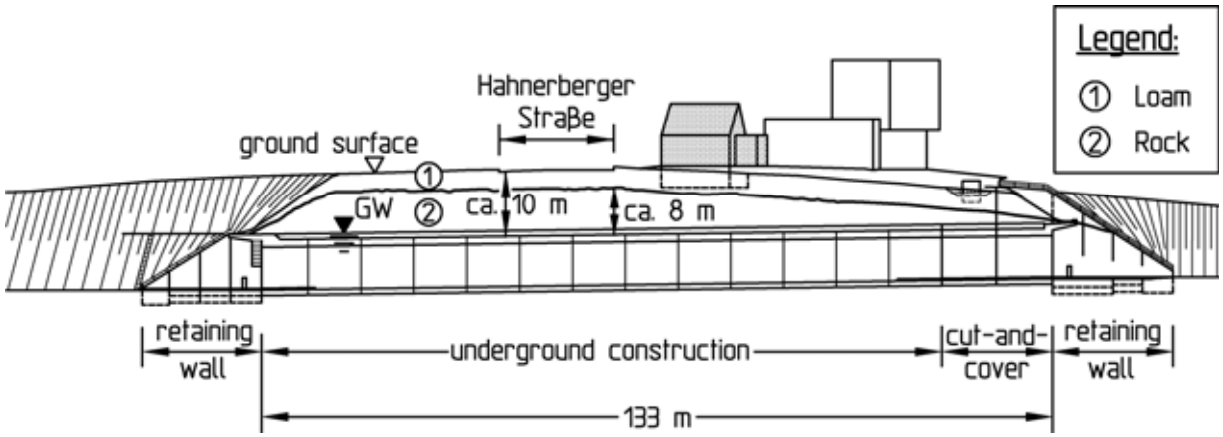

Fig. 5.2: Road tunnel Hahnerberger Straße, longitudinal section

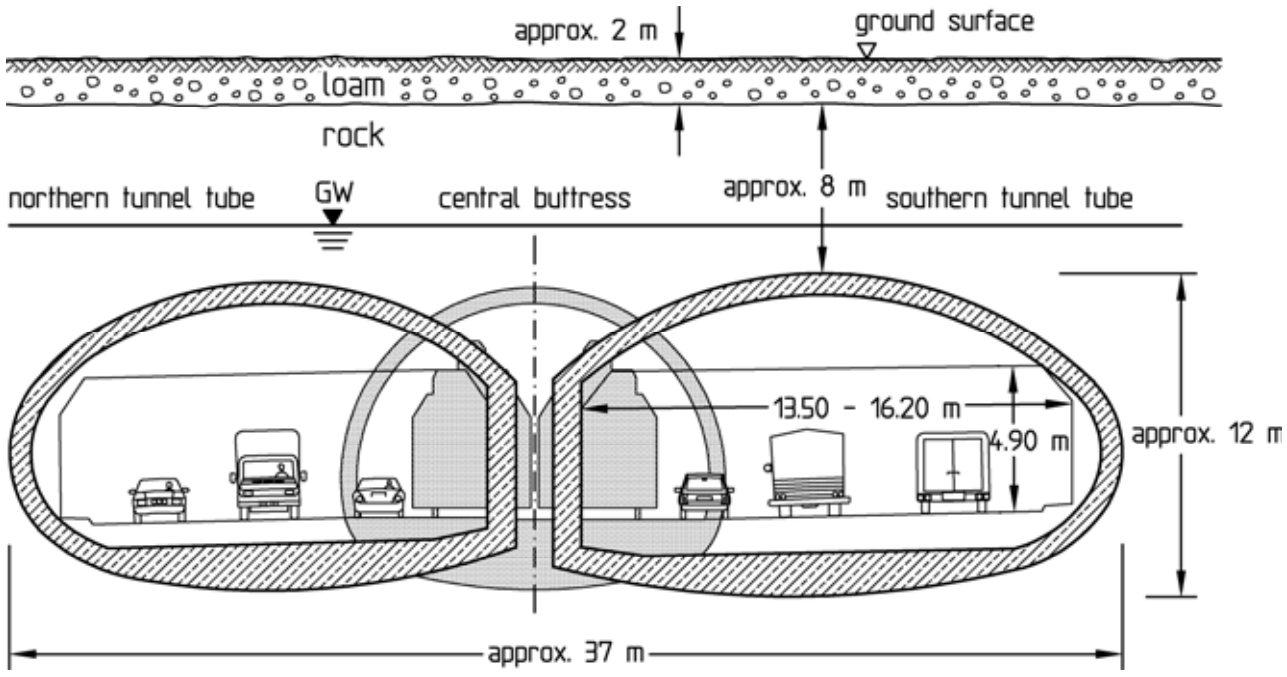

Fig. 5.3: Road tunnel Hahnerberger Straße, cross-section

The tunnel has an overburden height of approx. 10 m (Fig. 5.2). To avoid damage to the buildings above the tunnel and to the water and gas mains running along the Hahnerberger Straße, the subsidence due to tunneling was to be limited to a magnitude of 2 cm.

5.1.3 Exploration

Within the framework of route planning and in order to assess the feasibility of underground construction, an investigation program was carried out to explore the ground conditions and to determine the rock mechanical parameters. Test pits were excavated and core drillings were sunk with depths ranging between 10 and 34 m (Fig. 5.1).

According to the exploration results, below an about 2 to 4 m thick layer of top soil and loam with cobbles, a narrowly bedded alternating sequence of sandstones and claystones of the Middle Devonian Brandenberg layers is found. The sandstones and claystones are weathered close to the surface and intensely jointed. The orientation of the bedding planes and joints in the rock mass was measured on oriented drill cores and in test pits using a geological compass. Fig. 5.4 shows the idealization of the discontinuity fabric of the rock by a structural model (see Chapter 2.5.1). The rock mass is separated by bedding planes (B), which dip shallowly at approx. 30° and persist widely, and by three steeply dipping main joint sets (J1 to J3). According to the drilling results, the spacing of the bedding planes ranges between several centimeters and a few decimeters. The joint spacing amounts to a few decimeters on average.

The bedding planes are partially filled with clay and mixed-grained soils at a thickness of up to 10 to 40 cm. This leads to a greater deformability perpendicular to the bedding than parallel to it. After Wittke (1990), transversely isotropic deformation behavior can be assumed in the elastic stress domain for an alternating sequence of this kind. This kind of anisotropy can be described by 5 independent elastic constants: Two Young's moduli E_1 and E_2, one shear modulus G_2 and two Poisson's ratios ν_1 and ν_2 (Fig. 5.4).

The modulus E_1 relevant for loading parallel to the bedding was derived from the results of the pressuremeter tests and from experi-

ence gained from other projects with comparable ground conditions as E_1 = 1000 MN/m² (Fig. 5.4).

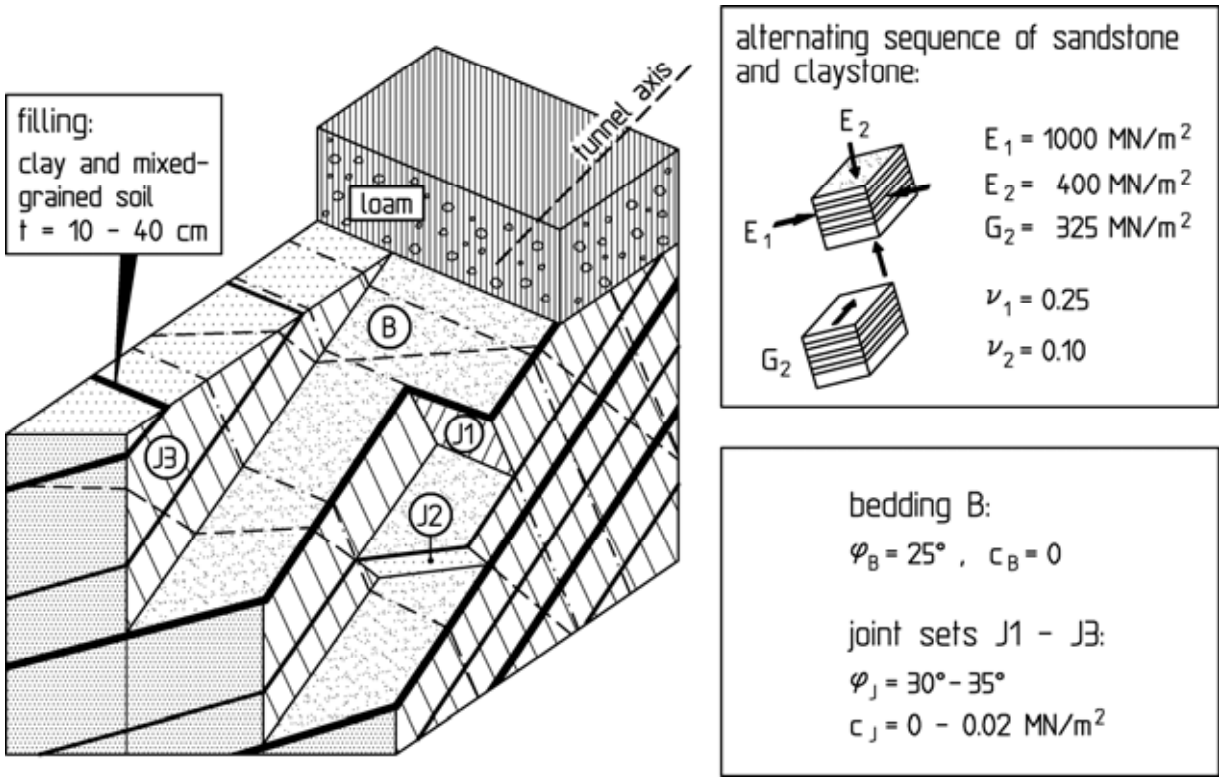

Fig. 5.4: Structural model and rock mechanical parameters

The modulus E_2, relevant for loading perpendicular to the bedding which is smaller than E_1, was determined according to Wittke (1990) from the following relation:

$$E_2 = \frac{1}{\frac{\alpha}{E_{IR}} + \frac{\beta}{E_{BF}}} = \frac{1}{\frac{0.9}{1000} + \frac{0.1}{70}} \approx 400 \text{ MN/m}^2 \qquad (5.1)$$

The symbols in (5.1) denote:

α = 0.9: Fraction of the sandstone in the alternating sequence.

β = 0.1: Fraction of the bedding plane filling in the alternating sequence.

E_{IR} = 1000 MN/m²: Young's modulus of the jointed sandstone with the bedding plane filling not taken into account.

E_{BF} = 70 MN/m²: Bulk modulus of the bedding plane filling.

α and β were derived from a statistical evaluation of the mapping results of the drill cores and test pits. Taking the joints in the sandstone into account, the modulus E_1 derived from the pressuremeter test results was chosen to E_{IR} as represented above. The bulk modulus of the bedding plane filling E_{BF} was estimated on the basis of the results of soil mechanical laboratory tests.

The shear modulus G_2, relevant for shear loading parallel to the bedding and thus strongly dependent on the mechanical properties of the bedding plane filling, was estimated at $G_2 = 325$ MN/m^2.

Poisson's ratio ν_1 corresponds approximately to Poisson's ratio of the sandstone. In unconfined compression tests on intact rock specimens a value of $\nu_{IR} = 0.25$ resulted on average for the latter. This value was taken as a basis for the analyses.

According to Wittke (1990), Poisson's ratio ν_2 can be computed as follows:

$$\nu_2 = \frac{E_{BF} \cdot \nu_{IR}}{\alpha \cdot E_{BF} + \beta \cdot E_{IR}} = \frac{70 \cdot 0.25}{0.9 \cdot 70 \cdot + 0.1 \cdot 1000} \approx 0.1 \qquad (5.2)$$

Laboratory tests resulted in very high values for the shear parameters of the intact rock. The failure behavior of the rock is thus essentially determined by the shear strength along the discontinuities, which was modeled by the Mohr-Coulomb failure criterion. For the shear strength parallel to the bedding, the bedding plane filling is relevant. On the basis of the grain-size distribution and water content and of experience, a friction angle of $\varphi_B = 25°$ and no cohesion were assumed (Fig. 5.4).

Unlike the bedding planes, the joints are mostly undulating and contain sandy, rusty coatings. Close to the surface, however, they are also partially filled with clayey, sandy silt. It is essential for the assessment of their shear strength that they mostly only extend through one layer and thus extend considerably less far than the bedding. Therefore, a cohesion of $c_J \approx 0$ to 0.02 MN/m^2 and a friction angle of $\varphi_J \approx 30$ to 35° were assumed for the joints (J1 to J3) (Fig. 5.4).

A tensile strength normal to the discontinuities was not accounted for.

The water permeability of the rock is relatively low perpendicularly to the bedding, because the bedding plane filling has a sealing effect. The groundwater table is located approx. 2 m above the tunnel roof.

To further explore the rock mass conditions and to test the planned construction method, an adit was driven in the middle between the two tunnel tubes as an advance construction measure (Fig. 5.5). In the course of construction, a reinforced concrete buttress was installed in the adit. The additional ground exposure by the adit confirmed the findings about the ground which had been gained in the first exploration phase.

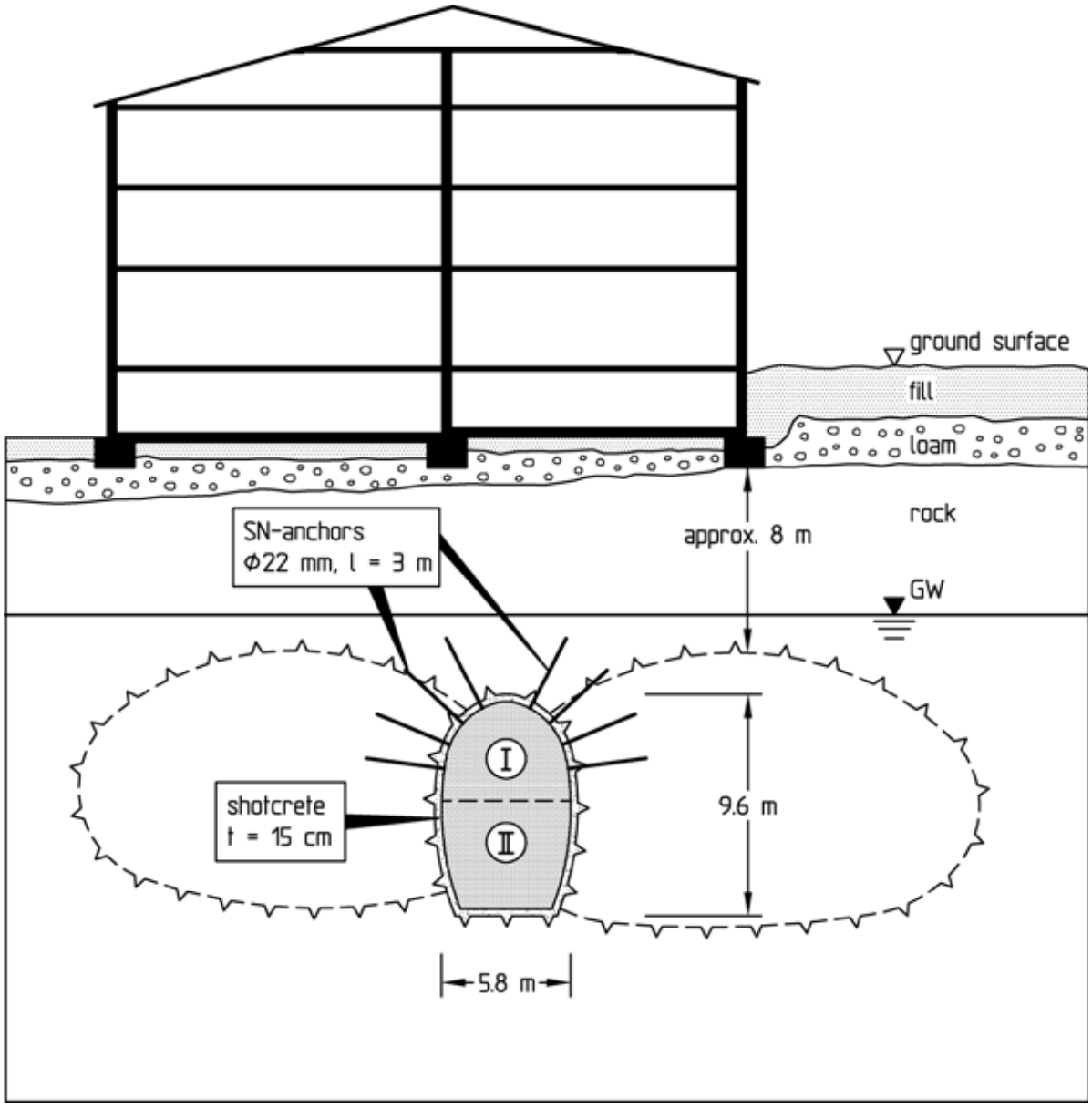

Fig. 5.5: Central adit for additional exploration and for testing of construction techniques

The adit was driven by means of smooth and true to profile blasting. To keep the blasting-induced vibrations low, the round lengths and the charges per ignition step were limited. Especially close to the buildings, the excavation profile had to be subdivided for the same reasons (I and II in Fig. 5.5). This experience could be used for the further planning and tendering of the tunnel.

During the heading displacements were measured in the adit and at the ground surface and interpreted using FE-analyses based on the rock mechanical parameters given above (back analysis). The measured and the computed displacements were in substantial agreement. The derived parameters were thus confirmed and remained unchanged in the further course of the design (Modemann and Wittke, 1988).

5.1.4 Design and construction

In the conditions present here, only the NATM is suitable for an underground construction of the tunnel. In view of the width of the tunnel structure of approx. 37 m and of the overburden of approx. 10 m, which is very low by comparison, it was necessary to provide for one tunnel tube for each direction. For reasons of the alignment only a width of approx. 1 to 2 m was available for the buttress between the two tunnel tubes. The option to leave a rock pillar between the tubes was thus ruled out. Therefore, as mentioned above already, a 1.2 m thick reinforced concrete buttress with a mushroom-shaped widening of the head and a base enlargement was constructed in the exploration adit driven in advance (Fig. 5.6 and 5.7). The two tunnel tubes thus formed still have a very large span compared to the overburden.

To enable at least a slight an arching effect in the remaining rock mass above the tunnel tubes, the tunnel profiles were designed with a very small camber above the prescribed clearance. The rounding of the inverts served to carry the water pressure on the interior lining better. Only a slight rounding was necessary here in spite of the wide span, because due to the small height of the clearance sufficient space was available to strengthen the invert of the interior lining.

Since the groundwater table could be lowered during the heading, the shotcrete support did not have to be dimensioned for water pressure. The interior lining, however, was to be constructed wa-

tertight. By request of the client, a PVC sealing was planned between the shotcrete membrane and the interior lining (Fig. 5.6). As a consequence of the shape of the cross-section, each tunnel tube was provided with a separate sealing, which did not include the central buttress. The arrangement and installation of the sealing was considerably simplified this way.

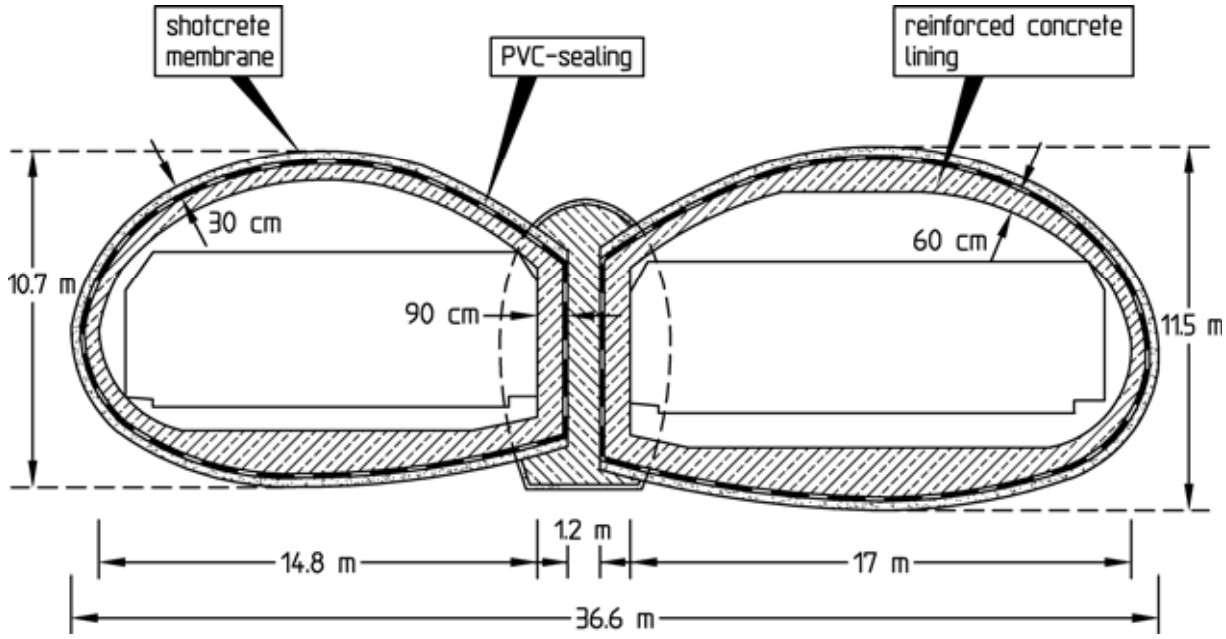

Fig. 5.6: Design

The reinforced concrete buttress was constructed in segments of 9 m each. Connecting reinforcement was provided for at the head and at the base for the shotcrete support of the two tunnel tubes to be constructed later (Fig. 5.7). Further, a sound load transfer between the concrete buttress and the rock mass above was effected by means of a contact injection. After that, the tunnel tubes were excavated in parts of the cross-section for reasons of stability, limitation of the heading-induced subsidence and vibrations.

The first step was the excavation and support of a sidewall adit in the northern tube. The cross-section of the sidewall adit was again subdivided by a crown heading with trailing invert (Fig. 5.8 and 5.9). As illustrated in Fig. 5.8, the outside sidewall was supported by a lattice girder and a 30 cm thick shotcrete membrane as well as by SN-anchors. The side of the sidewall adit facing the tunnel tube, on the other hand, was supported by only 15 cm of shotcrete. Glass fiber anchors were further installed on this side. This part of the support was removed again in the further course of the works.

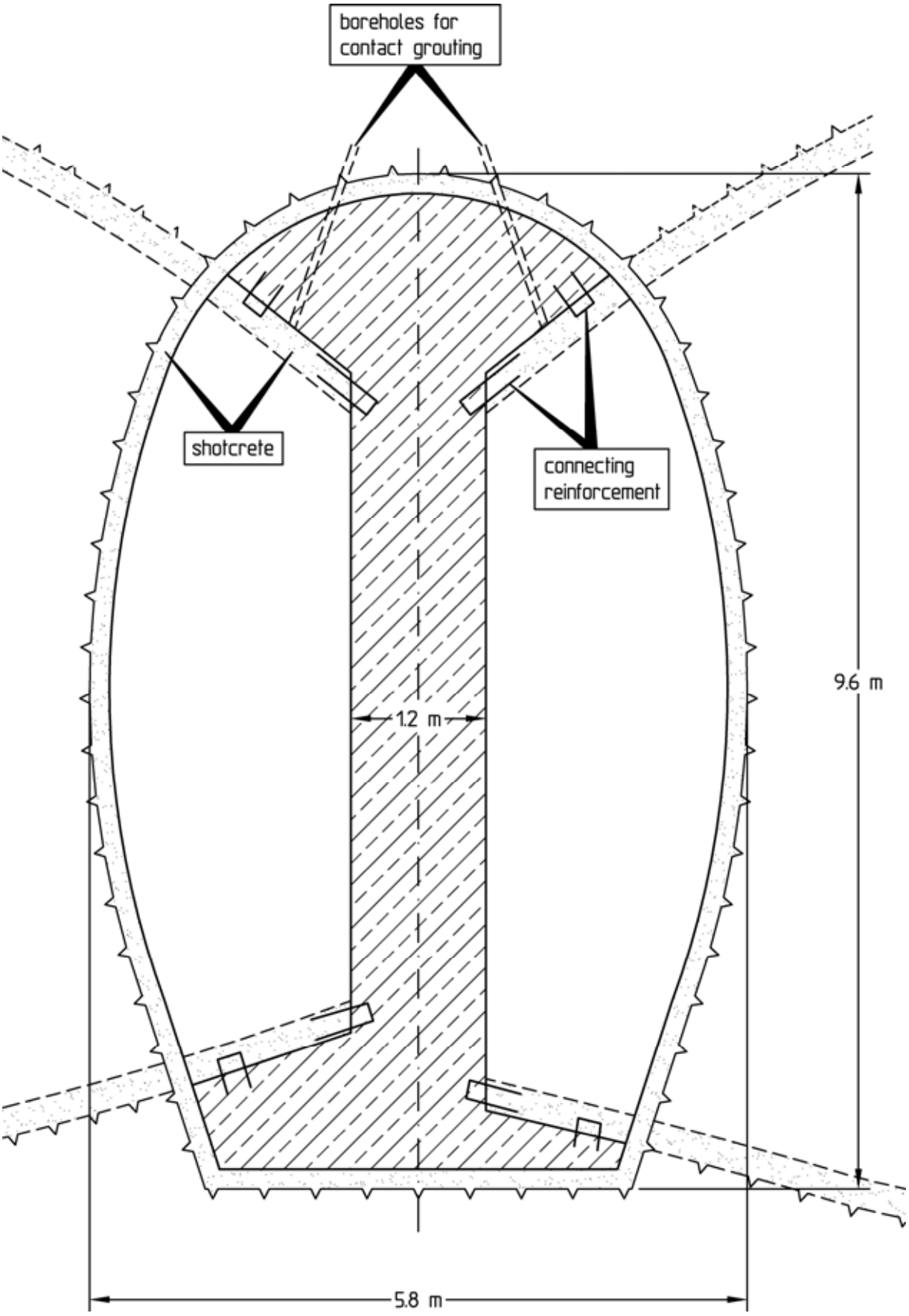

Fig. 5.7: Reinforced concrete buttress

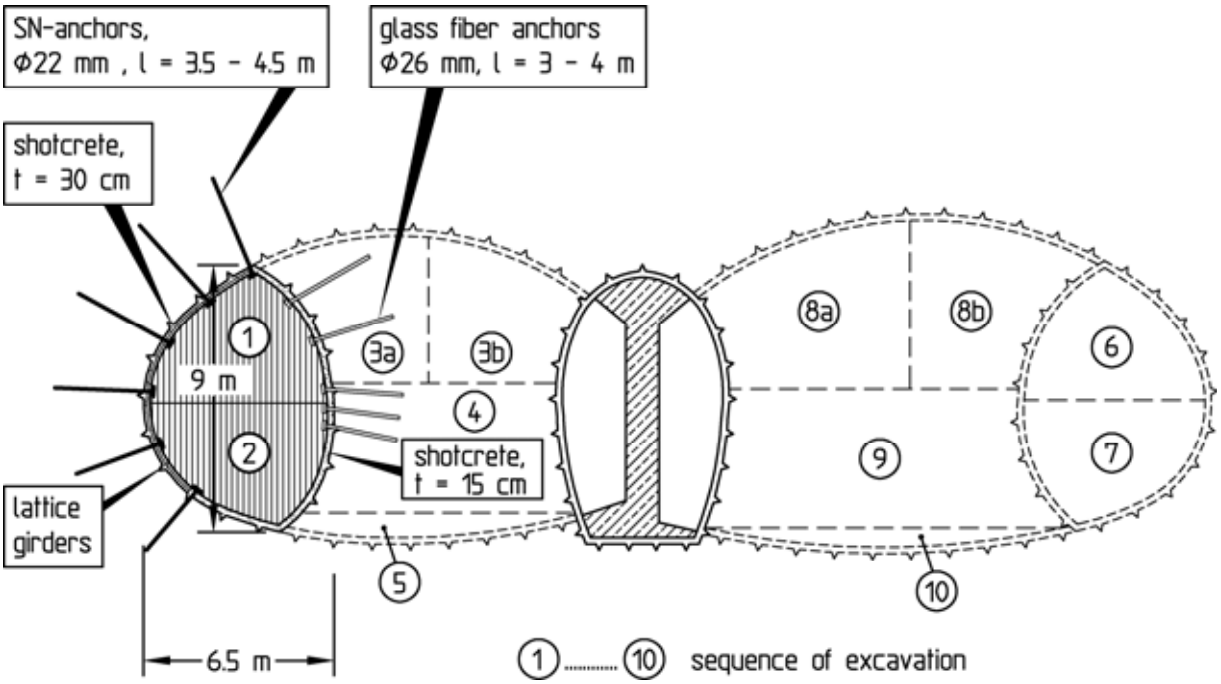

Fig. 5.8: Sidewall adit excavation and support

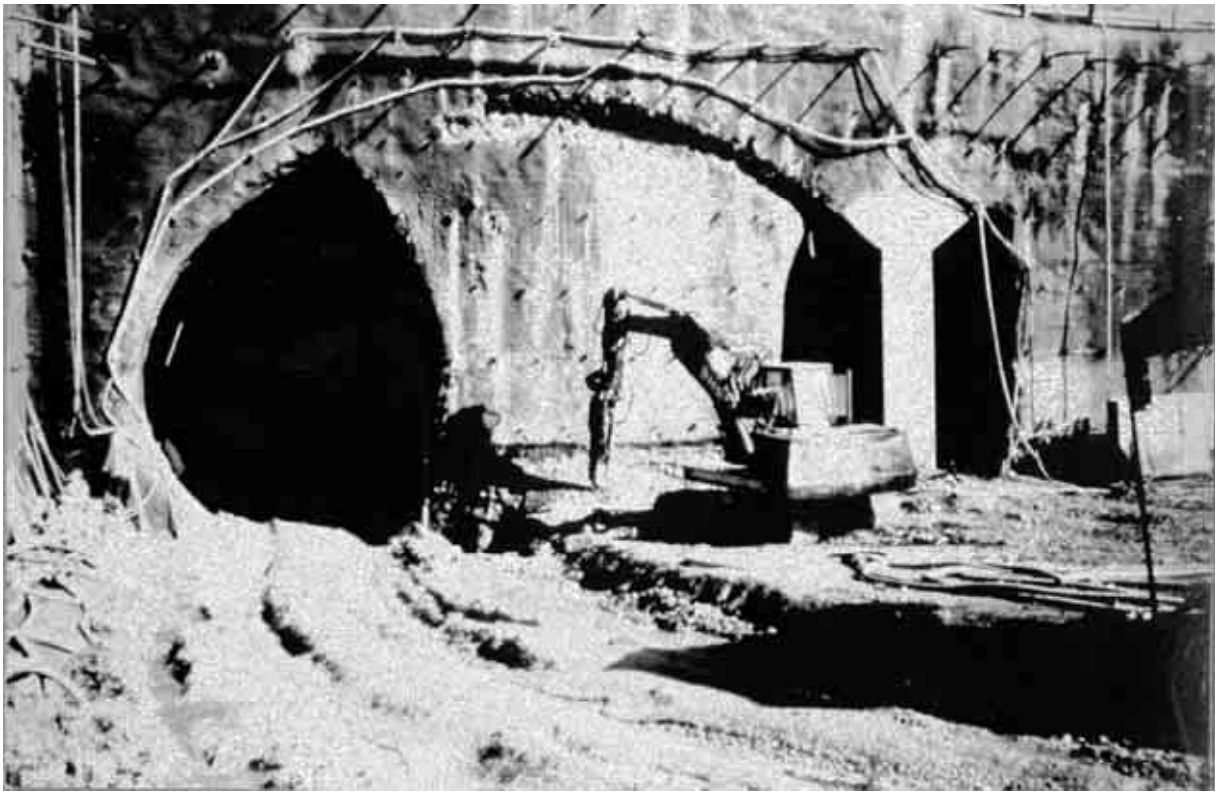

Fig. 5.9: Sidewall adit and central adit

In the third step, the crown of the northern tube was excavated and supported in sections (Fig. 5.10 and 5.11). The lattice girders and the reinforcement of the shotcrete membrane were connected

with the corresponding support elements of the sidewall adit in the process. The connection of the support to the central buttress was already mentioned above (see Fig. 5.7). The length of the SN-anchors was increased in the vault area to improve the arching effect in the rock above the tunnel roof.

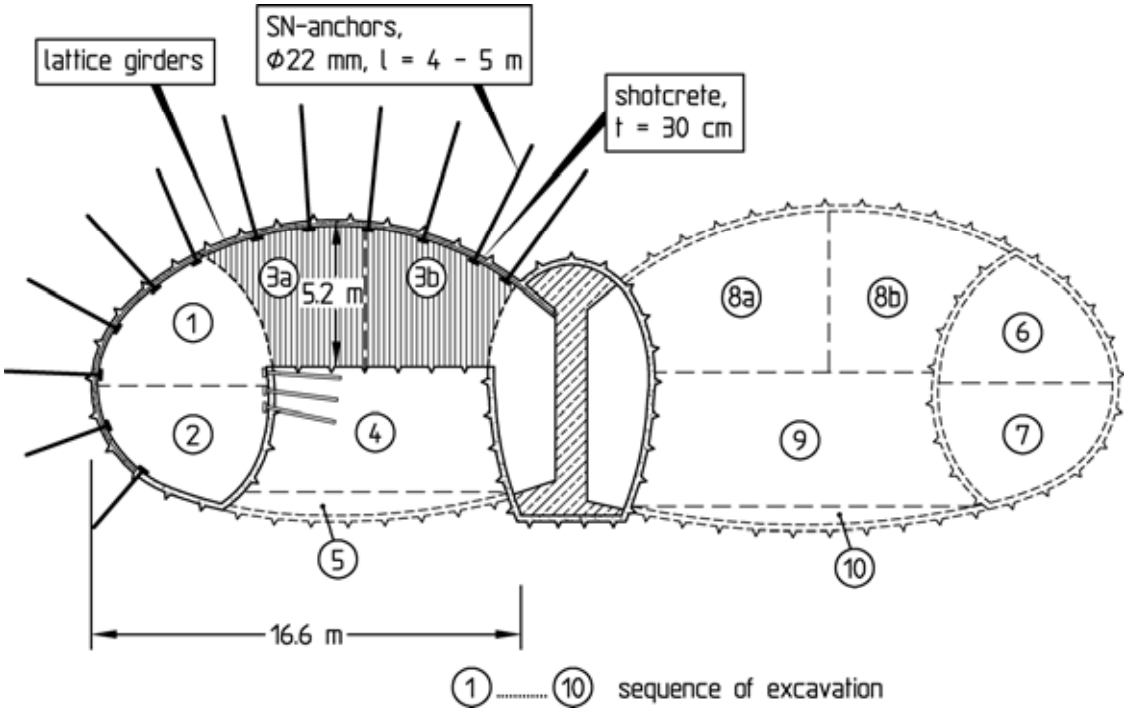

Fig. 5.10: Crown excavation and support

Fig. 5.11: Crown heading

The excavation of the bench and the invert constituted the last steps of the excavation sequence of the northern tube (Fig. 5.12 and 5.13). The invert was supported by 30 cm of shotcrete. Lattice girders and an invert anchoring could be dispensed with.

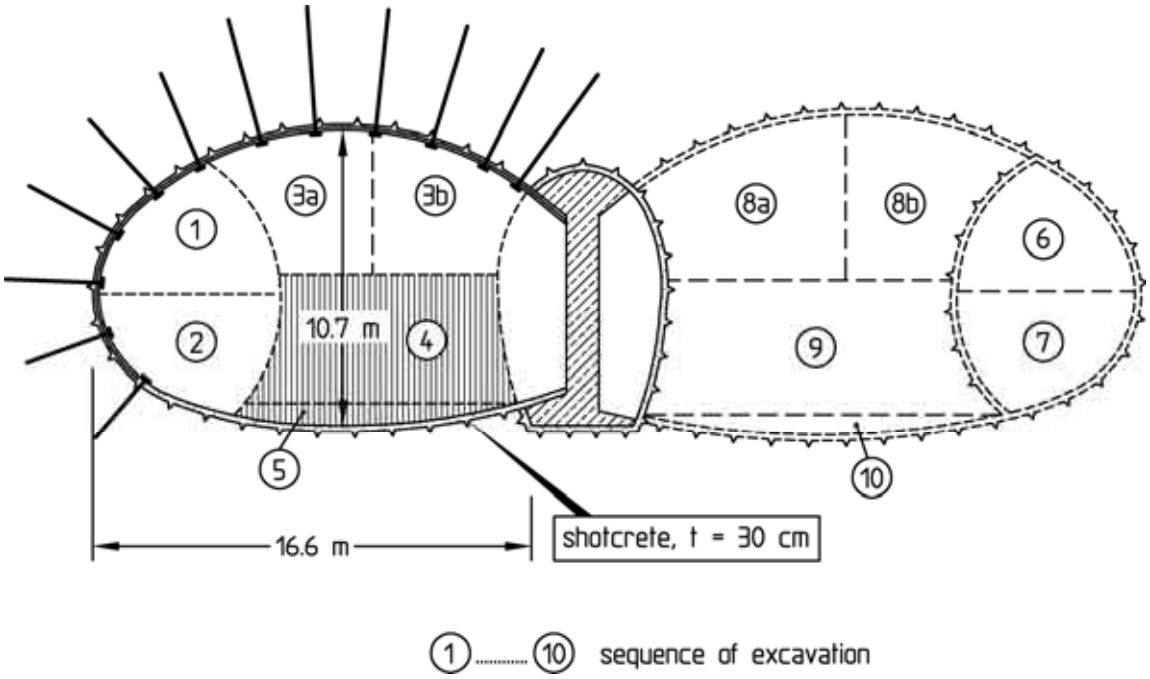

Fig. 5.12: Bench and invert excavation with closed invert support

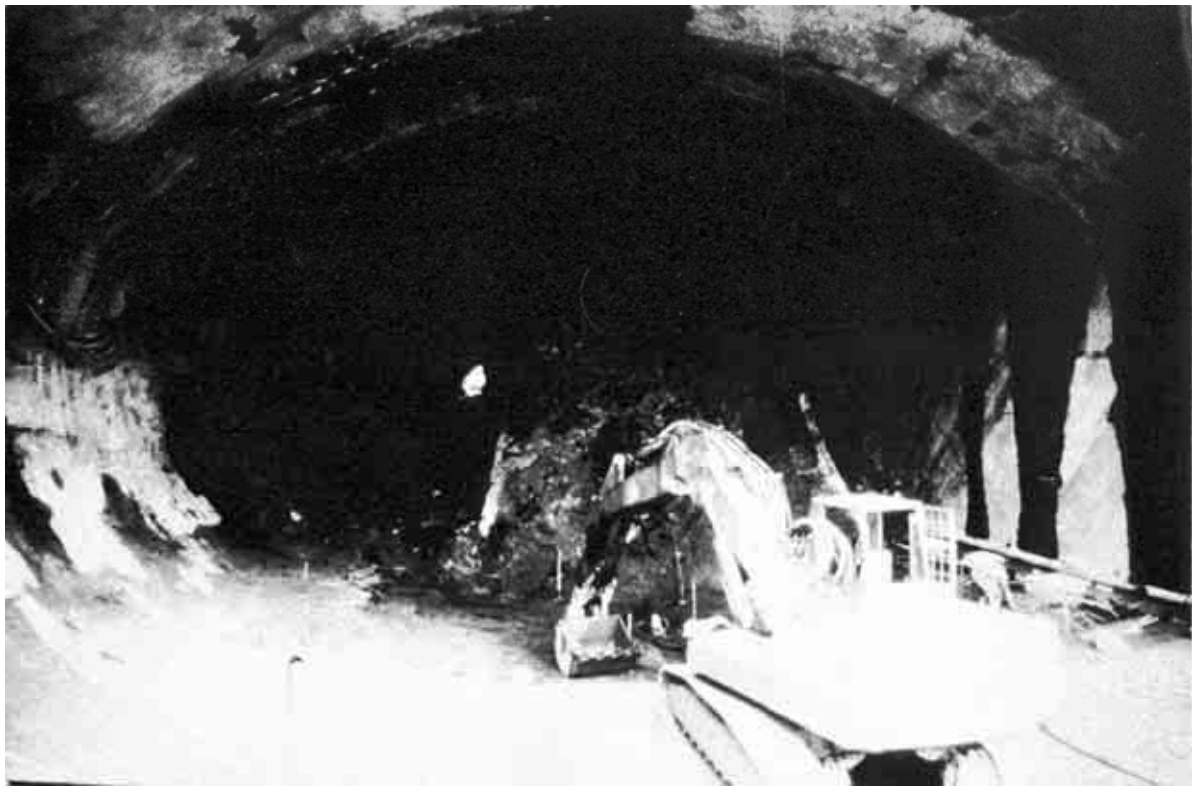

Fig. 5.13: Bench and invert excavation

The stepwise excavation and installation of the support measures and the short round lengths of approx. 1 m, specified for stability reasons and to limit the blasting vibrations, lead to a comparatively low heading performance. This had the advantage that the shotcrete membrane was only fully loaded when the shotcrete had mostly reached its final strength. The same applies to the SN-anchors.

To keep the heading-induced subsidence as small as possible, the interior lining of the northern tube was to be installed before the southern tube was excavated. For reasons of construction management the contractor was allowed, however, to carry out the excavation and support of the southern sidewall adit in parallel with the concreting works in the northern tube. The sequence of construction in the southern tube was analogous to the northern tube (Modemann and Wittke, 1988).

5.1.5 Stability analyses for the stages of construction

A rock slice with a width of 65 m and a height of 37 m was specified as computation section for the stability analyses for the construction stages (Fig. 5.14). The FE-mesh was subdivided into 440 three-dimensional isoparametric elements with 1140 nodes.

Sliding supports were specified as boundary conditions for the nodes of the lower boundary plane (z = 0).

Since the rock mass is anisotropic and the bedding is neither oriented perpendicularly nor parallel to the tunnel axis (see Fig. 5.4 and 5.14), displacements in x- and y-direction already occur due to the dead weight of the rock mass. Therefore the nodes on the vertical boundary planes of the computation section must not be fixed perpendicularly to the respective boundary plane.

The displacements in x- and y-direction resulting from the dead weight of the rock mass were determined by an advance analysis using a column-like computation section. These displacements were introduced as boundary conditions for the nodes on the vertical lateral boundary planes (x = 0 and x = 65 m) (Wittke, 2000).

For the two planes normal to the tunnel axis equal displacements were assumed as boundary conditions for opposite nodes with equal x- and z-coordinates (Wittke, 2000).

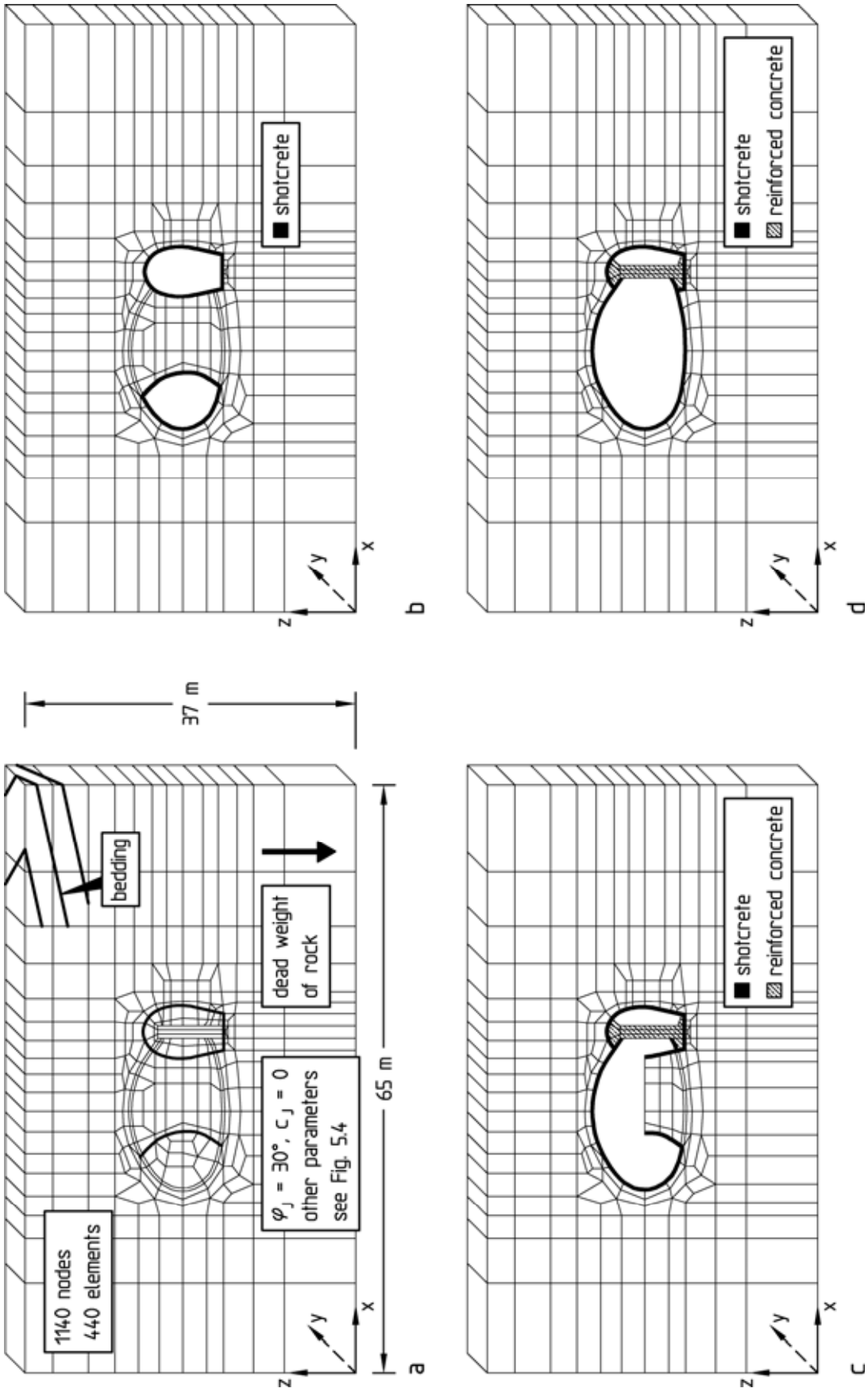

Fig. 5.14: FE-mesh and computation steps, northern tube: a) 1st computation step; b) 2nd computation step; c) 3rd computation step; d) 4th computation step

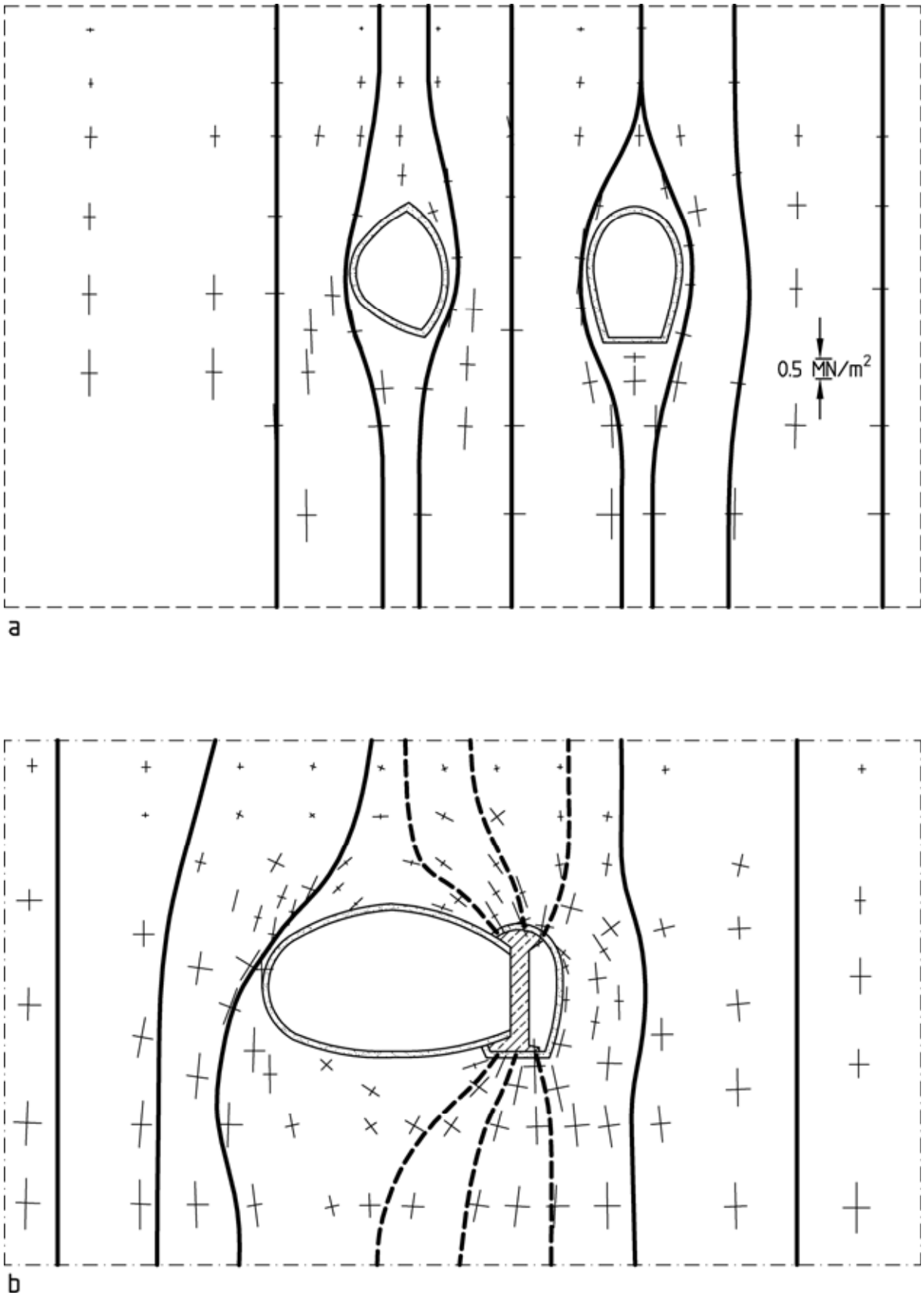

Fig. 5.15: Principal normal stresses and stress trajectories: a) 2nd computation step; b) 4th computation step

The stability analyses were carried out with the program system FEST03 (Wittke, 2000) in 4 computation steps: In the 1st computation step, the stresses and deformations in the rock mass resulting from the dead weight of the rock (in-situ state) are determined. In the 2nd computation step, the central adit as well as the northern sidewall adit are simulated to be excavated and supported. The 3rd computation step further accounts for the installation of the reinforced concrete buttress in the central adit and the crown excavation in the northern tunnel tube. Then, in the 4th computation step, the stresses and deformations occurring after the complete excavation and support of the northern tunnel tube are computed.

The principal normal stresses determined for the 2nd computation step show clearly how the loads resulting from the overburden weight are diverted around the central adit and the sidewall adit (Fig. 5.15a). A mutual influence of the two excavations is not apparent.

In the 4th computation step the loads resulting from the overburden weight are diverted around the entire excavation. Above and below the tunnel unloaded areas develop, whereas stress concentrations occur in the rock mass beside the northern tunnel tube as well as above and below the central buttress (Fig. 5.15b and 5.16).

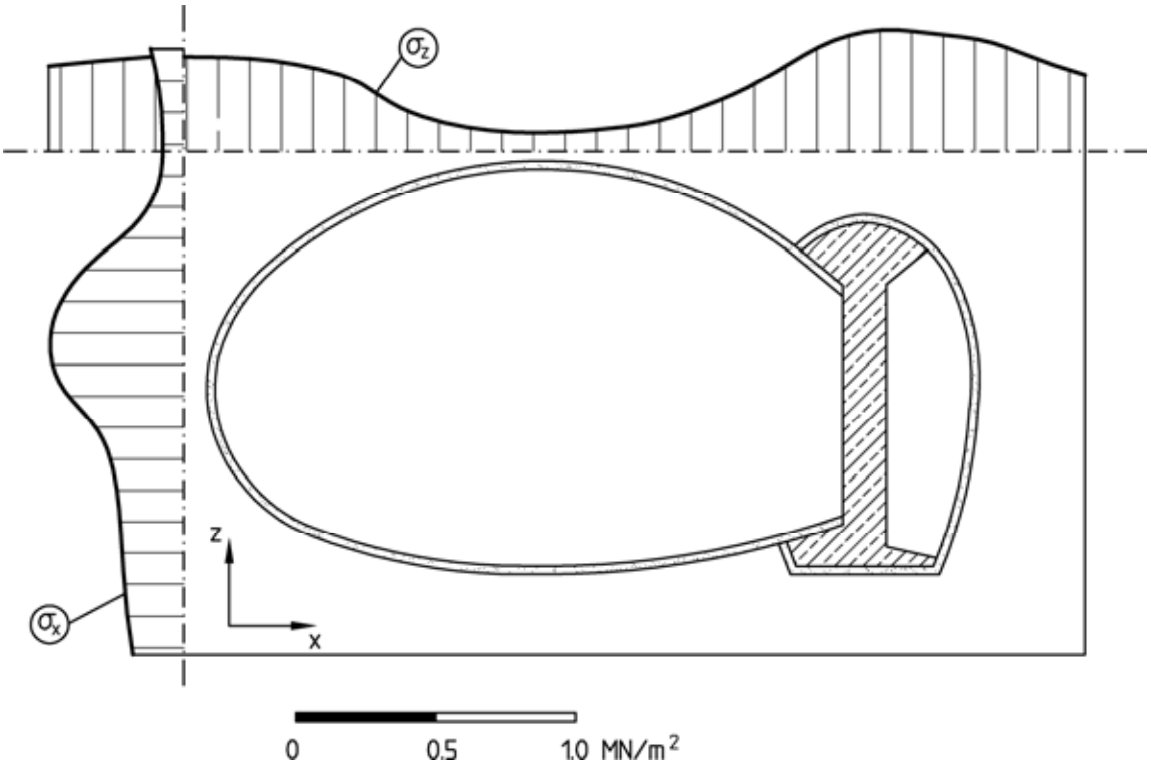

Fig. 5.16: Normal stresses in a horizontal and a vertical section, 4th computation step

According to the results of the analyses, the dead weight of the overburden is supported to a large degree by the rock mass beside the tunnel and by the central buttress. The resulting stress distribution in the concrete buttress is shown in Fig. 5.17. It becomes apparent that a horizontal tension loading results for the mushroom-shaped buttress head, whereas the shaft is loaded by normal thrust and bending.

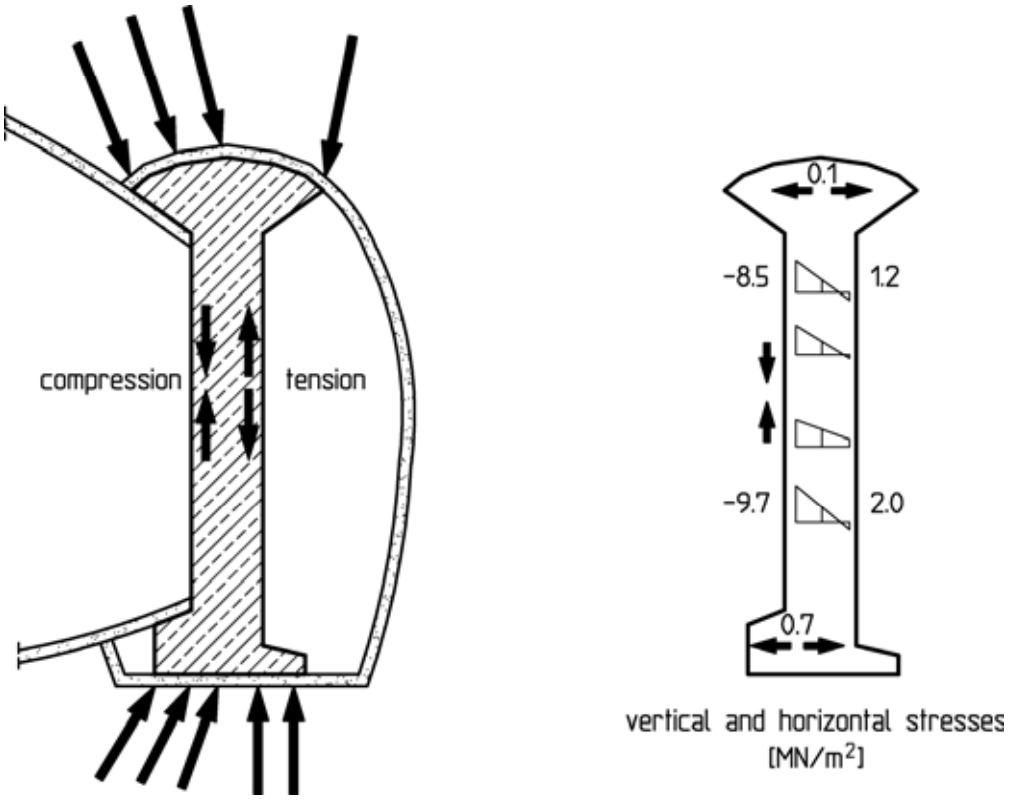

Fig. 5.17: Stresses in the central buttress, 4th computation step

An appreciable bending loading of the shotcrete membrane only occurs at the connection to the central buttress (Fig. 5.18). A connecting reinforcement is provided for to carry this bending loading (Fig. 5.18).

The maximum computed displacements due to the excavation of the northern tunnel tube amount to 22 mm at the tunnel's roof and to 8 mm at the ground surface (Fig. 5.19).

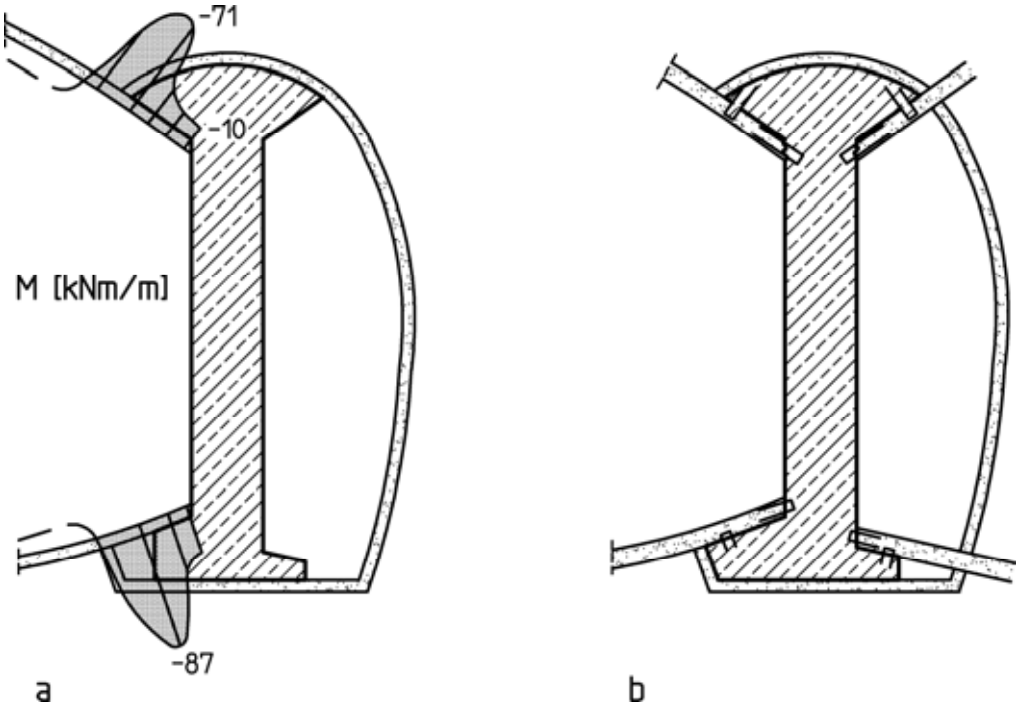

Fig. 5.18: Connection of the shotcrete membrane to the central buttress: a) Bending moments, 4th computation step; b) connecting reinforcement

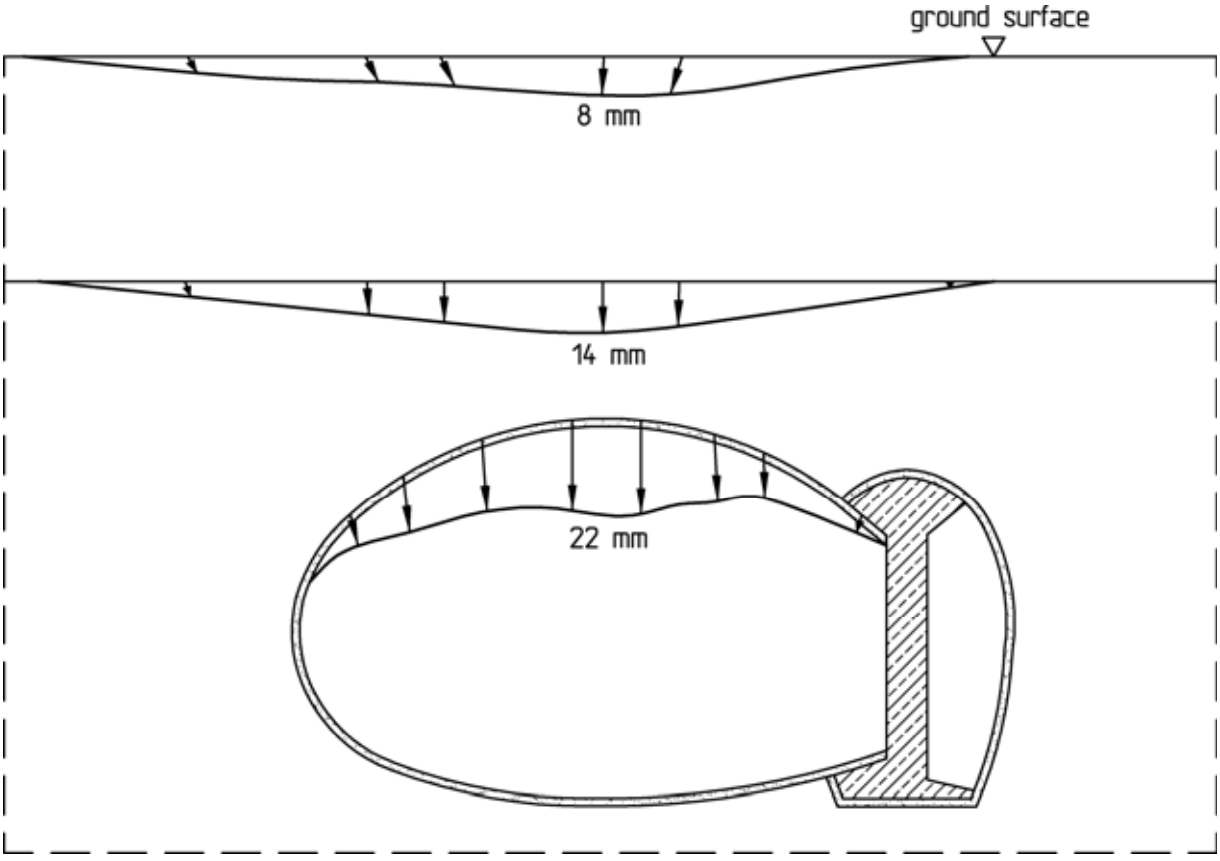

Fig. 5.19: Displacements, 4th – 1st computation step

An interpretation of the loading of the shotcrete membrane and the central buttress shows that due to the arching in the rock mass above the tunnel (see Fig. 5.15) only a portion of the overburden weight is carried by the shotcrete membrane. To determine whether the shotcrete membrane and the central buttress can carry the overburden weight alone, an analysis in which no arching can develop in the rock mass above the tunnel was carried out within the framework of safety considerations. For this purpose, above and beside the tunnel tube a vertical discontinuity set was assumed in the rock mass, striking parallel to the tunnel axis and having no shear strength ($\varphi = 0$, $c = 0$). Shear stresses thus cannot be transferred across these discontinuities. The principal normal stresses and stress trajectories determined for this case show clearly that the weight of the overburden must be completely carried by the shotcrete membrane and the central buttress (Fig. 5.20).

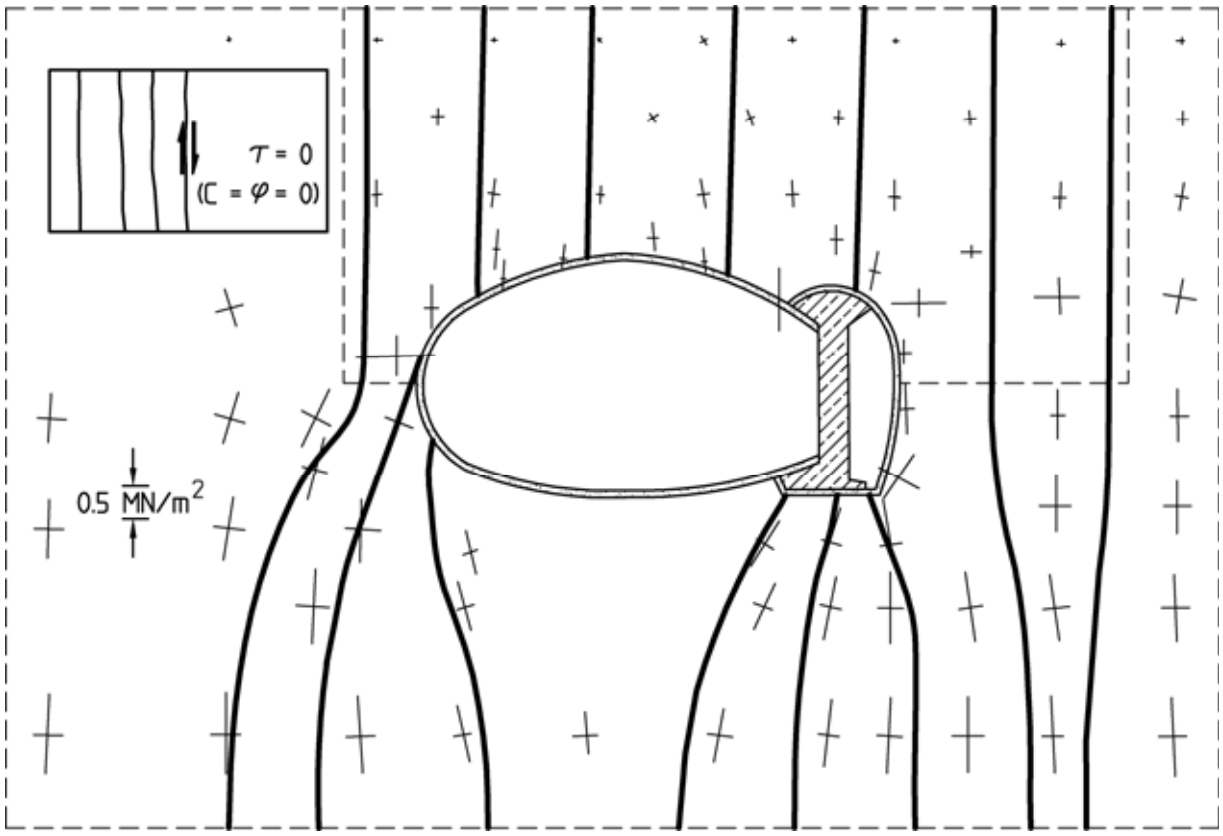

Fig. 5.20: Principal normal stresses and stress trajectories without arching in the rock mass, 4th computation step

A comparison of the normal thrust in the shotcrete membrane computed for this case with the ones of the previously investigated

case, in which arching was possible in the rock mass above the tunnel, shows that the normal thrust increases considerably (Fig. 5.21). Also for this case, however, it was possible to dimension the shotcrete membrane taking into account the inside and outside steel fabric mats Q221.

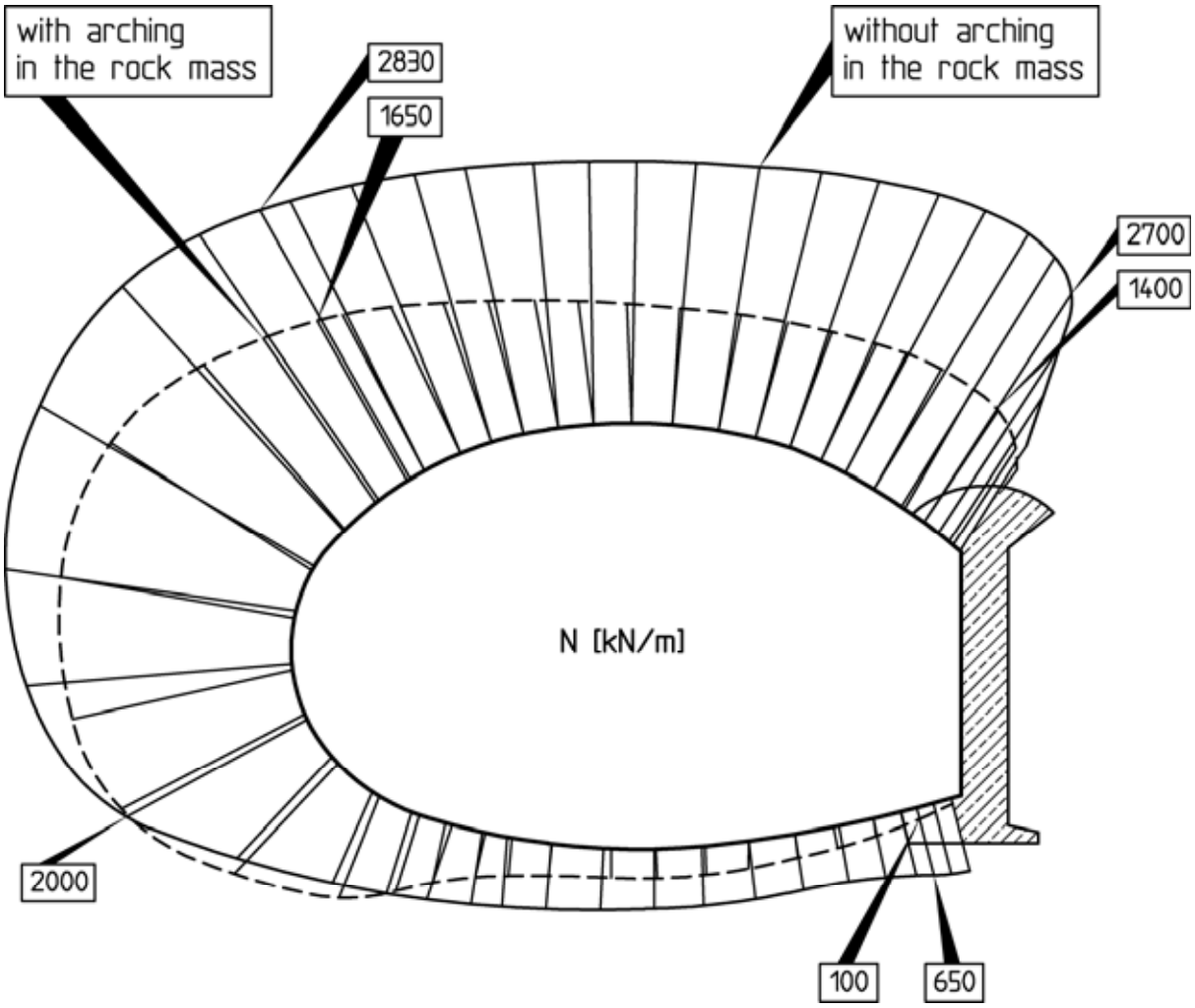

Fig. 5.21: Normal thrust in the shotcrete membrane with and without arching in the rock mass above the tunnel, 4th computation step

5.1.6 Stability analyses for the design of the interior lining

A number of stability analyses with varying assumptions was carried out for the design of the interior lining of the two tunnel tubes. Among other things it was assumed that the shotcrete membrane becomes ineffective over time.

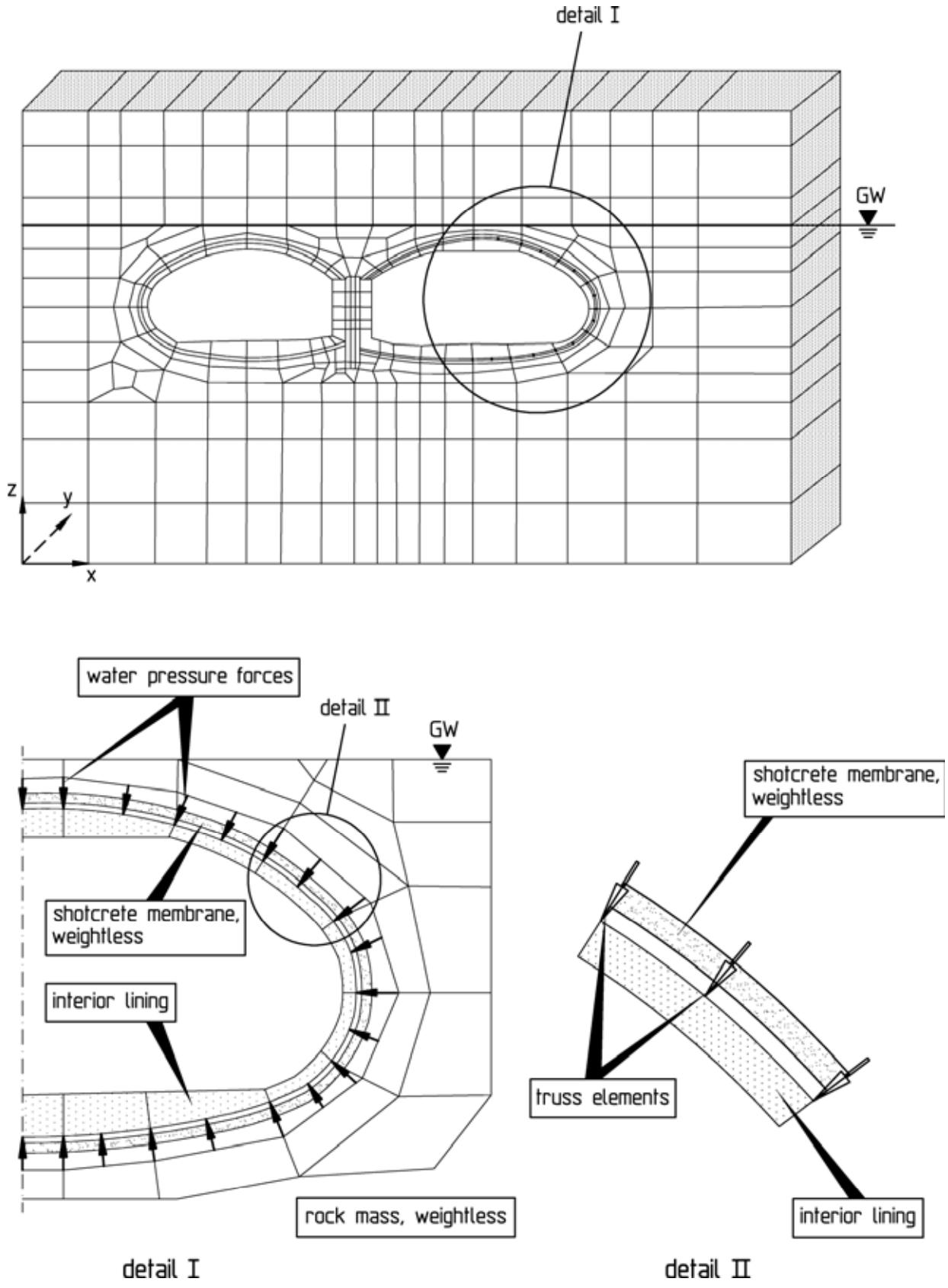

Fig. 5.22: Simulation of the water pressure acting on the interior lining

A corresponding assumption was made in some analyses for the central buttress as well, since it is not protected from the groundwater by the PVC sealing. Furthermore, cases with and without arching in the rock mass were investigated.

The result of merely one analysis shall be presented here, in which the interior linings are only loaded by their dead weight and by the water pressure. This case is relevant as long as the shotcrete membrane remains intact and carries the rock mass pressure. The water pressure is applied to the linings in the form of equivalent nodal forces (Fig. 5.22, detail I). The bedding of the interior lining is simulated by truss elements arranged between corresponding nodes of the shotcrete membrane and the interior lining and by the behavior of the shotcrete membrane and the rock mass, which is assumed elastic (Fig. 5.22, detail II). The truss elements possess a very high stiffness. They can only transfer compressive stresses, but not tensile or shear stresses. In this way the lack of a shear bond between the interior lining and the shotcrete membrane due to the PVC sealing is simulated. Since the rock mass pressure is not to be taken into account for the load case "dead weight and water pressure", the rock mass is assumed weightless.

The computed bending moment distribution represented in Fig. 5.23 shows clearly the bending loading of the inverts and the central buttress resulting from the water pressure. The corresponding distribution of the normal thrust is shown in Fig. 5.24.

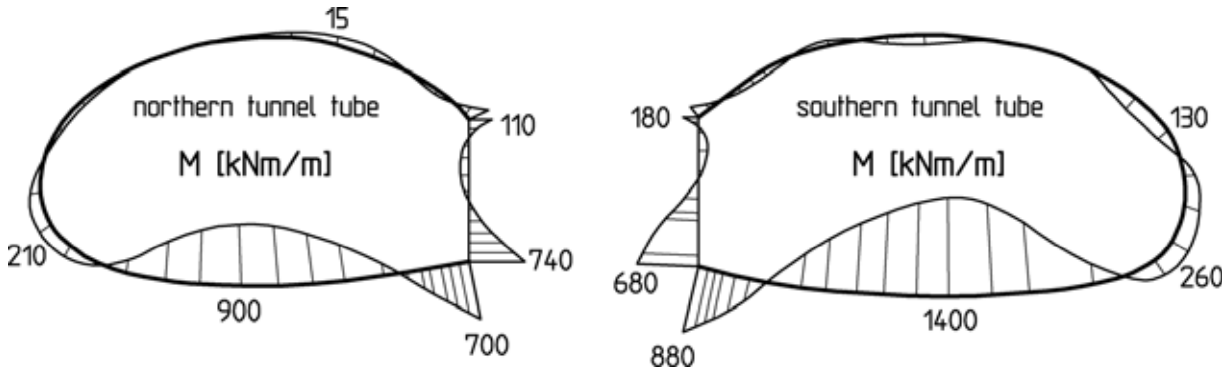

Fig. 5.23: Bending moments in the interior lining, load case "dead weight and water pressure"

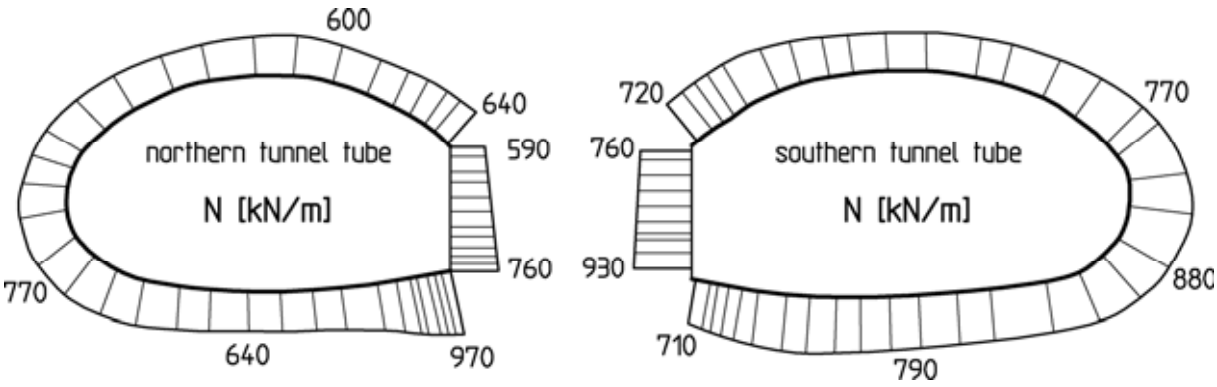

Fig. 5.24: Normal thrust in the interior lining, load case "dead weight and water pressure"

5.1.7 Monitoring

A measuring program was planned to monitor the stability as well as the subsidence occurring at the ground surface and at the buildings. It included leveling and convergency measurements in the tunnel. In addition, extensometer measurements as well as levelings at the ground surface and at buildings were carried out during construction. Further, the groundwater levels in observation wells located beside the tunnel (see Fig. 5.1) were read continuously, and the blasting-induced vibrations were measured at the buildings. Of course, evidence was perpetuated at the buildings before the start and after the end of construction.

The subsidence measured at a building located right above the tunnel is shown exemplarily in Fig. 5.25 for different stages of construction. It can be seen that the subsidence of the building at the end of construction is distinctly less than 2 cm, and that the building has subsided almost evenly. In the course of the different construction stages only small differential subsidence of the buildings occurred as well. No damage was found on this or the surrounding buildings (Modemann and Wittke, 1988).

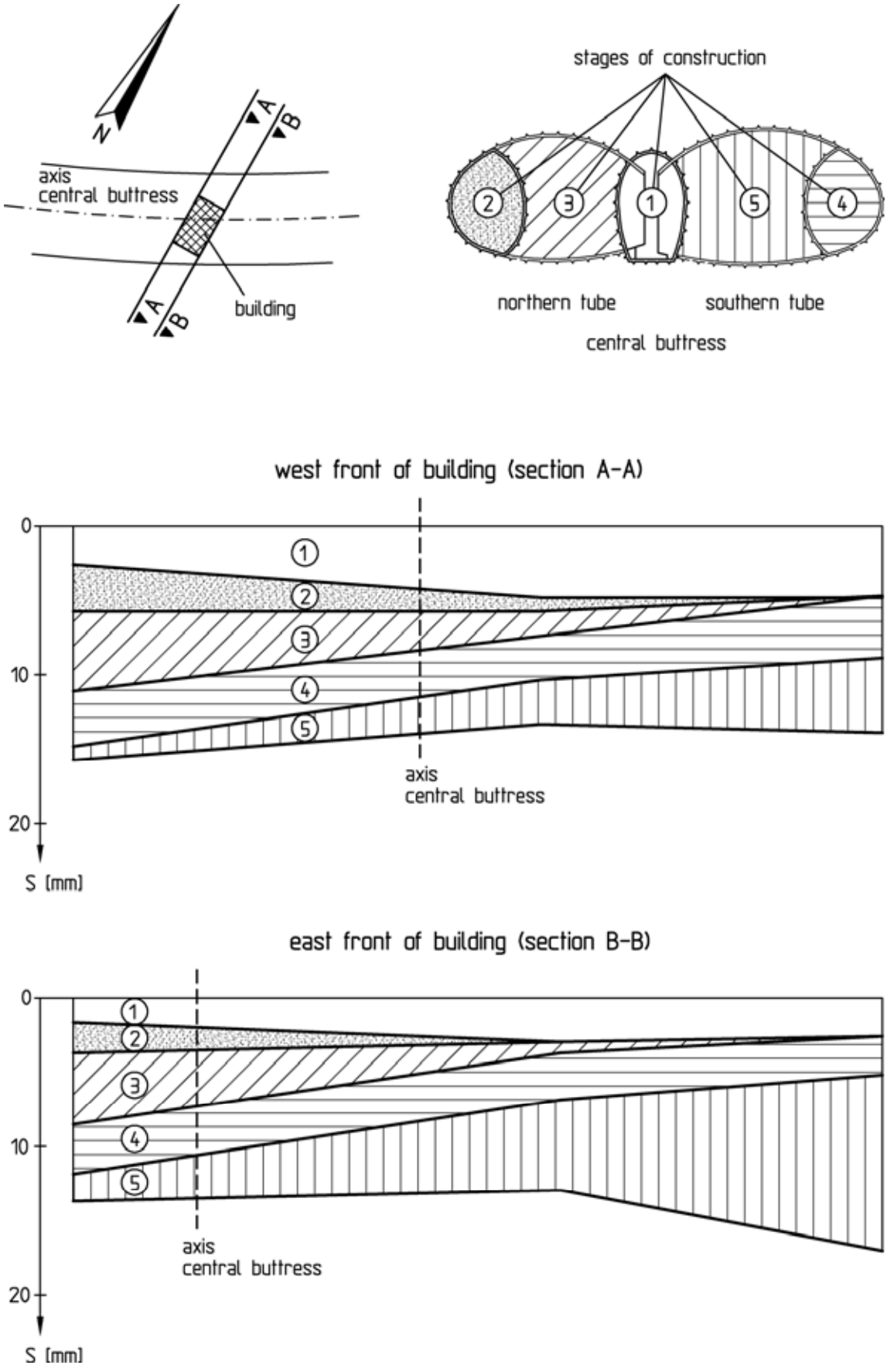

Fig. 5.25: Measured subsidence of a building located above the tunnel

5.1.8 Conclusions

The road tunnel Hahnerberger Straße is a tunnel with a very large span and low overburden, for which the requirement was made to keep the heading-induced subsidence at the ground surface and vibrations as small as possible.

This task was solved with the following measures:

- Construction of two tunnel tubes with a reinforced concrete buttress in the middle providing additional support of the rock mass,

- subdividing the cross-section of both tunnel tubes into several parts,

- limiting the round length to approx. 1 m,

- rounding the cross-sections of the two tunnel tubes in the vault area to enable the formation of a vault in the shotcrete membrane, the interior lining and the rock mass,

- designing the shotcrete membrane and the reinforced concrete buttress in such a way that they can carry the complete rock mass pressure,

- installation of the interior lining after the first tube was excavated and before the excavation of the second tube started,

- smooth blasting.

Essential for the success of the construction project were furthermore the appropriate characterization of the ground and the proofs of stability established using the FE-program developed by the authors and their co-workers.

5.2 Limburg Tunnel, Germany

5.2.1 Introduction

The new railway line Cologne-Rhine/Main undercrosses a business area of the city of Limburg in a approx. 2.4 km long tunnel between chainage km 109+680 and km 112+075.

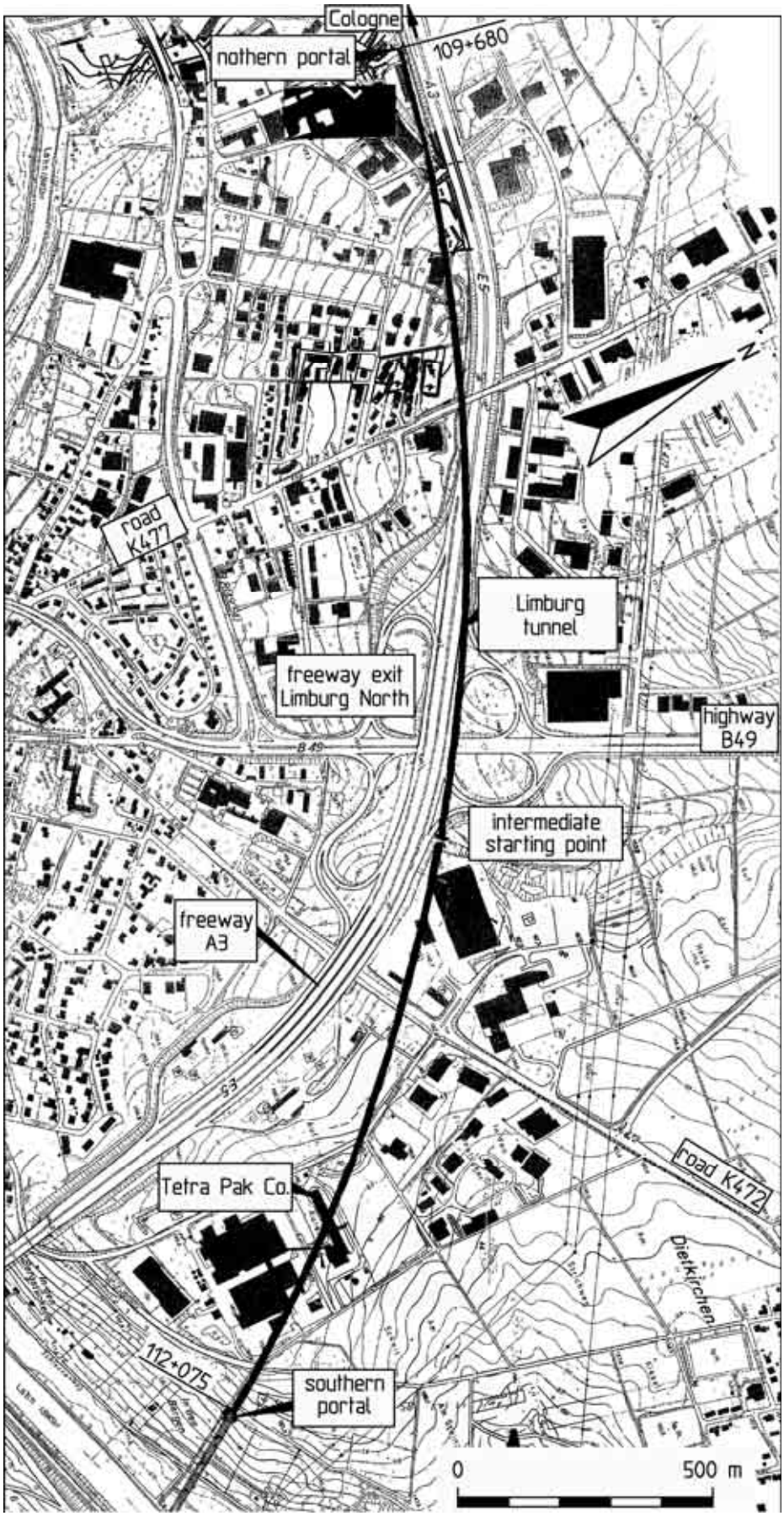

Fig. 5.26: Limburg Tunnel, site plan

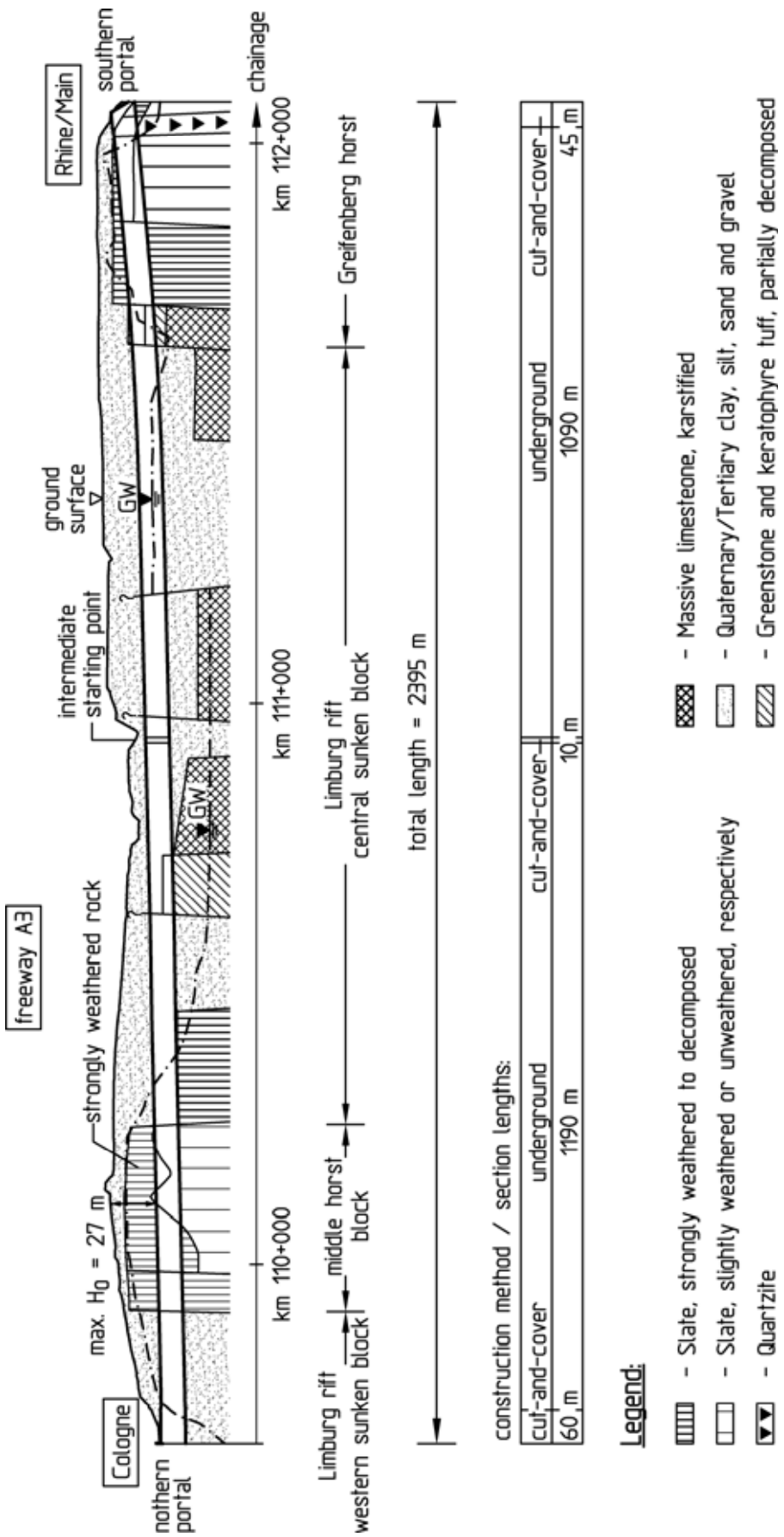

Fig. 5.27: Limburg Tunnel, longitudinal section with ground profile

In addition to business and industrial structures, the tunnel undercrosses among other things the freeway (Autobahn) A3 and the highway B 49 (Fig. 5.26 and 5.27). With overburden heights from 10 to 30 m it crosses through varying and geotechnically difficult ground in the form of predominantly weathered to decomposed slate as well as Tertiary and Quaternary clay, silt and sand (Fig. 5.27).

For reasons of stability the excavation profile had to be subdivided during tunnel heading. In most parts a sidewall adit excavation with additional tunnel face support measures was carried out.

5.2.2 Structure

In the portal areas and in a short middle section (intermediate starting point), the Limburg Tunnel was constructed by the cut-and-cover method. The sections in between, approx. 1190 m and 1090 m in length, were excavated by underground construction (Fig. 5.27).

Seen from the direction of Cologne, the tunnel undercrosses first the sports grounds "Im Finken" with an overburden of approx. 16 m. Next, it undercrosses the freeway A3 and the traffic lanes of the freeway exit Limburg North at an acute angle with an overburden varying between 10 and 20 m. Between chainage km 110+750 and km 110+810, the highway B 49 and its underpass of freeway A3 are undercrossed with a small roof cover of approx. 4 m. Afterwards, the tunnel crosses under parts of the Massa shopping center and under the county road K 472 with an overburden of approx. 15 to 19 m. At chainage km 111+680 the tunnel undercrosses a high bay warehouse and between chainage km 111+800 and km 111+870 a warehouse of Tetra-Pak Co. (Fig. 5.26).

Fig. 5.28 shows the geometry of the standard profile and of the sidewall adits. The double-tracked tunnel was constructed with a mouth-shaped profile with a width of 15.2 m and a height of 12.4 m. In the vault area a radius of curvature of R = 7.28 m was selected. The transition from the sidewalls to the invert was constructed with a radius of R = 4.43 m. For statical reasons the invert was deeply rounded with R = 11.63 m. The inside walls of the sidewall adits had a radius of curvature of R = 8.0 m. The roof and the invert of the sidewall adits were rounded with small radii of R = 0.4 m (Fig. 5.28).

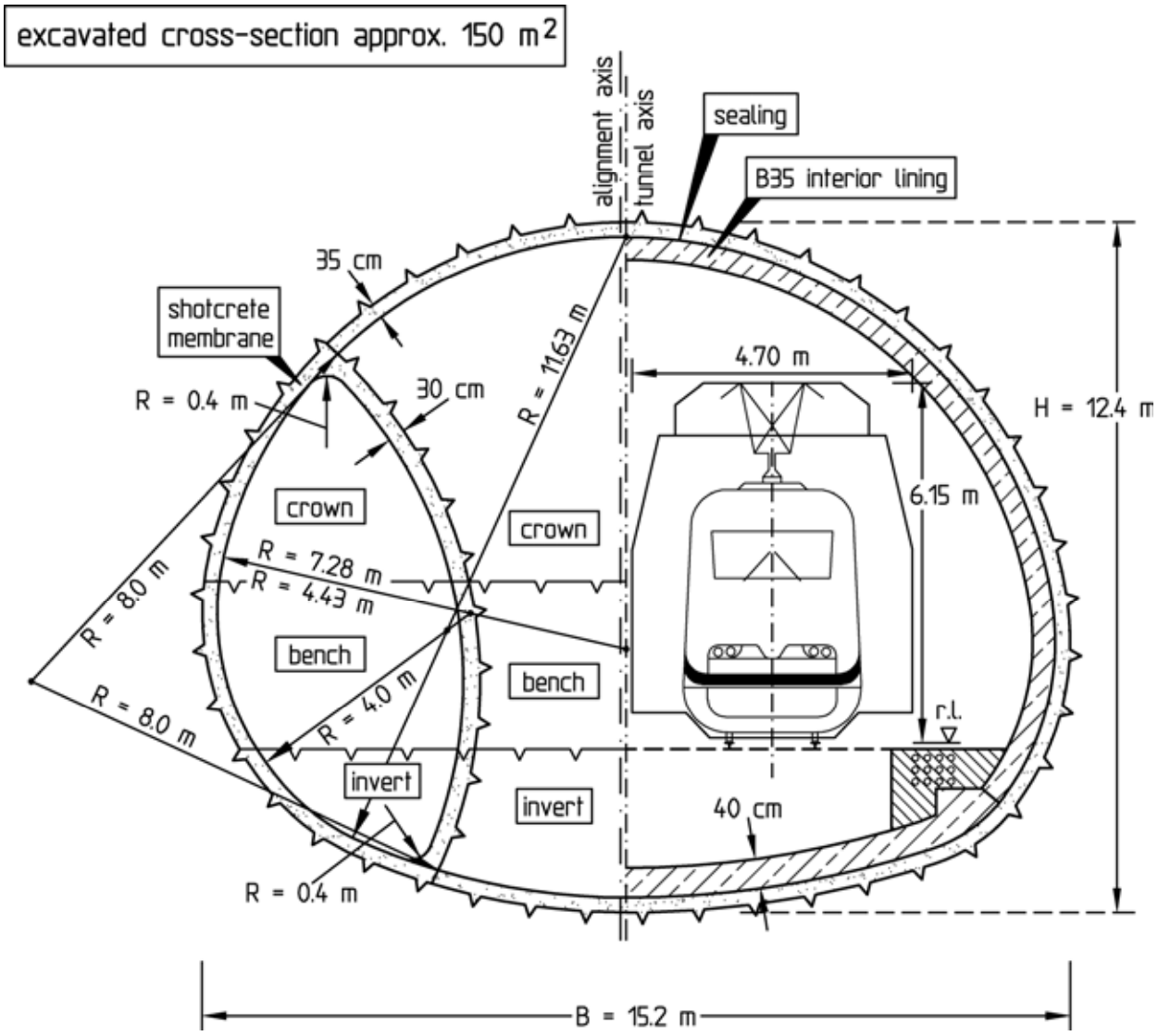

Fig. 5.28: Limburg Tunnel, standard profile

The excavated cross-section amounts to approx. 150 m^2. The sidewall adits as well as the remaining cross-section (core) were subdivided for the excavation into crown, bench and invert (Fig. 5.28).

The shotcrete membrane has a thickness of 35 cm. The thickness of the inside shotcrete membranes of the sidewall adits amounts to 30 cm. The interior lining is 40 cm thick (Fig. 5.28).

Fig. 5.29 shows the start of underground excavation at the northern portal.

Fig. 5.29: Limburg Tunnel, start of underground excavation at the northern portal

5.2.3 Ground and groundwater conditions

The ground at the alignment of the Limburg Tunnel was explored by core drillings, some of which were equipped as observation wells.

In the area of the northern portal the tunnel is located in the Tertiary clays of the western sunken block of the Limburg rift. This formation consists predominantly of silty clay with intercalated 1 to 9 m thick sand and gravel layers (Fig. 5.27).

At about chainage km 109+915 follows the middle horst block of the Limburg rift, consisting at first of slate decomposed to sandy and clayey silt. At the core of the uplifted block, solid Devonian slate is encountered. The slate has been strongly loaded in terms of fracture tectonics. It is strongly weathered in the upper zone up to a depth of approx. 45 m.

At approx. chainage km 110+250, the tunnel leaves the uplifted block and crosses through the central sunken block of the Limburg

rift up to about chainage km 111+640. As in the western sunken block, predominantly Tertiary clays are encountered here.

At about chainage km 111+640, in the area of the high bay warehouse of Tetra Pak Co., the tunnel reaches the uplifted block of the Greifenberg horst. On the first approx. 70 m, the tunnel is located partially in decomposed keratophyre tuff and partially in strongly weathered, in some areas also completely decomposed slate, into which the tunnel enters completely in the following section. From about chainage km 111+910 to the southern portal, the tunnel crosses through slightly weathered to decomposed slate (Fig. 5.27).

The foliation represents the dominant discontinuity set in the Devonian slate. It strikes from southwest to northeast and dips mostly at 40 to 70° in southeastern direction. Because of the tight (isoclinal) folding, however, foliation planes dipping steeply to the northwest occur as well. In connection with two steeply dipping joint sets, an approximately orthogonal discontinuity fabric exists in most cases.

To determine the deformability of the ground, 9 dilatometer tests and 40 borehole jack tests were carried out in exploration boreholes located in the area of the Limburg Tunnel. According to these tests, a modulus of deformation for initial loading of 200 to 1000 MN/m^2 can be assumed for slightly weathered slate. In decomposed slate, however, comparatively small moduli of deformation for initial loading of 5 to 80 MN/m^2 were determined. Even smaller values of 5 to 60 MN/m^2 resulted for the soil.

For 63 samples from the clayey and silty surface layers as well as from the decomposed rock the unconfined compressive strength was determined. The unconfined compressive strength of the clay and silt of the surface layers scatters over the relatively wide range of 50 to 1900 kN/m^2. The results of the tests on decomposed rock, however, are in the range of 100 to 500 kN/m^2. The strength of the slightly to strongly weathered or decomposed slate is substantially determined by the low strengths on the discontinuities (see Chapter 5.2.6).

Between the northern portal and the eastern boundary of the middle horst block, the groundwater table follows the course of the ground surface at a depth of approx. 5 to 10 m (Fig. 5.27). In the

area of the central sunken block of the Limburg rift, the groundwater table is located at a depth of about 25 to 45 m at the level of the two receiving streams, the Elbach and the Lahn. To the east of the central sunken block, at the Greifenberg horst, the groundwater table rises again to approx. 5 to 10 m below the ground surface (Fig. 5.27). The seasonal variations in the water table can amount to several meters. The groundwater table shown in the longitudinal section (Fig. 5.27) is based on the highest groundwater levels measured in the boreholes equipped as observation wells. The groundwater is assumed to flow roughly from northeast to southwest.

The water permeability of the Devonian rock and the Tertiary layers is estimated at 10^{-7} to 10^{-5} m/s.

5.2.4 Excavation and support

In the areas of the Greifenberg horst and the middle horst block, in which the tunnel cross-section is located in slightly weathered slate, a crown excavation with closed invert was planned according to excavation classes 5A-K, 6A-K or 7A-K, depending on the degree of weathering. In the other much longer sections the tunnel is located in soil or in decomposed slate. Here, a sidewall adit excavation was planned according to excavation classes 4A-U, 5A-U, 6A-U or 7A-U (see DGGT, 1995: Table 1).

Fig. 5.30 shows the sequence of excavation and the support for excavation class 7A-U-0, which was carried out for the most part. Excavation class 7A-U-0 is characterized by short round lengths for crown and bench (A = 0.6 m to 0.8 m), tunnel face support with plain shotcrete (t ≥ 7 cm), advance support with spiles and early closing of the invert (C ≤ 3.2 m). The tunnel profile is supported by a reinforced shotcrete membrane with two layers of steel fabric mats Q285 and by steel sets spaced at e_a = 0.6 to 0.8 m. A systematic anchoring of the sidewall adits with SN-anchors was planned on the outside and as required also on the inside.

Just as the excavation of the advancing sidewall adits, the excavation of the core is characterized by a short round length at the crown, tunnel face support with plain shotcrete and advance support with spiles (Fig. 5.31). The round lengths at bench and invert amounted to B = 2.8 to 3.2 m. The support was closed at the

invert at a maximum of approx. 18 m behind the crown excavation (Fig. 5.31).

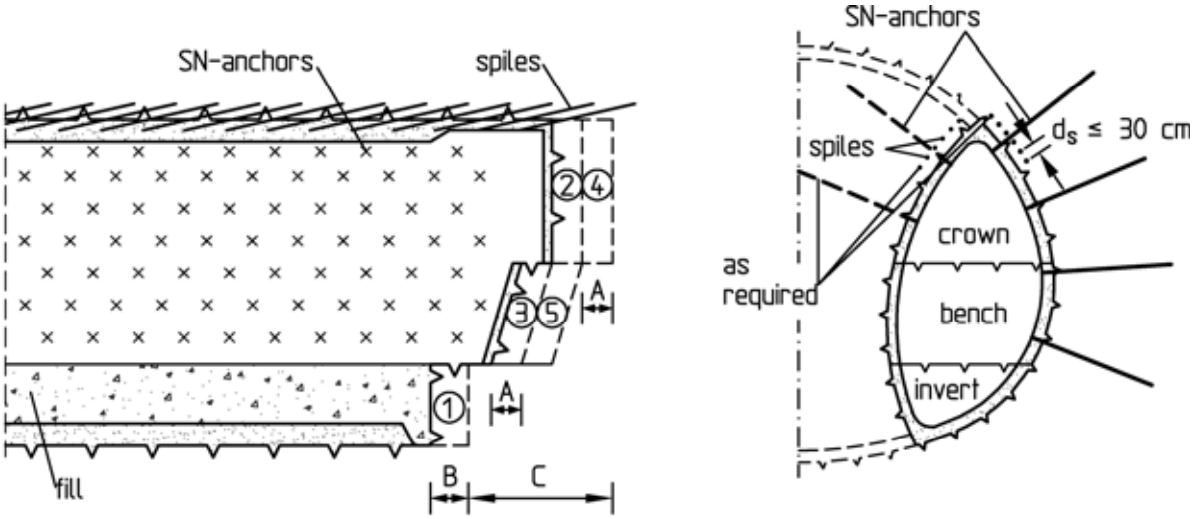

excavation class	7A-U-0		
	crown	bench	invert
excavation method	tunnel excavator		
round length	A = 0.6 - 0.8 m		B = 1.2 - 1.6 m
tunnel face support	shotcrete ≥ 7 cm		-
advance support	spiles l_S = 3 - 4 m $d_S \leq 30$ cm	-	
B25 shotcrete	outside 35 cm, inside 30 cm		
reinforcement	steel fabric mats (2 layers) outside Q378, inside Q188		
steel sets	d_a = 0.6 - 0.8 m outside GI120, inside GI100		-
anchoring	l_A = 4 m 1 - 2 pcs./round	l_A = 4 m 1 - 2 pcs./round	-
trailing distance	-	A = 0.6 - 0.8 m	C ≤ 4A ≤ 3.2 m

Fig. 5.30: Excavation and support of the sidewall adits, excavation class 7A-U-0

The rock mass and the soil could be excavated mechanically using a tunnel excavator.

The excavation was carried out temporarily at four locations simultaneously:

- Excavation north (starting from the northern portal),

- excavation south (starting from the southern portal),

- excavations center north and center south (starting from the intermediate starting point, see Fig. 5.27).

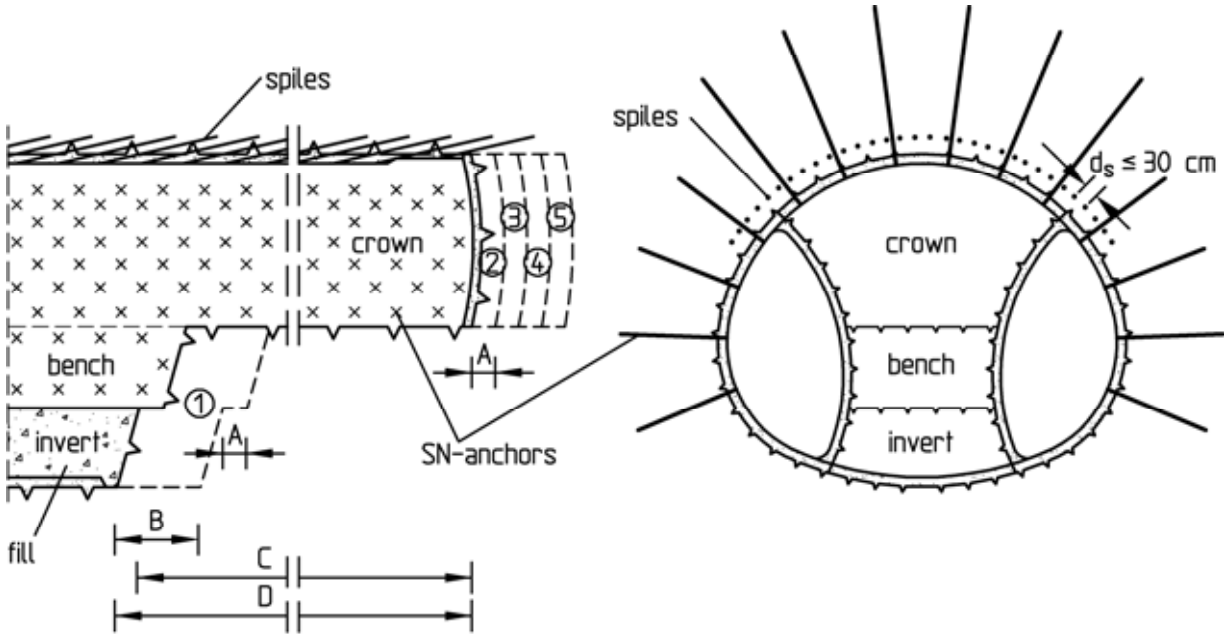

excavation class	7A-U-0		
	crown	bench	invert
excavation method	tunnel excavator		
round length	A = 0.6 - 0.8 m		B = 2.8 - 3.2 m
tunnel face support	shotcrete ≥ 7 cm		-
advance support	spiles l_S = 3 - 4 m $d_S \leq 30$ cm	-	
B25 shotcrete	35 cm		
reinforcement	steel fabric mats (2 layers) Q295		
steel sets	d_a = 0.6 - 0.8 m, GI120		
anchoring	l_A = 6 m 5 - 6 pcs./round	-	
trailing distance	-	C = 17.4 - 17.6 m	D ≤ 18.2 m

Fig. 5.31: Excavation and support of the core, excavation class 7A-U-0

5.2.5 Sidewall adit excavation north

The sidewall adit excavation north (Fig. 5.32 to 5.35) started at first with the excavation class 7A-U-0 with the support being closed at the invert after 4 rounds (C = 4A ≤ 3.2 m, see Fig. 5.30).

Fig. 5.32: Excavation north, right sidewall adit

Fig. 5.33: Excavation of the crown of the sidewall adit

After 160 m, as the heading reached the decomposed slates, which were fractured to small sizes, water entered more intensely through joints and foliation parallel discontinuities within the area of the tunnel face. This lead to stability problems at the vertical tunnel face and thus impeded the heading.

Starting at chainage 193 m the excavation sequence was therefore modified. The step between crown and bench excavation was extended and the bench face was steepened. The support was closed at the invert at a distance of 6 rounds behind the crown excavation (Fig.

5.36). In this manner a tunnel face more shallowly inclined on average was achieved. In addition, the safety of the staff during closing of the invert was increased.

Fig. 5.34: Excavation of the bench of the sidewall adit

Fig. 5.35: Invert of the sidewall adit

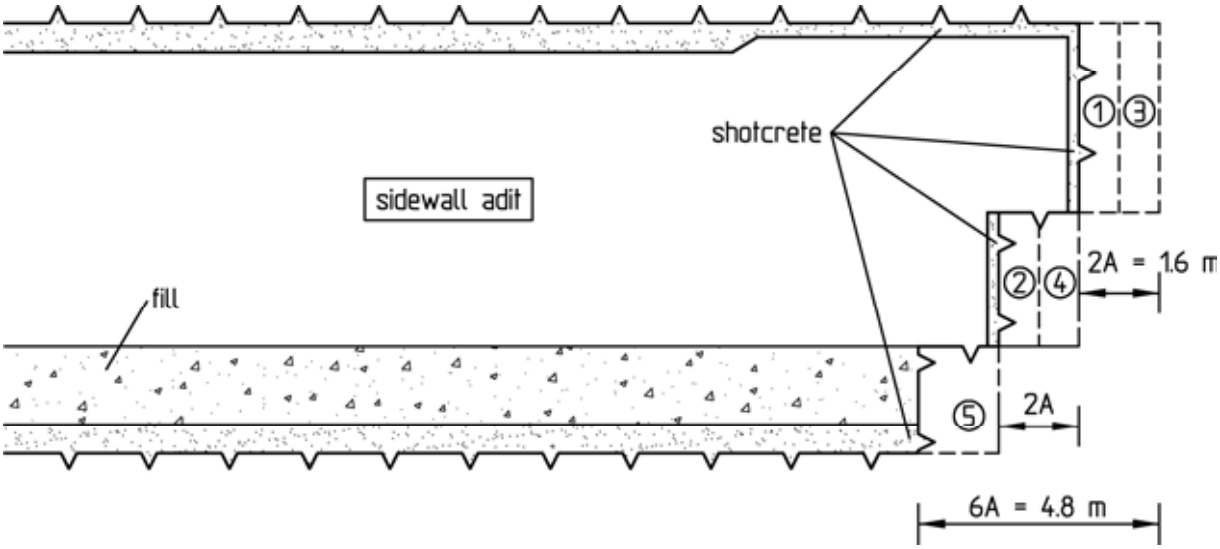

Fig. 5.36: Modified sequence of excavation and closing of invert support after 6 rounds, sidewall adits, excavation north, chainage 193 to 267 m

As stability problems continued at the tunnel face, an inclined crown and bench face supported with plain shotcrete was constructed starting at chainage 267 m. In addition, a reinforced shotcrete support was installed at the invert of the temporary bench of the sidewall adits to achieve a rapid stabilization of the excavation. Furthermore, the final closing of the support at the invert was carried out separately for the crown and bench heading. After the excavation and support of the crown and the bench of the sidewall adits had been completed ≤ 20 m in advance, the heading was interrupted and the tunnel face was sealed with plain shotcrete. Subsequently the excavation and support of the invert was carried out (Fig. 5.37). To drain off the water inflow through joints and foliation parallel discontinuities in the tunnel face area, a drainage was laid in the invert of the bench of the sidewall adits and a shaft sump reaching down to below the tunnel's invert was constructed every 10 to 20 m.

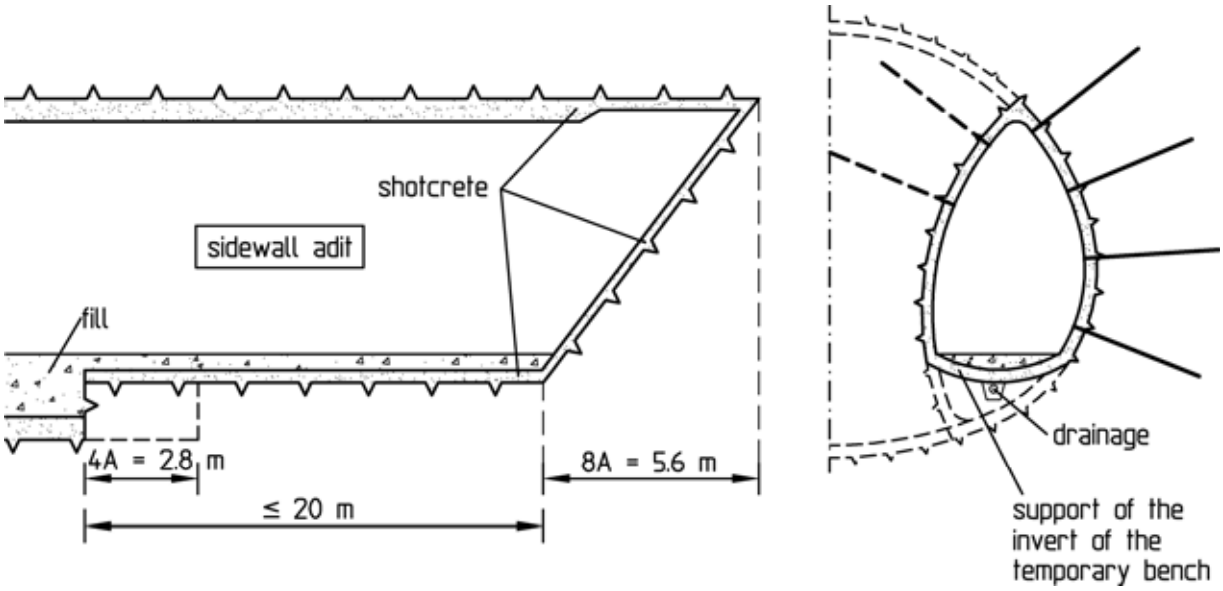

Fig. 5.37: Inclined tunnel face and support of the invert of the temporary bench of the sidewall adits, excavation north, chainage 267 to 336 m

At chainage 336 m the heading was changed back again to excavation class 7A-U-0, since the strength of the rock mass increased and the jointing as well as the water inflow decreased.

Fig. 5.38 is a photograph of the core excavation at excavation north.

Fig. 5.38: Excavation north, core excavation

5.2.6 Stability analyses for sidewall adit excavation north

The problems with the tunnel face stability that had occurred during the sidewall adit excavation north in the decomposed slate of the middle horst block (see Fig. 5.27) were attributed to the low shear strengths on the discontinuities of the strongly weathered to decomposed slate. The foliation and bedding parallel discontinuities F the orientations of which were measured during tunnel face mapping, strike approximately perpendicularly to the tunnel axis and dip mostly steeply with dip angles between 40° and 70° towards the tunnel face. In addition, two joint sets J1 and J2 exist, which strike in parallel and perpendicularly to the tunnel axis and dip steeply as well (Fig. 5.39).

The water pressure acting in the foliation and bedding discontinuities, respectively, and in the joints had a further unfavorable effect on the stability of the tunnel face.

Three-dimensional stability analyses were therefore carried out using the program system FEST03 (Wittke, 2000) for the sidewall adit excavation in the area of the middle horst block to investi-

gate the influence of the strength on the discontinuities and of the seepage pressure on the stability of the tunnel face.

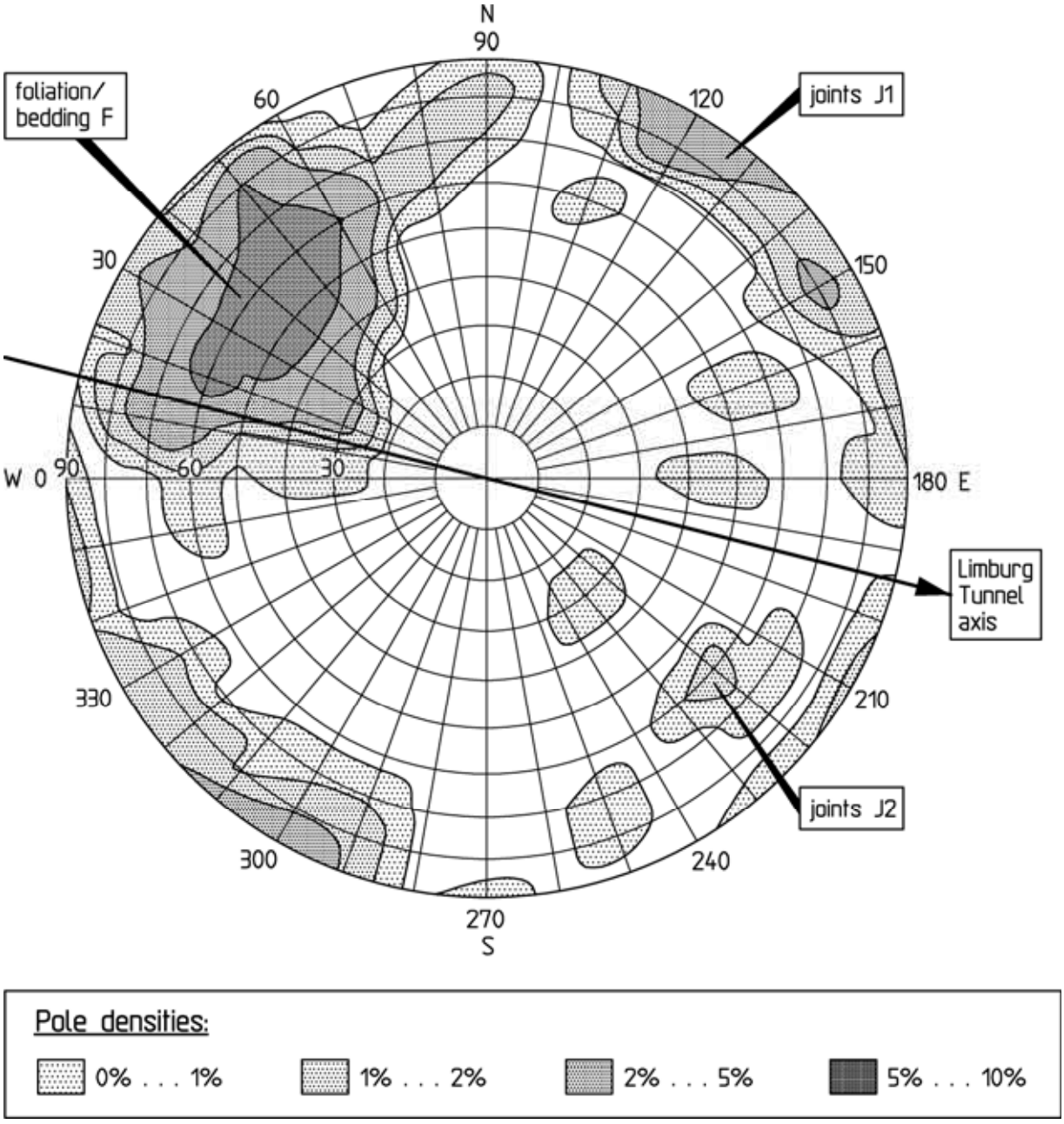

Fig. 5.39: Discontinuity orientations measured during sidewall adit excavation north, polar diagram

Fig. 5.40 shows the three-dimensional computation section, the FE-mesh and the parameters the analyses were based upon. One sidewall adit was modeled. The overburden amounts to 23 m.

In order to investigate the influence of the shear strengths on the discontinuities on the tunnel face stability three three-

dimensional analyses were carried out (cases A, B and C, Table 5.1).

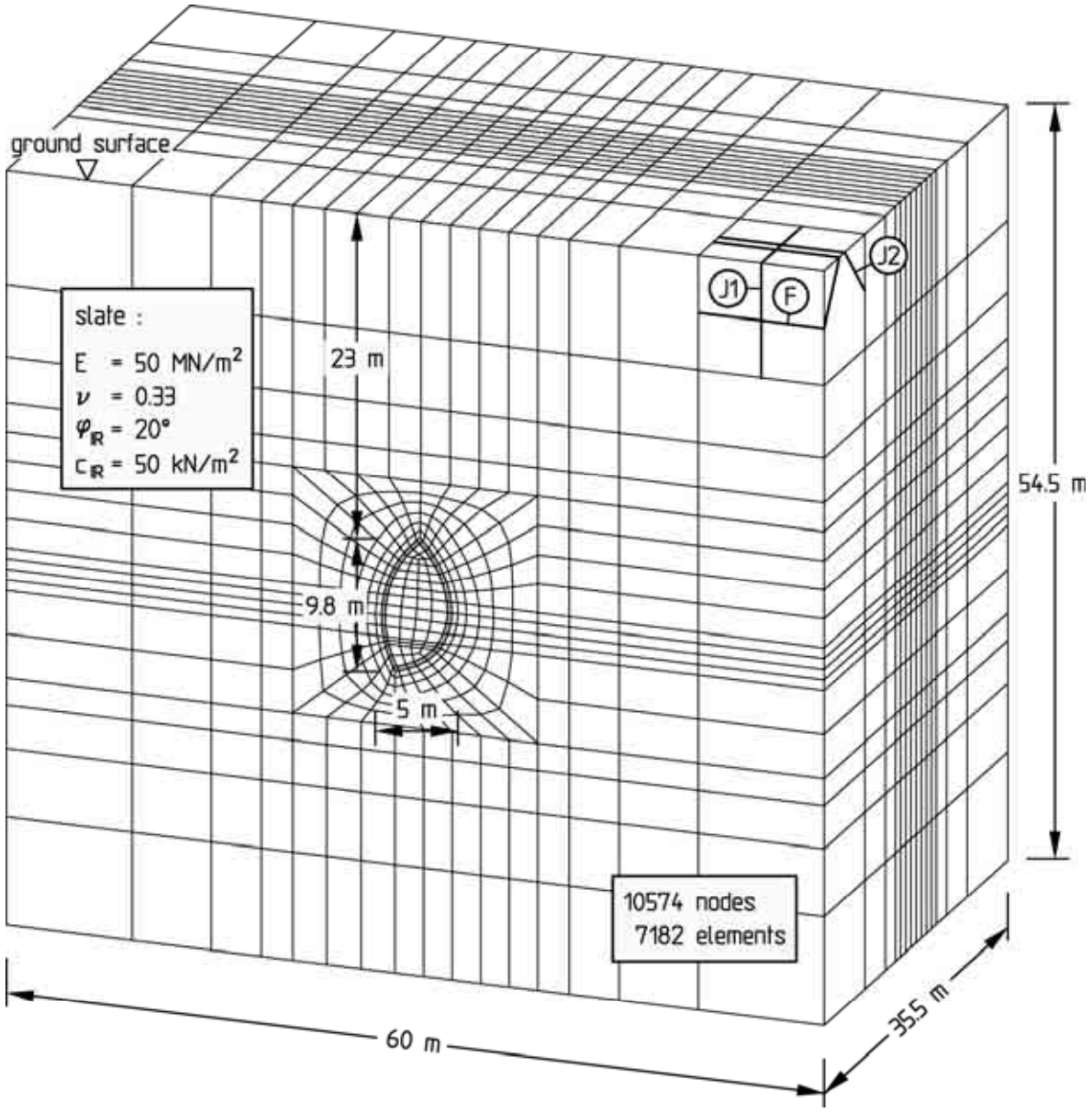

Fig. 5.40: Computation section, FE-mesh and parameters

Case	Discontinuities in the slate		
	φ_F [°]	φ_{J1} [°]	φ_{J2} [°]
A	no discontinuities		
B	20	20	20
C	10	10	10

Table 5.1: Limburg Tunnel, three-dimensional analyses regarding the tunnel face stability

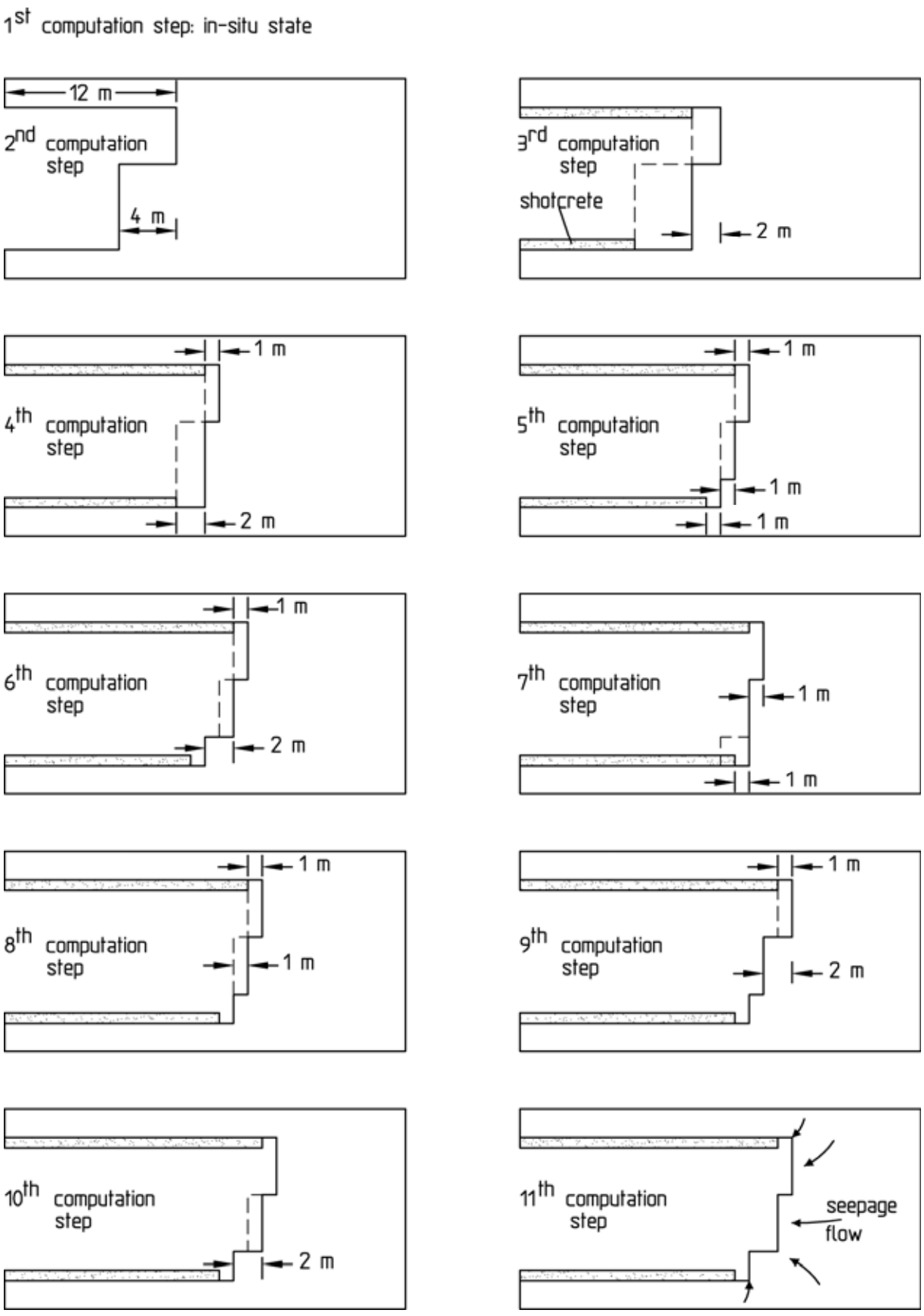

Fig. 5.41: Computation steps for the simulation of the sidewall adit heading

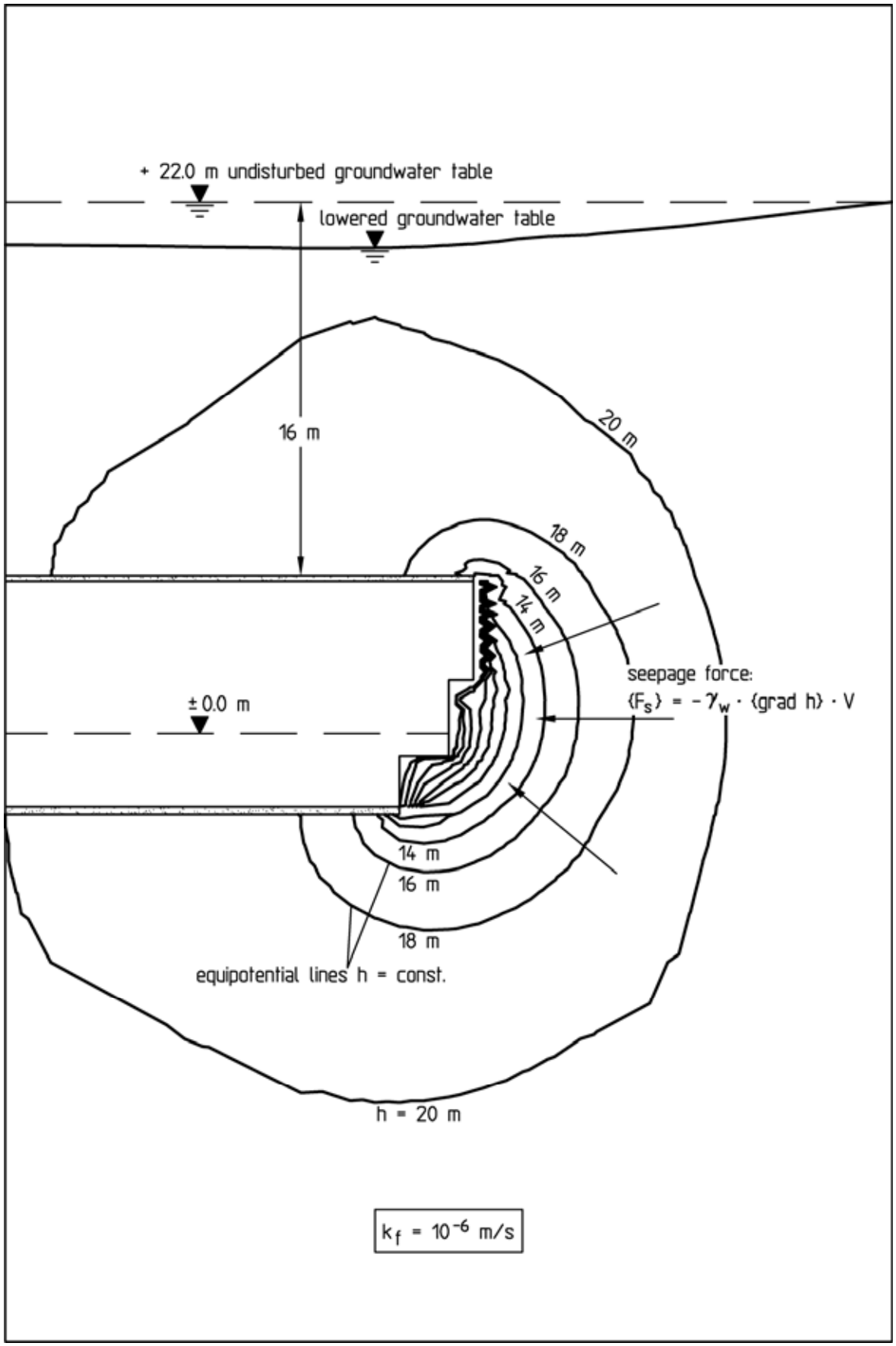

Fig. 5.42: Seepage flow analysis, equipotential lines and seepage forces

In case A discontinuities were not taken into account. In cases B and C the foliation/bedding F, dipping at 70° towards the tunnel face, was simulated, together with the joint set J1, vertical and striking parallel to the tunnel axis, and the joint set J2, dipping at 60° opposite to the direction of heading (see Fig. 5.40). In case B the friction angle on the discontinuities was chosen as $\varphi_{F/J}$ = 20° and in case C as $\varphi_{F/J}$ = 10° (Table 5.1). No cohesion was assumed on the discontinuities. Young's modulus of the slate was specified as E = 50 MN/m^2 in all cases (Fig. 5.40).

The heading of a sidewall adit with crown, bench and invert excavation was simulated in 10 computation steps, which are outlined in Fig. 5.41. In the 11th computation step the seepage forces due to the water seeping through the rock mass were applied (Fig. 5.41), which had been determined in a three-dimensional seepage flow analysis using the program system HYD03 (Wittke 2000). This seepage flow analysis results in the distribution of piezometric heads h, from which the seepage forces can be calculated. The analysis was based on an undisturbed groundwater table located 16 m above the roof of the sidewall adit. Fig. 5.42 shows the location of the groundwater table lowered due to the tunnel excavation, the computed equipotential lines (h = const.), as well as, qualitatively, the direction and magnitude of the seepage forces F_S oriented perpendicularly to the equipotential lines.

The slate was simplificatively assigned a homogeneous and isotropic permeability with a permeability coefficient of $k_f = 10^{-6}$ m/s. The distribution of the piezometric heads and the seepage forces is, however, independent of the selected permeability coefficient, since a homogeneous and isotropic ground was assumed for the analysis (Wittke, 2000).

Fig. 5.43 shows the development of the computed horizontal displacement δ_H of a point on the unsupported tunnel face in the course of the viscoplastic iterative analysis for computation steps 10 and 11.

Case A results in a stable tunnel face with a maximum horizontal displacement of $\delta_H \approx 3$ cm. In case B the displacements are larger than in case A, with max. $\delta_H \approx 6$ cm in the 10th computation step and max $\delta_H \approx 10$ cm in the 11th computation step (with seepage pressure). The tunnel face is stable, however, since the displacements converge in the course of the viscoplastic iterative analysis. Case C

results in a maximum displacement of $\delta_H \approx 22$ cm for the 10^{th} computation step and of $\delta_H \approx 35$ cm for the 11^{th} computation step. Although the displacement δ_H converges in this analysis as well, the tunnel face cannot be regarded stable anymore due to the magnitude of δ_H. For a horizontal displacement of 35 cm it must be assumed that the rock loosens up and disintegrates in the tunnel face area.

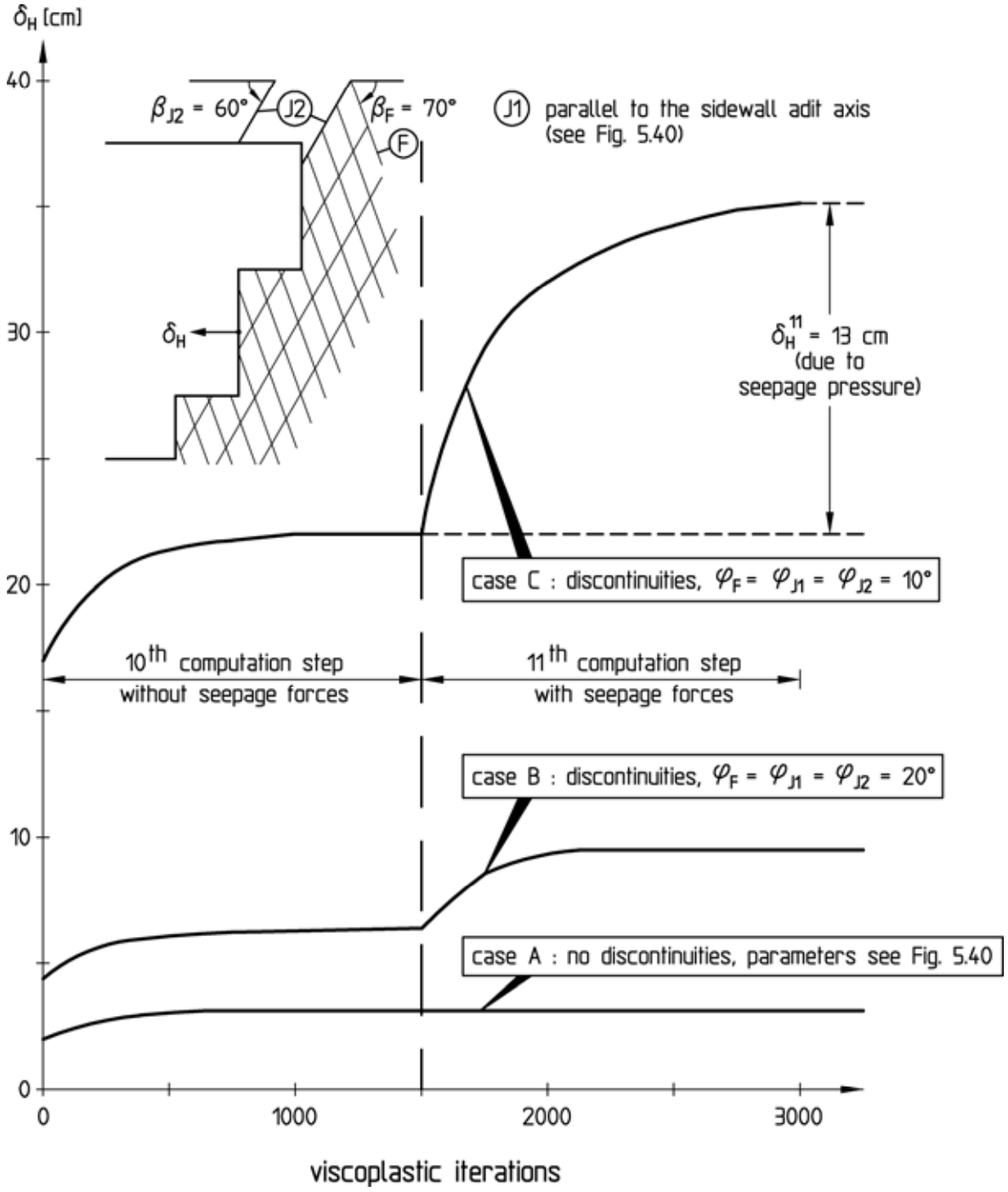

Fig. 5.43: Horizontal displacement of the tunnel face depending on the shear strength on the discontinuities

In summary it can be stated on the basis of the FE-analysis results that the stability of the tunnel face of the sidewall adit is substantially influenced by the discontinuity fabric. For shear parameters of $c_F = c_{J1} = c_{J2} = 0$ and $\varphi_F = \varphi_{J1} = \varphi_{J2} = 10°$, which had been estimated from the results of the geotechnical mapping during heading, the tunnel face must be considered unstable. The analysis results further show that for low shear strengths on the discontinuities the seepage pressure acting on the tunnel face has a strong influence on the magnitude of the horizontal displacements. If follows that by an efficient drainage of the rock in advance of the sidewall adit excavation the problems during the heading could have been reduced decisively.

5.2.7 Monitoring results

The heading of the Limburg Tunnel was accompanied by a geotechnical monitoring program including surface leveling, extensometer and inclinometer measurements as well as leveling and convergency measurements in the tunnel.

Fig. 5.44 shows exemplarily the vertical displacements of the sidewall adit roofs δ_{SL} and δ_{SR} and of the tunnel roof δ_R measured after the excavation of the entire cross-section in excavation north from chainage 160 to 375 m (km 109+900 to km 110+115). The measured vertical displacements of the roofs of the two sidewall adits are larger than the one of the roof of the total cross-section, because with the latter only a part of the displacements occurring during the core excavation can be captured. The measured displacements of the sidewall adit roofs include a part of the subsidence that occurred during the sidewall adit heading and in addition the subsidence resulting from the core excavation.

The maximum subsidence of $\delta_{SL} = 45$ mm was measured at chainage 300 m (Fig. 5.44). In this area the sidewall adit was excavated with an inclined tunnel face and with a supported invert of the temporary bench (see Fig. 5.37). From chainage approx. 340 m on the measured subsidence decreased to a few millimeters. In this area the sidewall adit excavation was changed over to excavation class 7A-U-0 (see Fig. 5.30). Starting with chainage approx. 360 m the roof was located in slightly weathered to unweathered slate. Here, the measured roof subsidence decreased to ≤ 3 mm (Fig. 5.44).

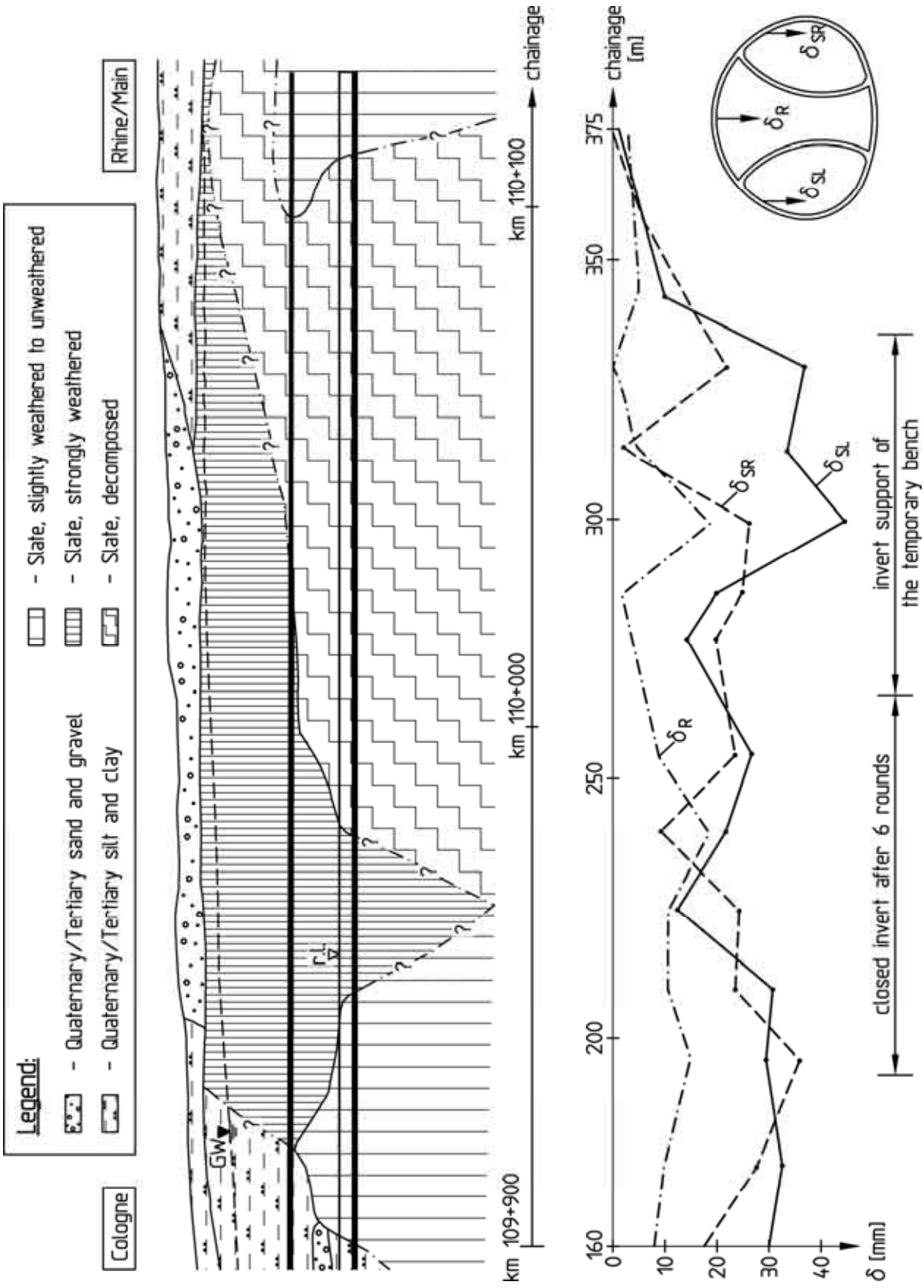

Fig. 5.44: Measured vertical displacements, chainage 160 to 375 m

5.2.8 Conclusions

With the Limburg Tunnel of the new railway line Cologne/Rhine-Main stability problems often occurred at the tunnel face during the sidewall adit excavation north in the area of the middle horst block. These problems impeded the heading and required intensified support measures. In this section the tunnel cross-section was located in strongly weathered slate which is strongly jointed to fractured to small sizes. The groundwater table was encountered approx. 15 m above the roof.

By three-dimensional FE-analyses the influence of the shear strength on the discontinuities of the slate and of the seepage pressure in the rock mass on the stability of the tunnel face was investigated. The results show that the tunnel face stability is substantially determined by the discontinuity fabric. It could further be proven that the seepage pressure resulting from the seepage flow in connection with the low strength on the discontinuities caused the stability problems during the sidewall adit excavation north. The impediments during the heading and the intensified support measures could have been considerably reduced by an efficient drainage of the rock mass in advance of the heading.

5.3 Niedernhausen Tunnel, Germany

5.3.1 Introduction

The Niedernhausen Tunnel lies in the southern part of the new railway line Cologne-Rhine/Main in the area of the town of Niedernhausen, south of Idstein, Germany.

Over a length of approx. 350 m following the northern portal the tunnel is located in the completely weathered and decomposed slates of the Schwall layers with an overburden of about 17 to 50 m. Further, the groundwater table lies at roof level or above in this area and the freeway A3 had to be undercrossed (Fig. 5.45). Under these conditions the tunnel face was not stable without supplementary support measures. Moreover, the tunneling-induced subsidence of the ground surface in the area of the undercrossing of the freeway A3 had to be kept small.

The high demands and the difficult ground conditions made it necessary to drain the rock in advance and to construct the tunnel in this area in partial excavations with additional tunnel face support measures.

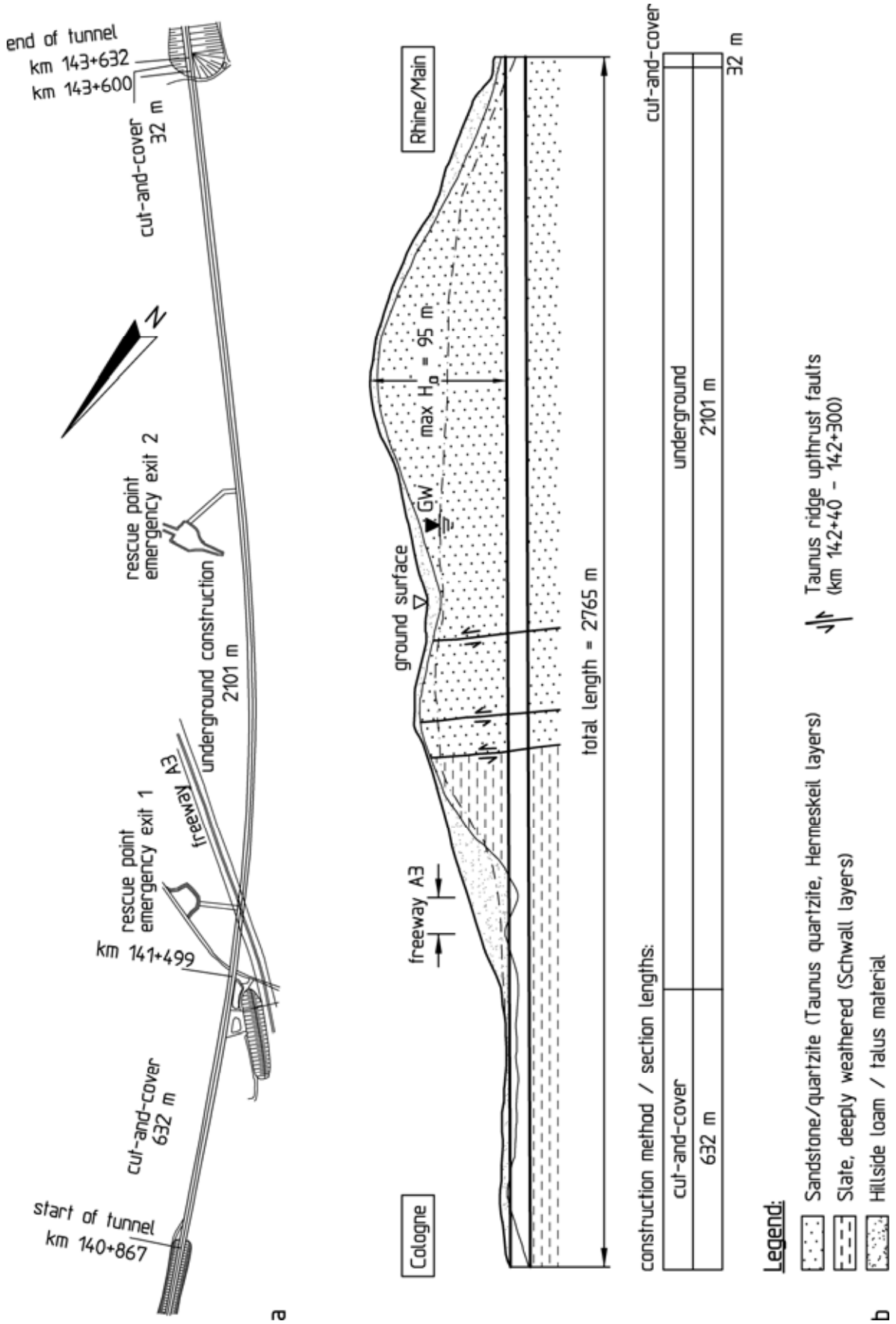

Fig. 5.45: Niedernhausen Tunnel: a) Site plan; b) longitudinal section with ground profile

5.3.2 Structure

The two-tracked Niedernhausen Tunnel is 2765 m long (Fig. 5.45). From chainage km 140+867 to km 141+499 as well as in the southern portal area the tunnel was constructed by the cut-and-cover method. The overburden in this area amounts to less than 10 m. Over the remaining 2101 m the tunnel was excavated by underground construction. The maximum overburden height is 95 m (Fig. 5.45b).

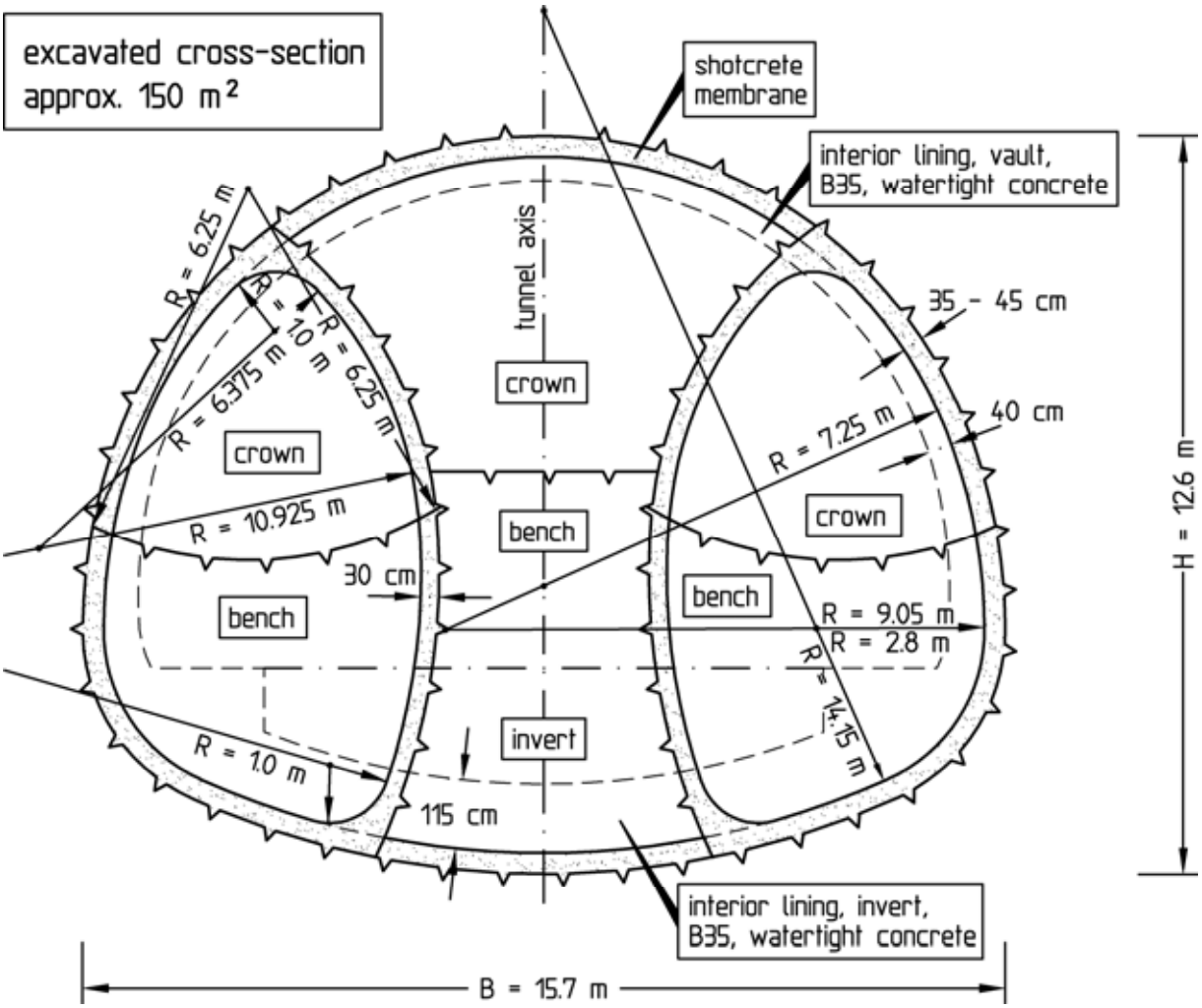

Fig. 5.46: Niedernhausen Tunnel, standard profile with sidewall adits

Between chainage km 141+600 and km 141+700 the tunnel undercrosses the federal highway A3 at an acute angle with an overburden of 20 to 30 m. The tunnel roof lies in the hillside loam in this area. The remainder of the cross-section is located in the already mentioned deeply weathered and decomposed Schwall layers (Fig. 5.45b). A sidewall adit heading was planned in this area.

Fig. 5.46 shows the 15.7 m wide and 12.6 m high standard profile with the geometry of the sidewall adits. The excavated cross-section amounts to approx. 150 m^2.

The vault area was constructed with a radius of curvature of R = 7.25 m. In the sidewalls a radius of R = 9.05 m was selected. The transitions from the sidewalls to the invert were constructed with a radius of R = 2.8 m. The invert was rounded with R = 14.15 m. The inside walls of the sidewall adits had radii of curvature of R = 6.375 m and R = 10.925 m, respectively. The roof and the invert of the sidewall adits were constructed with a small radius of R = 1.0 m. The temporary crown inverts of the sidewall adits were rounded with R = 6.25 m (Fig. 5.46).

The shotcrete membrane was carried out unusually strong with a thickness of 35 to 45 cm. The inside shotcrete membrane of the sidewall adits were constructed 30 cm thick. The thickness of the interior lining amounts to 40 cm (Fig. 5.46).

The sidewall adits were subdivided into crown and bench for the heading. The remaining cross-section (core) was subdivided into crown, bench and invert (Fig. 5.46).

Fig. 5.47 shows the starting wall of the northern heading at the northern portal.

Fig. 5.47: Niedernhausen Tunnel, starting wall of the northern heading

5.3.3 Ground and groundwater conditions

The ground at the alignment of the Niedernhausen Tunnel was explored by core drillings. Some of these boreholes were equipped as observation wells.

The Quaternary hillside loam and talus material extends to a depth of approx. 40 m in the northern tunnel section. In the southern tunnel area, however, the Quaternary surface layer is only 12 m thick at the most (Fig. 5.45b).

Below the Quaternary cover Devonian rock sequences follow (Fig. 5.45b) consisting of silty and finely sandy slate (Schwall layers), micaceous sandstone and quartzite with slate intercalations (Hermeskeil layers), quartzitic sandstone and quartzite with embedded sandy slate (Taunus quartzite) and phyllitic slate with sandstone and quartzite layers (Variegated Schist).

The slate of the Schwall layers is characterized by a far-reaching weathering which can extend to a depth of about 150 m. It corresponds in strength to a cohesive soil. Young's modulus, however, is roughly that of a well-compacted gravel sand. The discontinuity fabric has remained intact in spite of the weathering (Fig. 5.48).

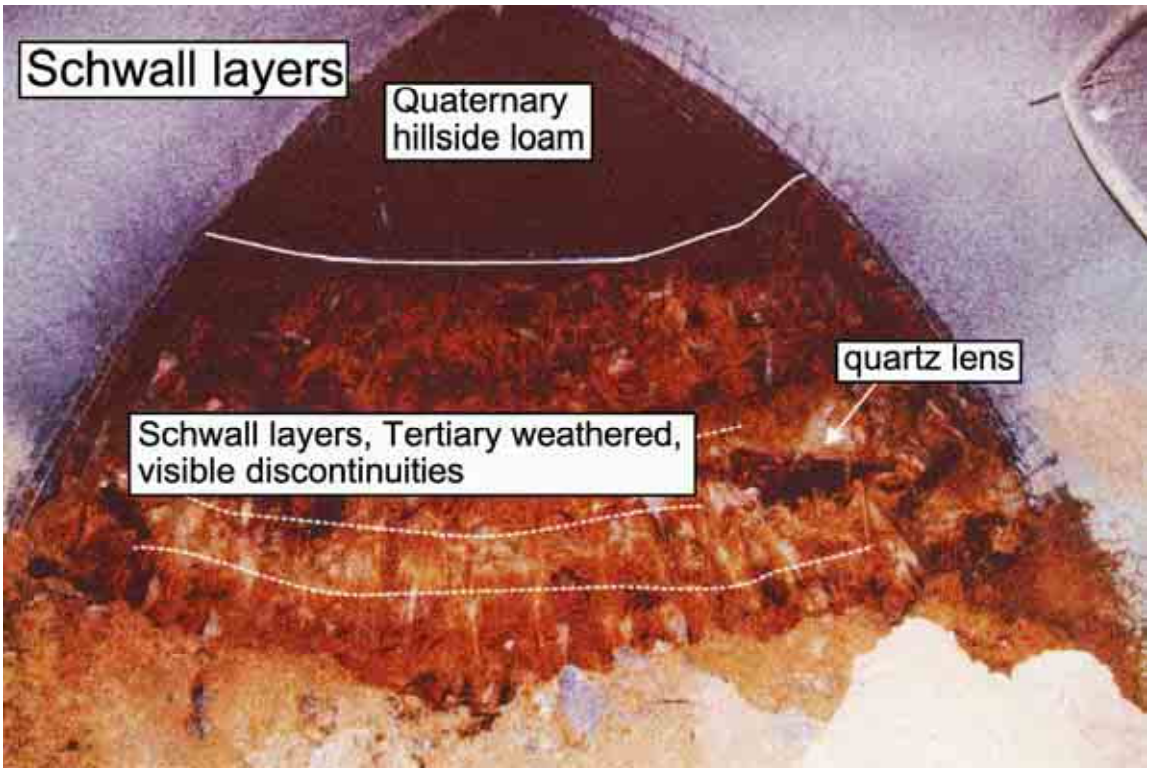

Fig. 5.48: Deeply weathered, decomposed slate of the Schwall layers

The bedding planes and foliation discontinuities strike in NE-SW direction, which is typical for the Rhine schist mountains, and dip mostly steeply at 60 to 90° in varying directions. In combination with two discontinuity sets usually an orthogonal discontinuity fabric exists.

To the south of the Taunus ridge upthrust, in the middle and the southern part of the tunnel, the rock mass is mostly unweathered. Individual steep bedding-parallel fault zones here exist (Fig. 5.45b).

From the northern tunnel portal to about km 142+500 the groundwater table follows roughly the course of the ground surface at a depth of 5 to 25 m. In the southern tunnel section it drops to approx. 50 m below the ground surface due to a drinking water supply facility. This level is still up to approx. 40 m above the tunnel roof, however (Fig. 5.45b).

The seasonal variations in the groundwater table amount to up to 10 m. The groundwater table shown in the longitudinal section (Fig. 5.45b) is based on the highest groundwater levels measured in the boreholes equipped as observation wells.

5.3.4 Excavation and support

In the approx. 350 m long section in which the tunnel's cross-section is partially or completely located in the weathered Schwall layers, a sidewall adit heading was planned according to excavation classes 7A-U-0 and 7A-U-1, respectively (Fig. 5.49, see DGGT, 1995: Table 1). The two excavation classes differ with regard to the unsupported round lengths, the spacing of the steel sets and the number of anchors per m^2 (Fig. 5.49).

In both excavation classes the shotcrete membrane is reinforced by two layers of steel fabric mats Q295. As mentioned above, the thickness of the shotcrete membrane of 35 to 45 cm is unusually strong. The inside shotcrete membrane of the sidewall adits was to be carried out with a thickness of at least 30 cm. Further, a tunnel face support with plain shotcrete ($t \geq 7$ cm) and an advancing support with spiles were planned (Fig. 5.49).

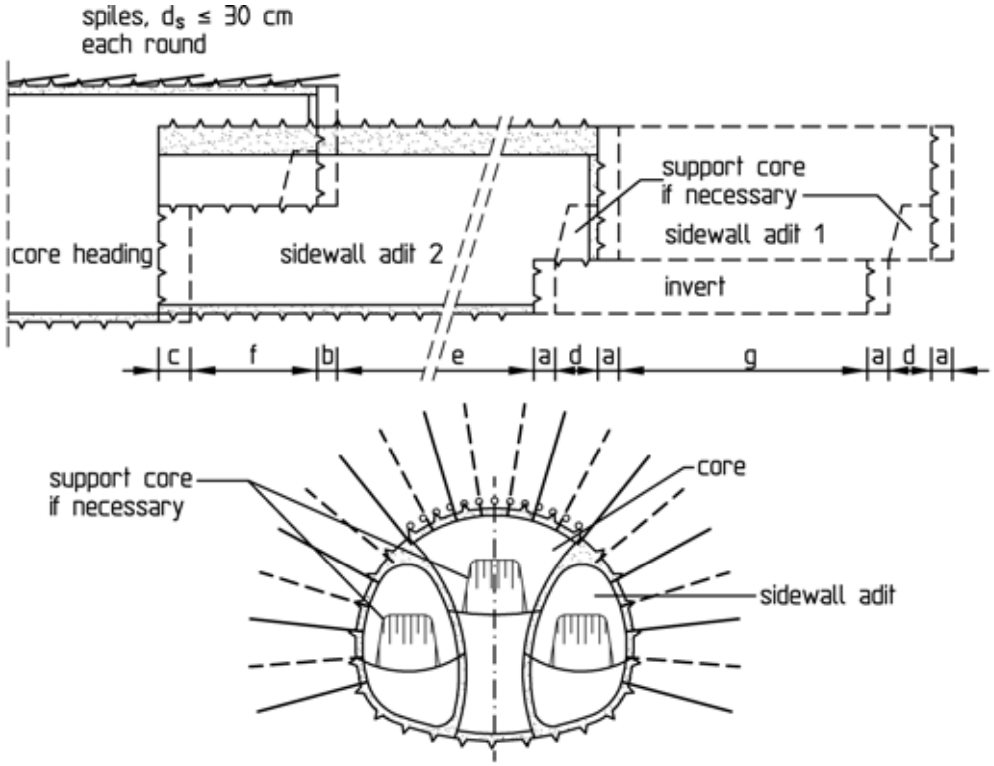

excavation class		7A-U-0	7A-U-1
excavation method		tunnel excavator	tunnel excavator
unsupported round length	sidewall adit (a)	0.61 – 0.80 m	0.81 – 1.20 m
	core/crown (b)	0.61 – 0.80 m	0.81 – 1.20 m
	core/invert (c)	≤ 3.20 m	≤ 5.00 m
tunnel face support		≧ 7 cm shotcrete possibly support core tunnel face anchoring if necessary	≧ 7 cm shotcrete possibly support core tunnel face anchoring if necessary
advance support		spiles (cemented or driven) depending on the encountered rock conditions $\Phi \geq 25$ mm, $L \geq 3.0$ m, $d_s \leq 30$ cm support length in the rock mass ≧ 1.0 m	spiles (cemented or driven) depending on the encountered rock conditions $\Phi \geq 25$ mm, $L \geq 3.0$ m, $d_s \leq 30$ cm support length in the rock mass ≧ 1.0 m
shotcrete B25	vault sidewall, stem	35 – 45 cm min. 30 cm	35 – 45 cm min. 30 cm
reinforcement	vault sidewall, stem	at least Q295, inside and outside 1 layer each	at least Q295, inside and outside 1 layer each
systematic anchoring vault sidewall, inside		l_A = 4 m, 1 pc./2 m² l_A = 4 m, 1 pc./1 m²	l_A = 4 m, 1 pc./2.5 m² l_A = 4 m, 1 pc./1.5 m²
steel sets		d = 0.61 – 0.80 m	d = 0.81 – 1.20 m
trailing distance	sidewall adits: crown – invert (d)	2 a ≦ d ≦ 5 a	2 a ≦ d ≦ 5 a
	sidewall adit 2 (invert) – core (crown) (e)	10 m ≦ e ≦ 20 m	10 m ≦ e ≦ 20 m
	core: crown – invert (f)	f ≦ 10 m	f ≦ 10 m
	sidewall adit 1 – sidewall adit 2 (g)	10 m ≦ g ≦ 20 m	10 m ≦ g ≦ 20 m

Fig. 5.49: Excavation and support, excavation classes 7A-U-0 and 7A-U-1

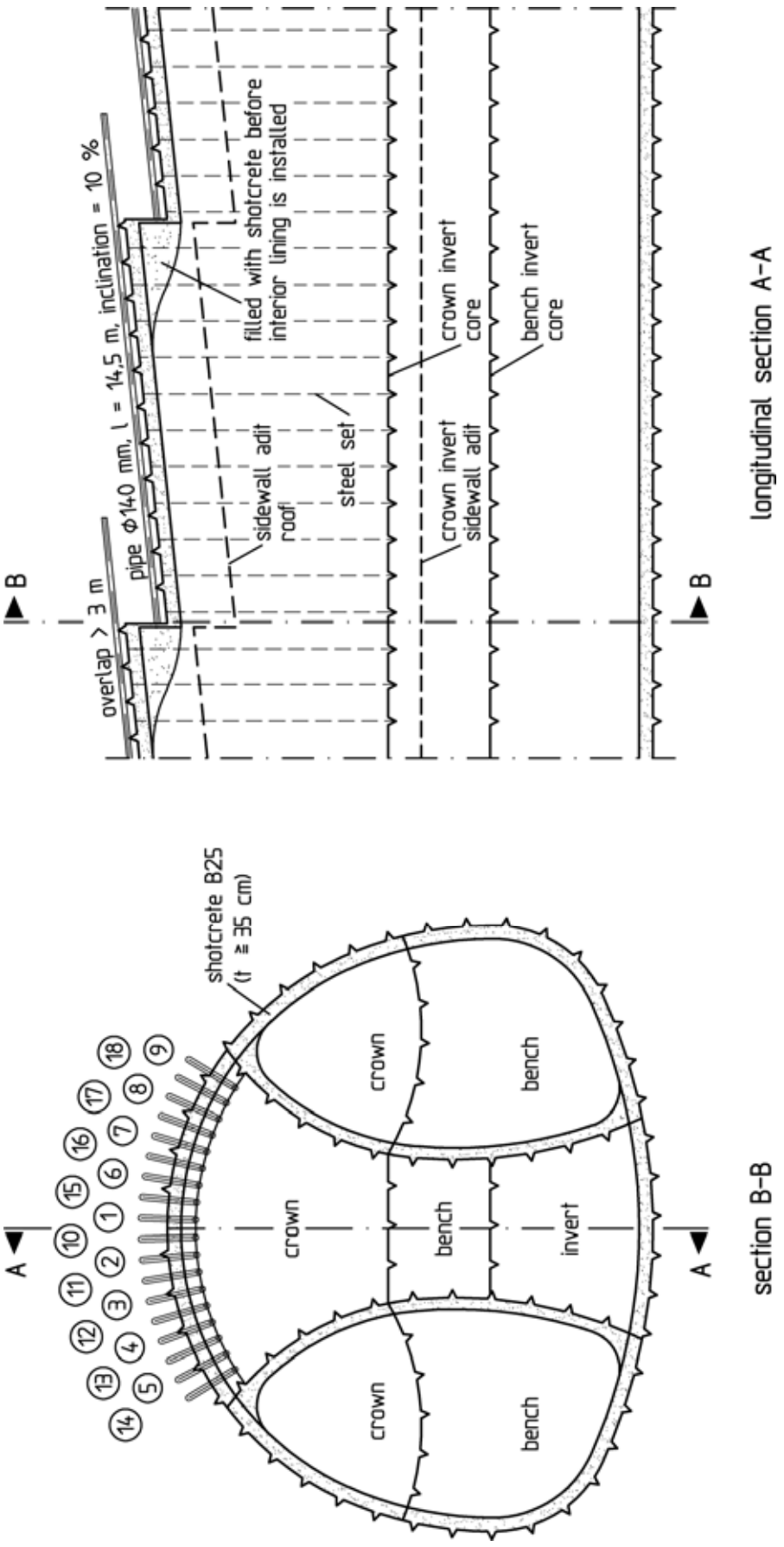

Fig. 5.50: Pipe umbrella for the undercrossing of freeway A3

In the area of the undercrossing of the freeway the workspace for the tunnel excavation was to be additionally supported by pipe umbrellas made of 14.5 m long pipes with an inclination of approx. 10 % and an overlap of > 3 m. The pipe umbrellas were to be constructed from niches (Fig. 5.50).

5.3.5 Three-dimensional stability analyses

Calibration of the analysis model (analysis cross-section AC 1)

In the course of the final design for the tunnel driven by sidewall adit excavation three-dimensional stability analyses were carried out with the program system FEST03 (Wittke, 2000).

A total of four cases were investigated (cases A, B, C and D, see Table 5.2).

Case	H_o [m]	Slate, decomposed			Temporary support of the sidewall adit invert	Tunnel face support	Unloading modulus
		E [MN/m²]	φ [°]	c [kN/m²]			
A	17	20	25	5	no	-	-
B	25	"	"	"	yes	crown: p = 0.04 MN/m²	E_U = 3E
C	"	"	"	"	no	"	"
D	"	40	27.5	10	yes	"	"

Table 5.2: Niedernhausen Tunnel, three-dimensional analyses of the sidewall adit heading

To calibrate the analysis model and to verify the soil and rock mechanical parameters the analyses were to be based upon, the vertical and horizontal ground displacements measured at measuring cross-section MC 2 (Fig. 5.51) during the sidewall adit heading were back-analyzed first. MC 2 (analysis cross-section AC 1) is located at km 141+580 approx. 20 m in front of the undercrossing of freeway A3 (Fig. 5.51). To record the vertical and horizontal displacements resulting from the heading, leveling points were set up at the ground surface and 3 multiple extensometers as well as 2 inclinometers were installed beside and above the tunnel. Zero readings were taken sufficiently ahead of the excavation. The ar-

rangement of these measuring devices is shown in Fig. 5.52 together with the tunnel's cross-section.

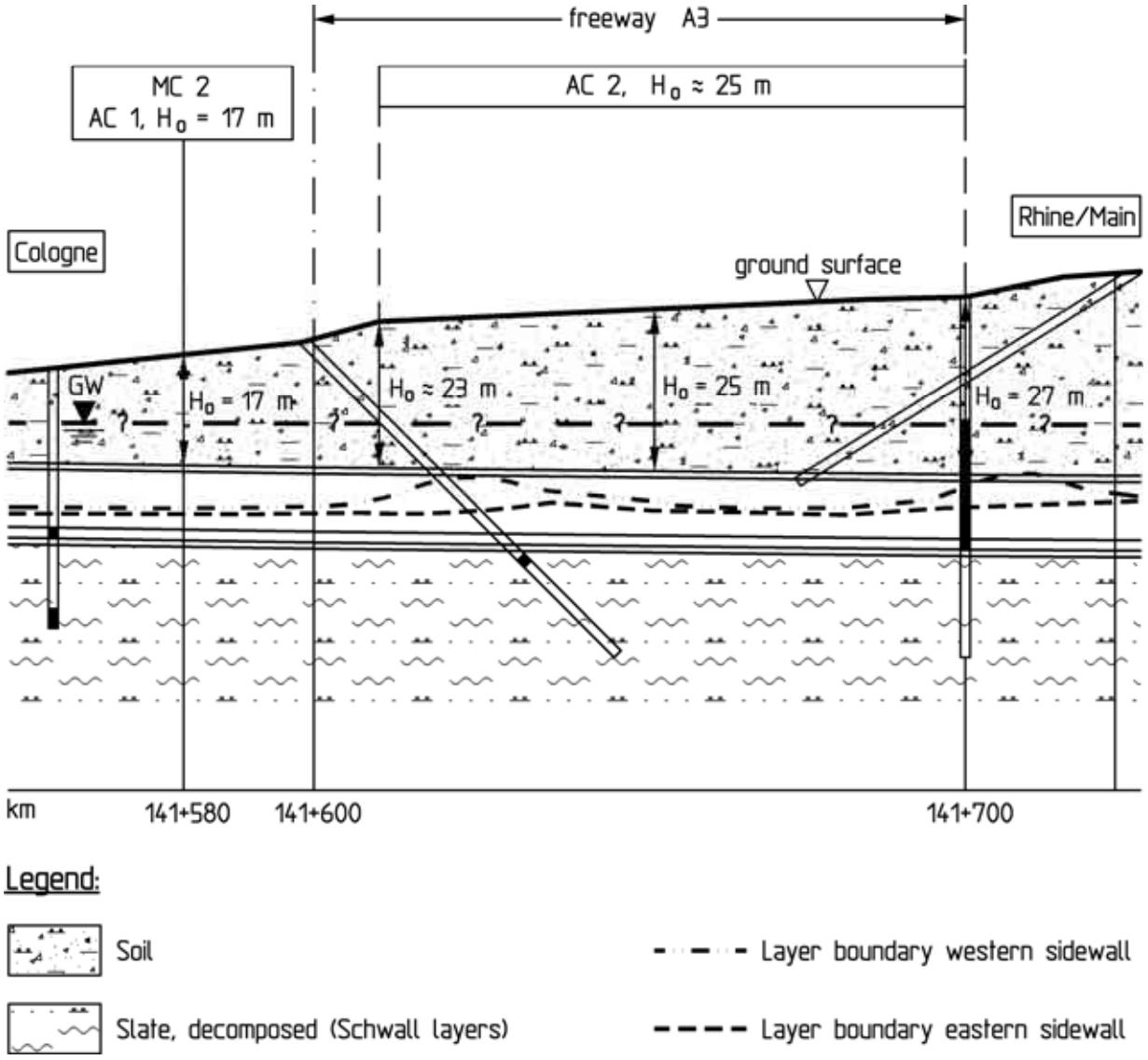

Fig. 5.51: Longitudinal section, location of measuring cross-section MC 2 and analysis cross-sections AC 1 and AC 2

Fig. 5.53 shows the three-dimensional FE-mesh for the back-analysis of the measured displacements together with its main dimensions, the boundary conditions and the modeled stratigraphy. To keep the computing time within justifiable bounds, symmetric ground conditions as well as a horizontal ground surface and horizontal layers were assumed. It was thus sufficient to model one half of the tunnel's cross-section and the surrounding ground.

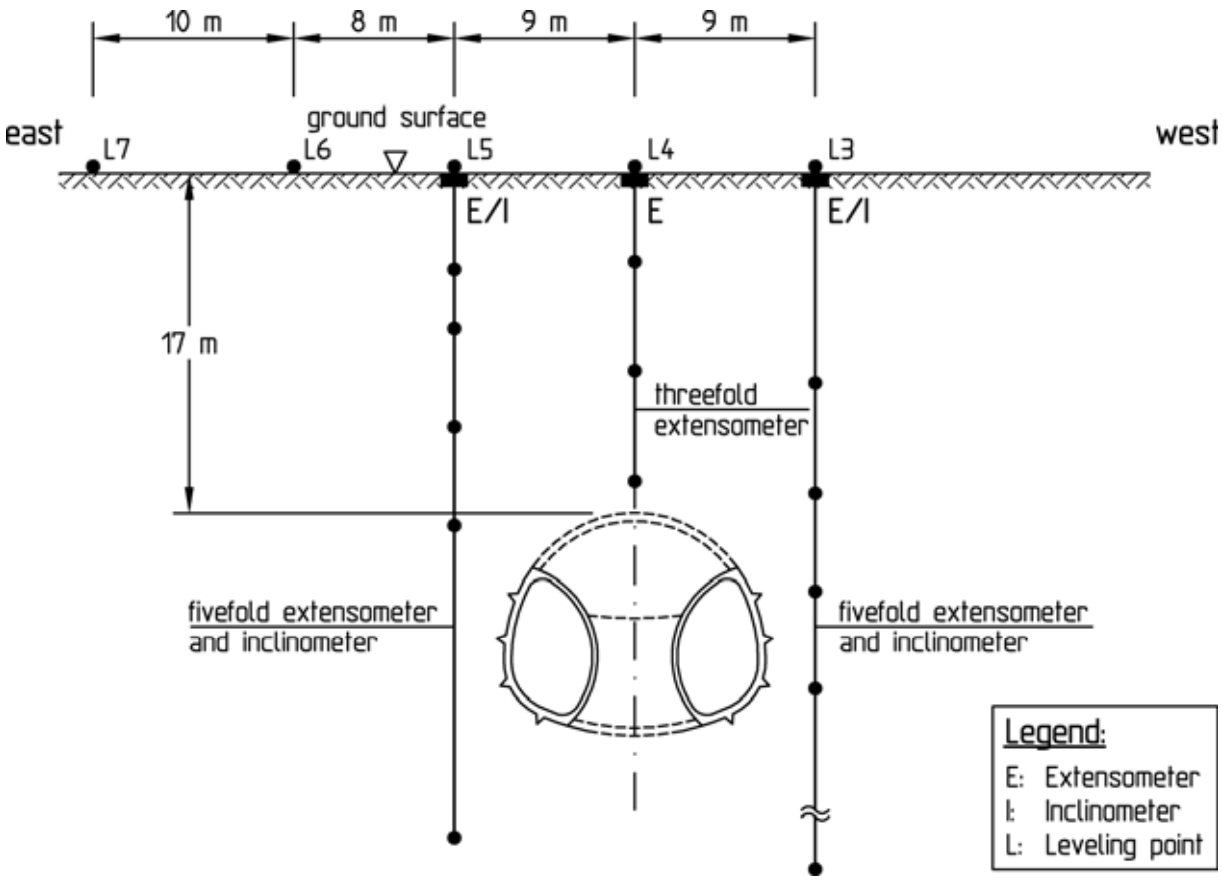

Fig. 5.52: MC 2 (km 141+580), measuring devices

According to the assumed symmetry the two sidewall adits are simulated as being excavated parallel in time in the analyses. In reality the western sidewall adit heading ran ahead of the eastern one by 10 to 20 m (g in Fig. 5.49). The influence of the simplified simulation in the analysis on the final result is small, however.

The overburden in the area of measuring cross-section MC 2 amounts approx. 17 m. The boundary between the soil and the strongly weathered rock mass was modeled in the FE-mesh at about half the height of the tunnel's cross-section.

The characteristic parameters of the soil include a Young's modulus of 10 MN/m^2 and shear parameters of $\varphi' = 25°$ and $c' = 7.5$ kN/m^2. For the weathered rock mass, the corresponding values are E = 20 MN/m^2 to 40 MN/m^2, $\varphi = 25°$ to 27.5° and c = 5 kN/m^2 to 10 kN/m^2 (Fig. 5.53). Thus both layers differ essentially in their deformability and only negligibly with respect to their shear strength.

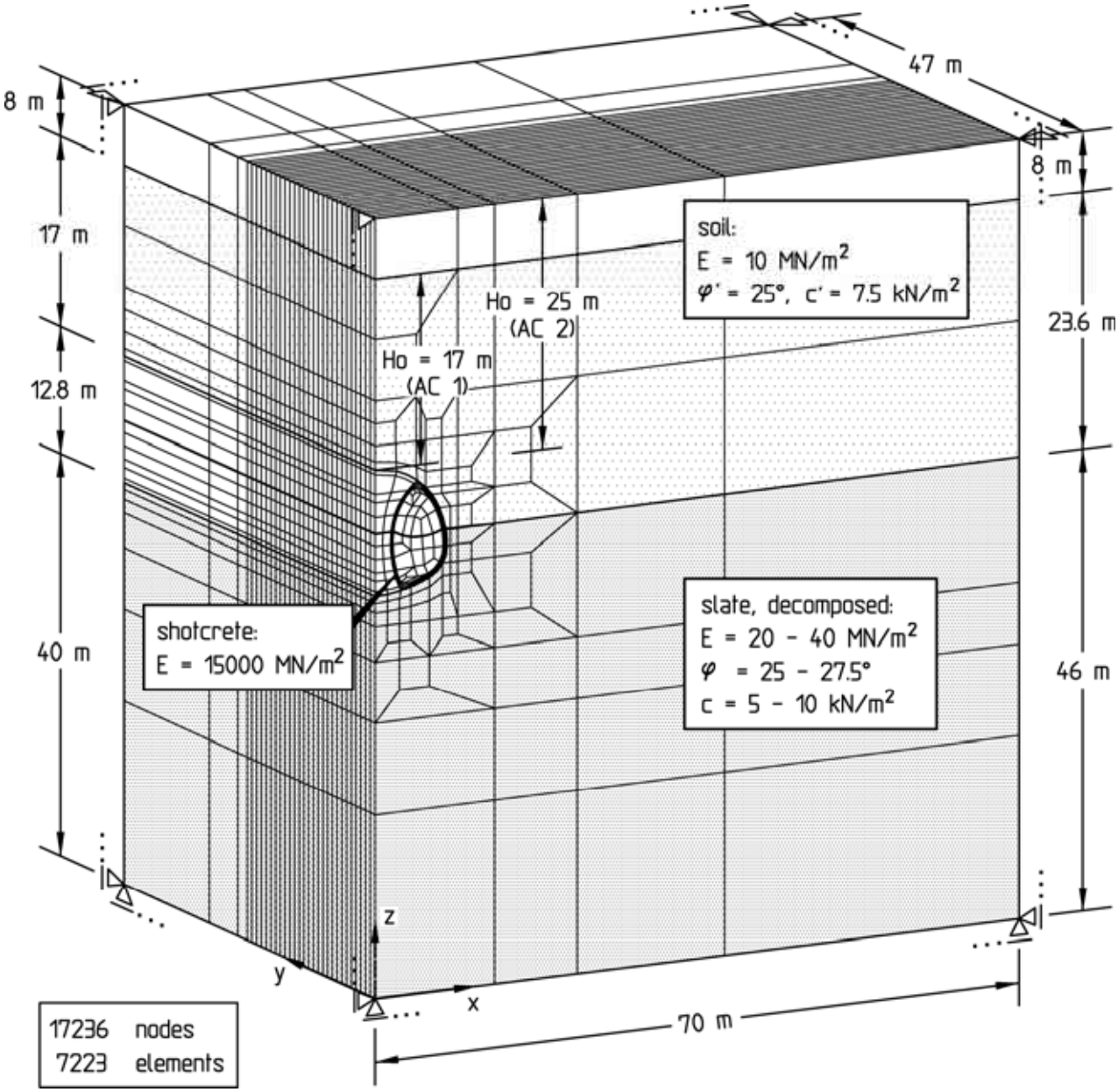

Fig. 5.53: Computation section, FE-mesh, boundary conditions, ground profile and parameters for the three-dimensional analyses (AC 1 and AC 2)

The outside shotcrete membrane was constructed 45 cm thick in the course of the sidewall adit heading, and it is modeled accordingly (Fig. 5.54). The shotcrete membrane of the inside walls of the sidewall adits is 30 cm thick. The shotcrete support of the temporary crown invert of the sidewall adits shown in Fig. 5.54 was not installed in the area of MC 2. It was therefore not modeled in analysis case A for the back-analysis of the measured displacements (see Table 5.2).

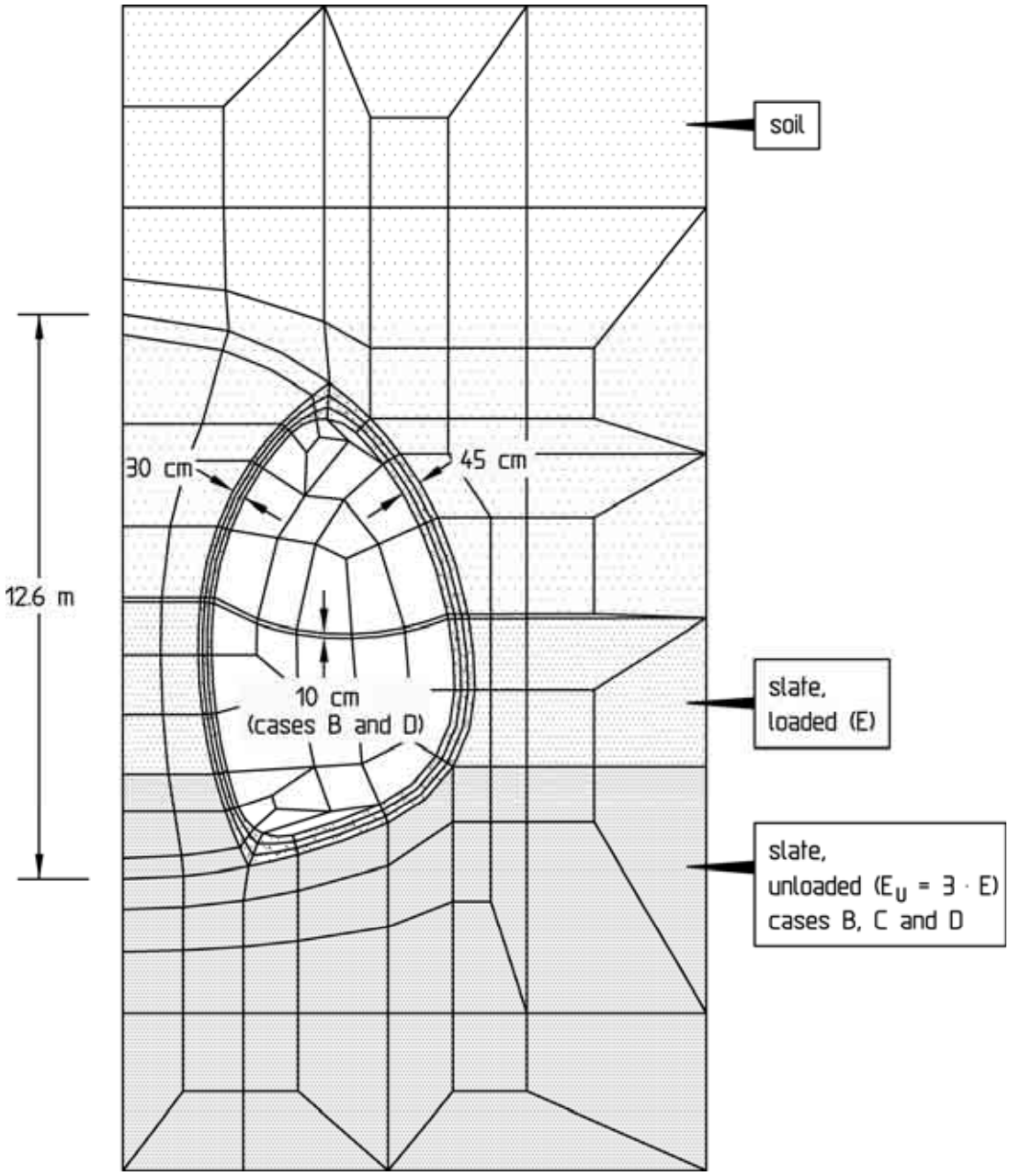

Fig. 5.54: FE-mesh, detail

The computation sequence of the analyses comprising a total of 36 computation steps is shown schematically in Fig. 5.55. The analysis of the in-situ state (1st computation step) is followed in the 2nd computation step by the excavation of a 23 m long crown section of the sidewall adits together with an invert section trailing by 2 m. The 2nd computation step is the starting stage for the actual heading simulation carried out in computation steps 4 to 36 according to the iteration technique described in detail in Wittke (2000).

1st computation step: in-situ state

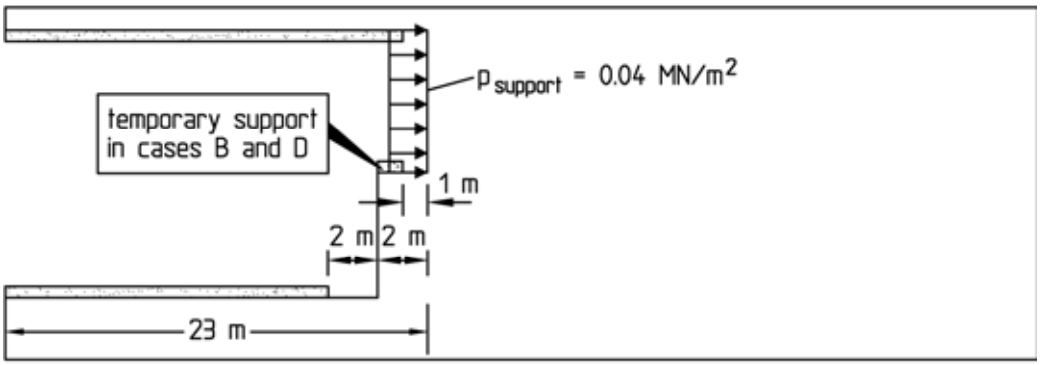

2nd computation step: excavation of 23 m of the crown and 21 m of the invert of the sidewall adit, shotcrete support up to 1 m (crown) and 2 m (invert) behind the tunnel face, tunnel face support [1] (starting stage)

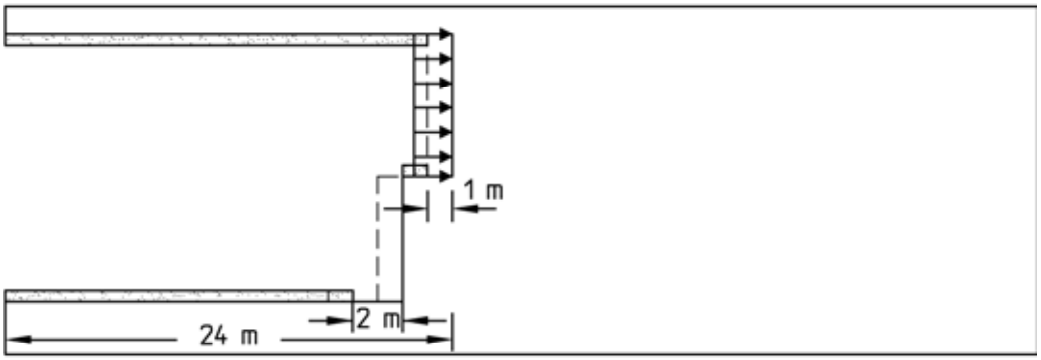

3rd computation step: round of 1 m each in crown and invert of the sidewall adit, shotcrete support up to 1 m (crown) and 2 m (invert) behind the tunnel face, tunnel face support [1]

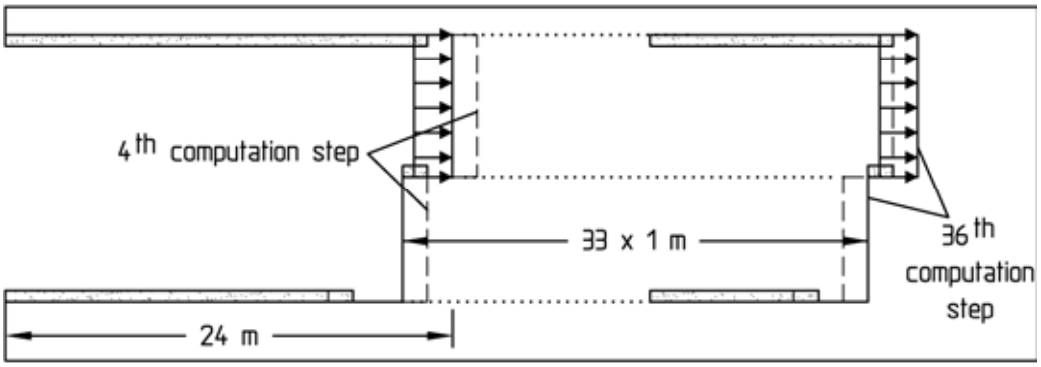

4th bis 36th computation step: heading simulation by moving the computation section, round length 1 m in crown and invert, shotcrete support up to 1 m (crown) and 2 m (invert) behind the tunnel face, tunnel face support [1]

[1] cases B, C and D (AC 2)

Fig. 5.55: Computation steps for the simulation of the sidewall adit heading

The basic idea of this iterative analysis is that the computation section moves with the heading or with the simulation of each round, respectively. With increasing number of iterations the constraints are reduced which develop in the starting stage due to the restraint of the displacements in longitudinal tunnel direction. In this way the computed displacements approach the actual displacements of the excavation surface at the time of the installation of the shotcrete membrane. In this manner the loading of the shotcrete membrane and the deformations due to the heading can be realistically determined.

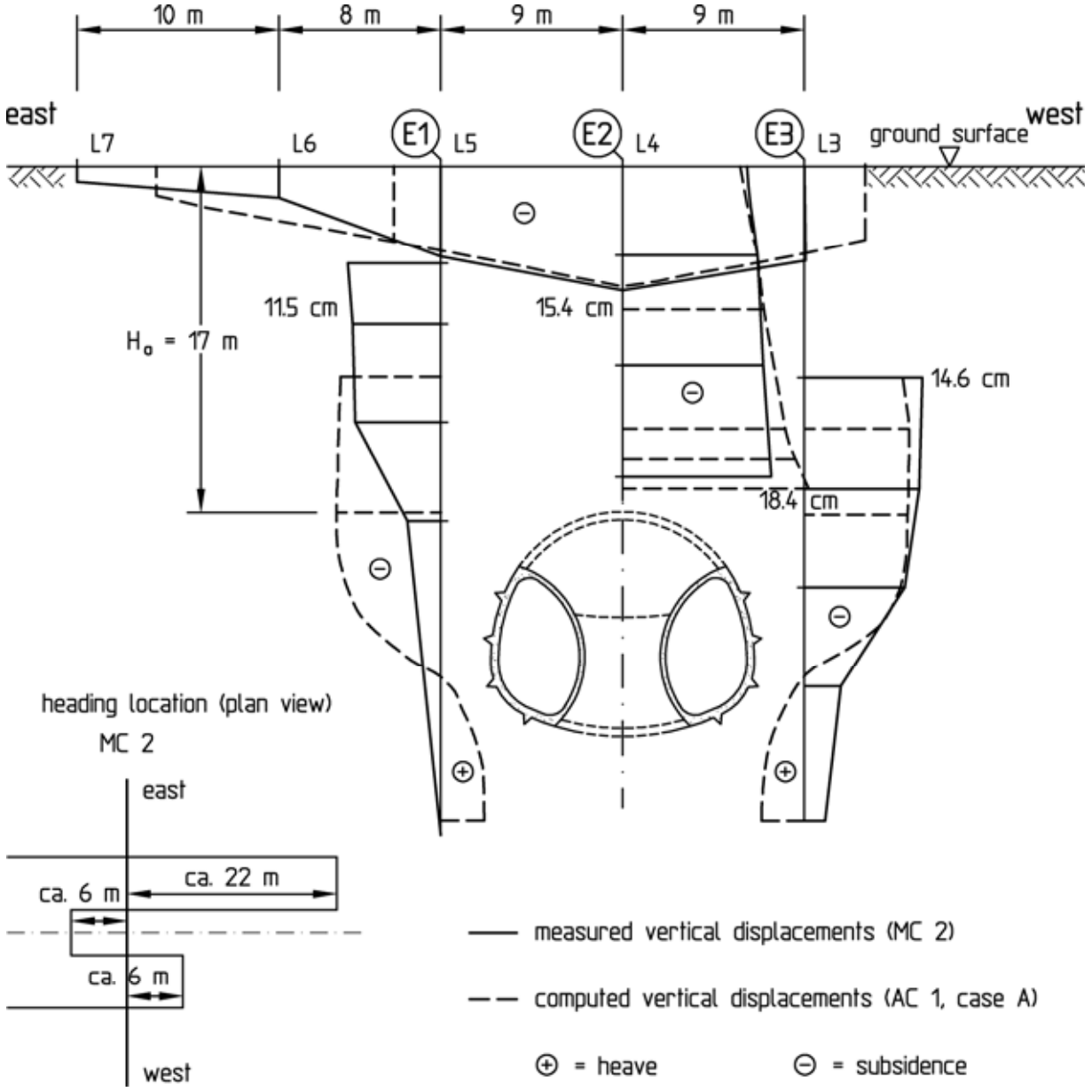

Fig. 5.56: Sidewall adit heading, comparison of measured and computed vertical displacements

According to excavation class 7A-U-1 applied in construction (see Fig. 5.49) a round length of 1 m is simulated. The distance between the shotcrete support and the temporary tunnel face amounts to 1 m in the crown and 2 m in the invert. The closing of the invert of the sidewall adits is thus completed in each case at a distance of 4 m from the crown face (Fig. 5.55).

The tunnel face support using shotcrete is not taken into account.

The vertical and horizontal displacements in the rock mass and on the ground surface computed in case A for the sidewall adit heading are compared with the measurement results in Fig. 5.56 and 5.57. The computed displacements were taken from the plane located 14 m behind the crown face in the 36th computation step. This distance represents approximately the average of the distances of MC 2 to the crown faces of the two sidewall adit headings at the time of the measurement (see Fig. 5.56 and 5.57).

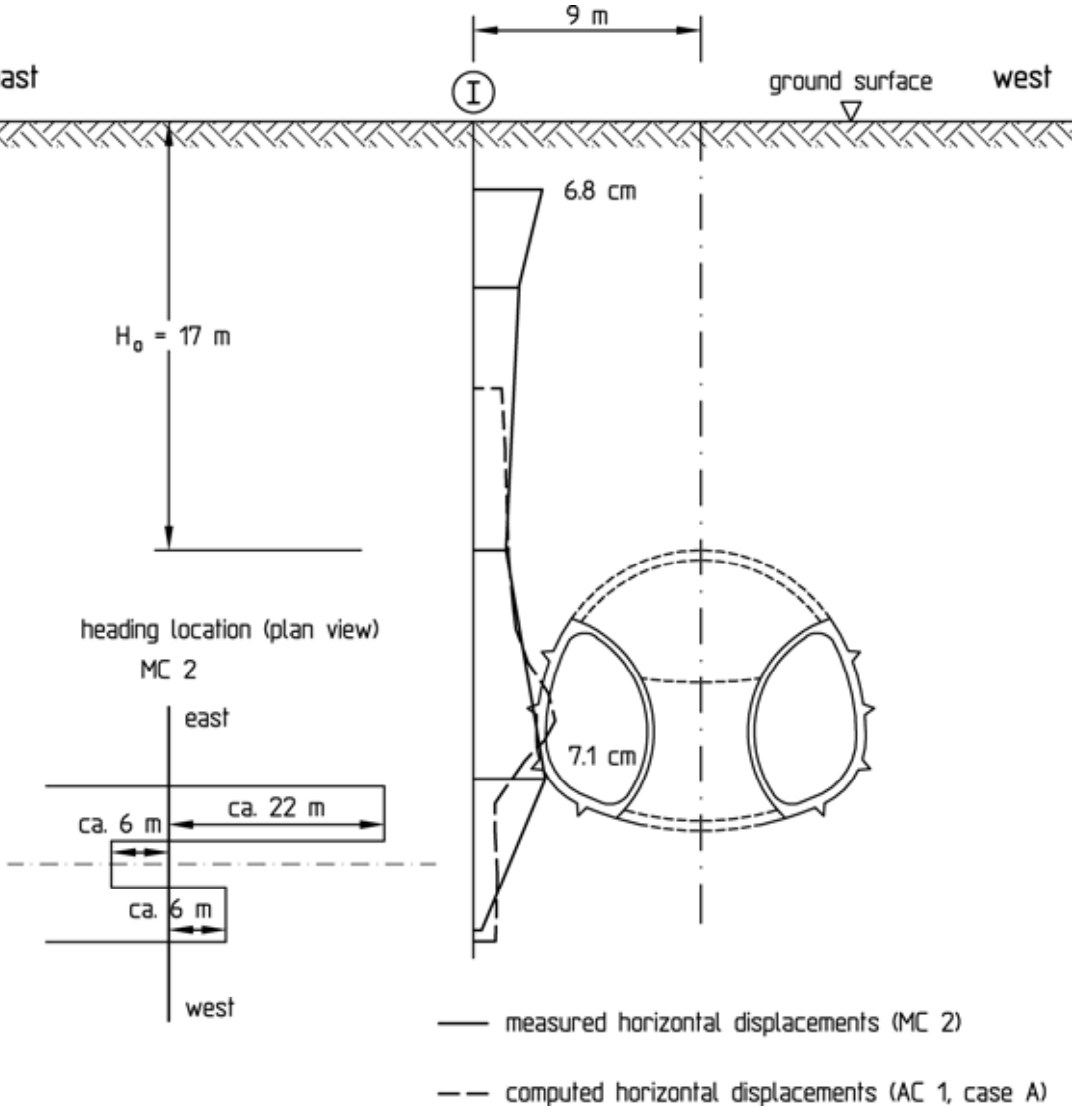

Fig. 5.57: Sidewall adit heading, comparison of measured and computed horizontal displacements

A comparatively good agreement results between the measured and the computed displacements (see Fig. 5.56 and 5.57). It is only in the computed vertical displacements that heave show at the level of the tunnel's invert and below which was not measured. According to experience this is because in the FE-analysis the same modulus was specified for the areas unloaded by the excavation as for the loaded areas above and beside the tunnel. The modulus relevant for unloading is generally markedly higher than the one for loading. In the stability analyses for the sidewall adit heading in the area of the undercrossing of the freeway (cases B, C and D, see Table 5.2), which are described in the following, an unloading modulus E_U equal to three times the loading modulus was therefore specified below the tunnel's invert level (see Fig. 5.54).

Three-dimensional analyses of the sidewall adit heading (analysis cross-section AC 2)

In the area of the undercrossing of the freeway (analysis cross-section AC 2) the overburden height varies between 23 and 27 m (see Fig. 5.51). The stability analyses for this area were correspondingly based on an average overburden of 25 m (see Fig. 5.53). The investigation included cases B, C and D (see Table 5.2). Differing from case A, an unloading modulus E_U = 3 E was specified below the invert in these analyses, as already mentioned (see Fig. 5.54), together with a crown face support with p = 0.04 MN/m^2 (see Fig. 5.55 and Table 5.2). In this way the supporting effect of horizontal cemented anchors installed in advance of the crown face was modeled.

In cases B and D a shotcrete support of the temporary crown invert (t = 10 cm, see Fig. 5.54) is accounted for. In case C the temporary crown invert support is not taken into account. In case D the specified shear strength of the decomposed slate is higher than in cases A, B and C (see Table 5.2).

In Fig. 5.58 the stress resultants are shown as a function of the distance from the tunnel face and from the boundary of the mesh for the example of the normal thrust and the moment in the roof. The broken lines in Fig. 5.58 show the extrapolated course of the stress resultants which would ensue without the influence of the boundaries. The stress resultants in the section located 16.5 m behind the tunnel face (dimensioning section) can be regarded as

decisive and taken as a basis for the design of the shotcrete membrane.

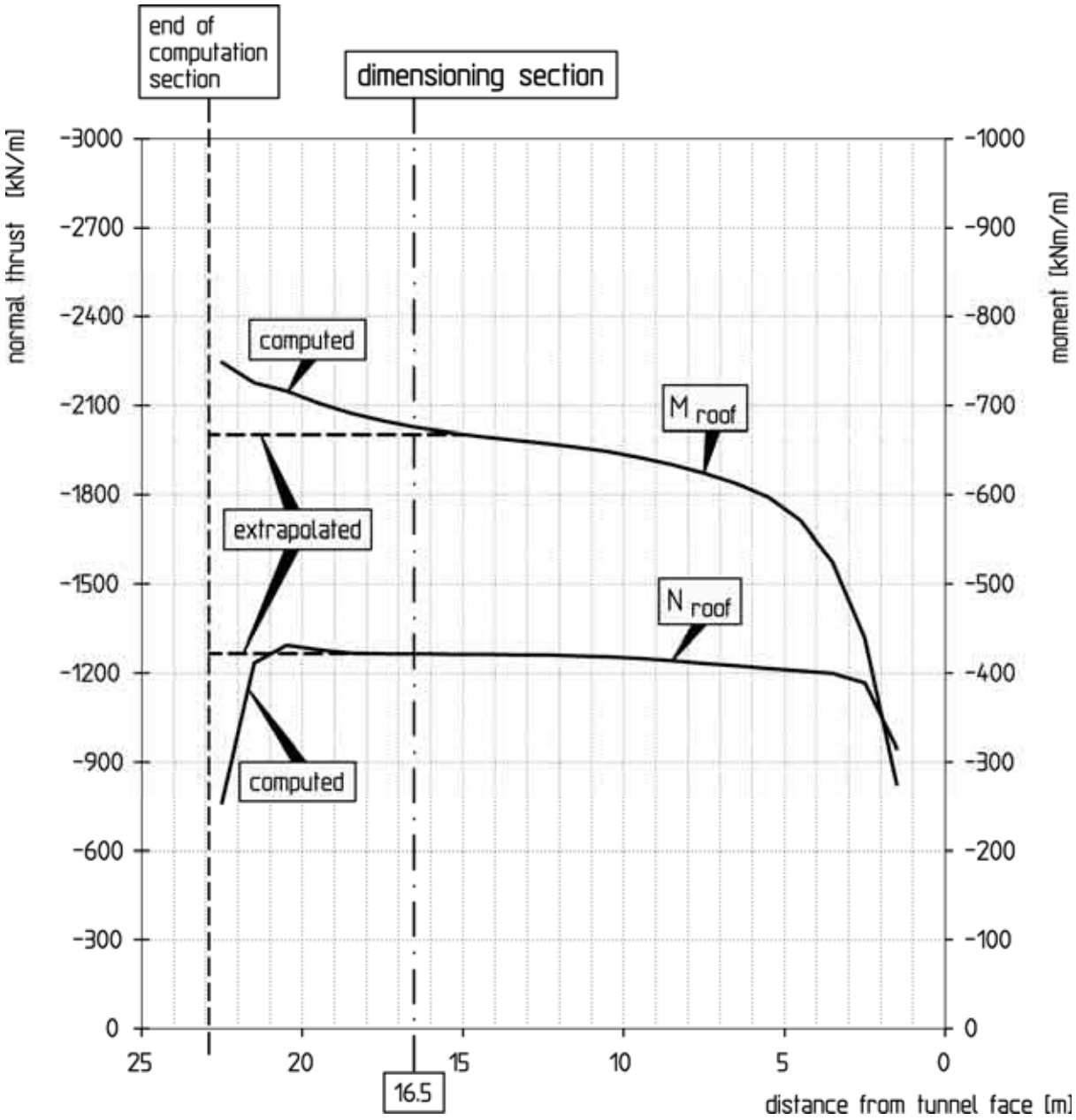

Fig. 5.58: Sidewall adit, stress resultants vs. distance from the crown face, case B, 36th computation step

Fig. 5.59 shows the stress resultants M, N and S in the dimensioning section for case B. Very large bending moments M occur in the areas of the small radii of curvature of 1.0 m at the roof and at the transition from the inside wall of the sidewall adit to the invert (see Fig. 5.46). It was assumed for the design of the shotcrete membrane that the computed bending moments would not develop in reality to their full extent since the shotcrete membrane is

installed in several working steps. The construction joints in the areas mentioned above enable the formation of links which result in a reduction of the bending moments but not of the normal thrust. In agreement with the parties concerned the calculated bending moments were reduced for the design to 65 %.

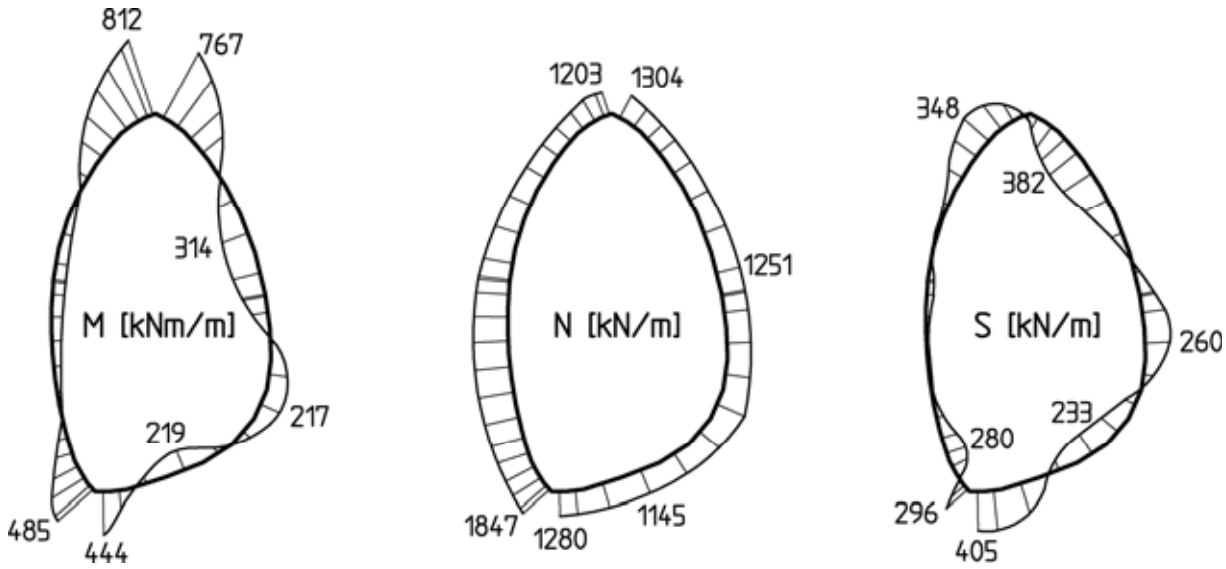

Fig. 5.59: Sidewall adit, stress resultants in the shotcrete membrane, dimensioning section, case B, 36th computation step

Fig. 5.60 shows the statically required reinforcement cross-sections for bending and normal thrust determined for cases B, C and D. In addition to the reduction of the moments already mentioned, the design was based on a B25 concrete grade, a BSt 500 steel grade and a distance of the reinforcement from the edge of t_1 = 4 cm. In the roof (sections 1 and 2) and at the transition from the outside wall of the sidewall adit to the invert (section 3) statically required reinforcement cross-sections are computed for case B which are not covered by the planned reinforcement (Q295 inside and outside) and require supplementary reinforcement. In the remaining area (section 4), no reinforcement is required for statical reasons. A minimum reinforcement of Q295 inside and outside suffices here. For case C, in which a support of the temporary crown invert is not accounted for, even larger statically required reinforcement cross-sections result in sections 1 to 3 than for case B (see Fig. 5.60). For case D, in which a higher Young's modulus and a higher shear strength are specified for the decomposed slate, statically required reinforcement cross-sections

larger than the minimum reinforcement only ensue in the roof (sections 1 and 2, Fig. 5.60).

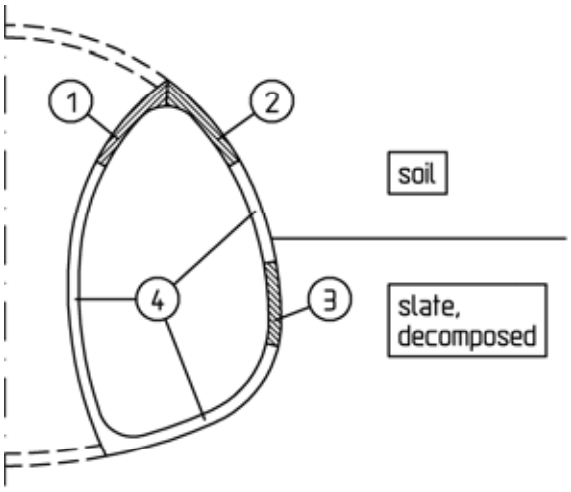

section		req. a_s [cm²/m] [1]		
		case B	case C	case D
1	outside	17.3	17.9	15.1
	inside	12.4	17.2	11.7
2	outside	14.0	34.9	12.2
	inside	0 [2]	4.6	0 [2]
3	outside	14.3	14.3	0 [2]
	inside	14.3	14.3	0 [2]
4	outside	0 [2]	0 [2]	0 [2]
	inside	0 [2]	0 [2]	0 [2]

[1] basis for design:
B25, BSt500/550, t_1 = 4 cm,
moments reduced to 65% of computed values,
safety factor: η = 1.75

[2] req. a_s = minimum reinforcement (Q295 inside and outside)

Fig. 5.60: Sidewall adit, required reinforcement cross-sections for bending and normal thrust

As a consequence of the results of these analyses, during the undercrossing of the freeway A3 by sidewall adit excavation supplementary reinforcement was installed in the roof area and the temporary invert of the crown of the sidewall adits was supported with shotcrete. The tunnel face was additionally supported by tunnel face anchors (see Chapter 5.3.6). Further, an advancing pipe umbrella was installed for the excavation of the core (see Fig. 5.50).

Three-dimensional analyses of a crown heading with closed invert and tunnel face anchoring

Because only a low heading performance could be achieved with the sidewall adit heading due to the extensive support measures, WBI investigated in further analyses whether in the section following the undercrossing of freeway A3 also a crown heading with closed invert and tunnel face anchoring could be carried out in a stable way for the same ground conditions and higher overburden (see Fig.

5.45b; Wittke and Pierau, 2000; Wittke and Sternath, 2000). For this purpose three-dimensional FE-analyses were carried out for the computation section shown in Fig. 5.61 with the program system FEST03 (Wittke, 2000).

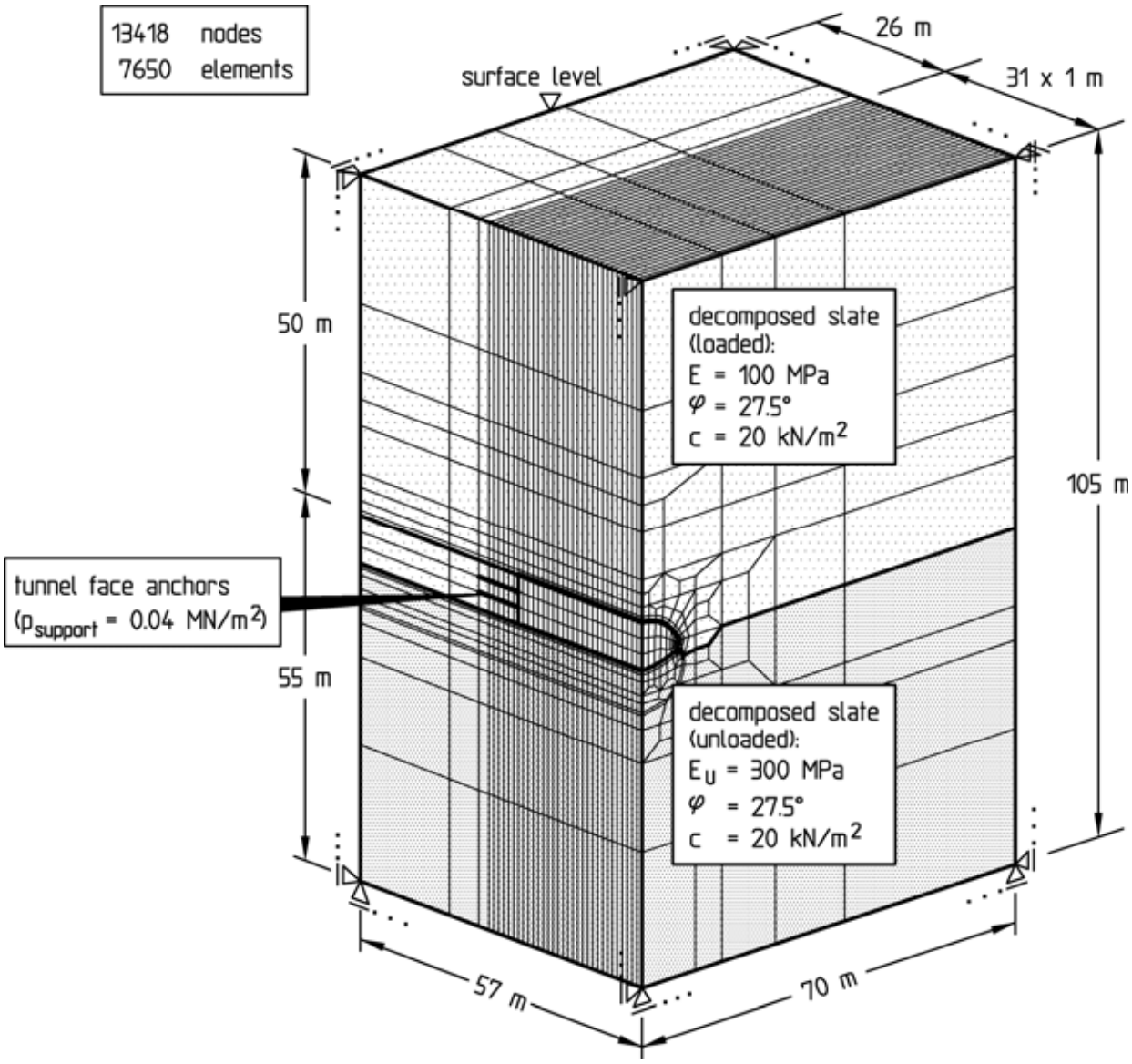

Fig. 5.61: Computation section, FE-mesh, boundary conditions and parameters for three-dimensional analyses of the crown heading with closed invert and tunnel face anchoring

The analyses were based on an overburden of 50 m. Because of the higher overburden compared to the undercrossing of freeway A3, a higher Young's modulus and a higher shear strength were assumed for the decomposed slate with $E = 100$ MN/m² and $E_U = 300$ MN/m², respectively, $\varphi = 27.5°$ and $c = 20$ kN/m² (see Table 5.2 and Fig. 5.61).

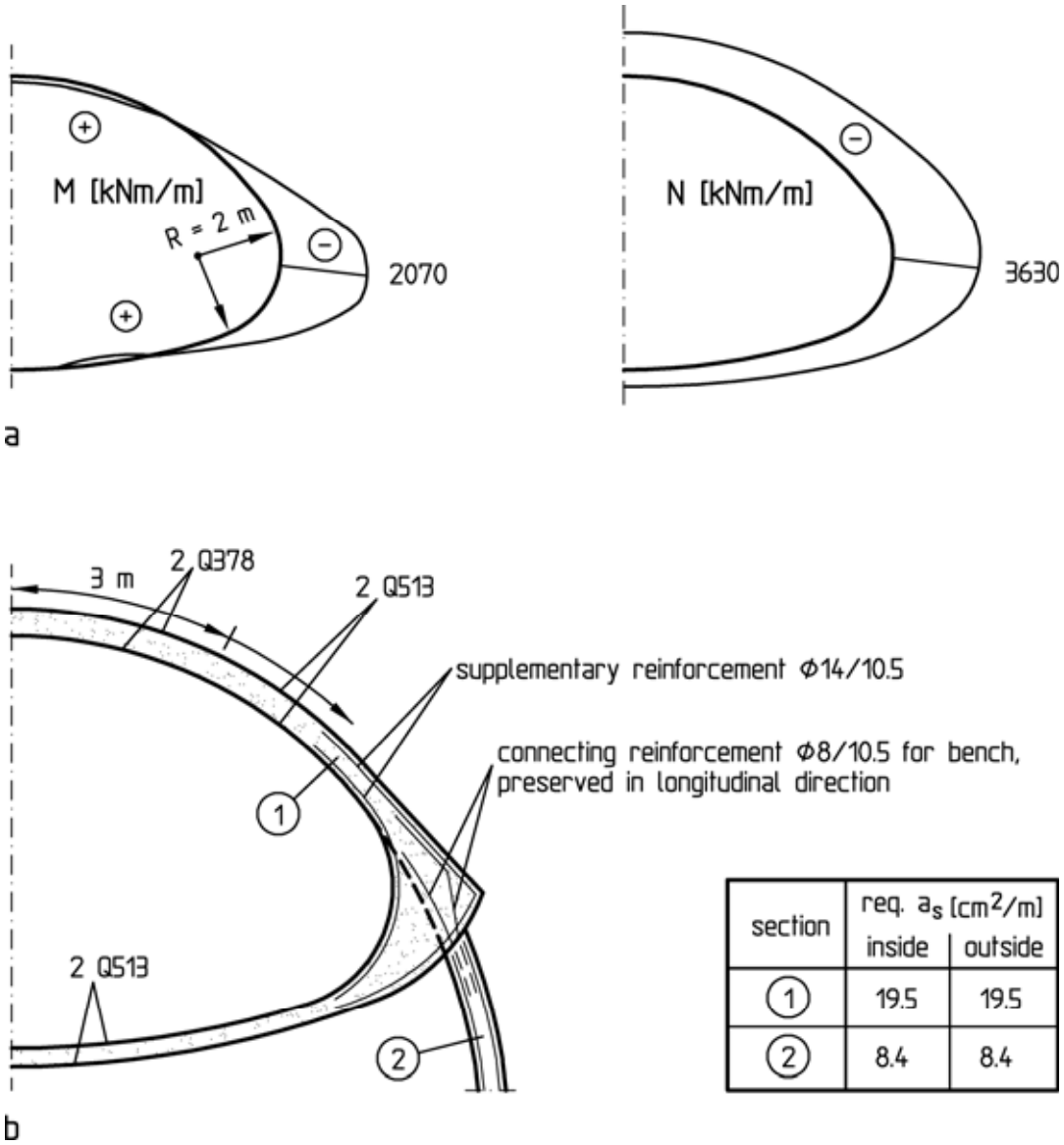

Fig. 5.62: Crown heading with closed invert and tunnel face anchoring: a) Stress resultants in the shotcrete membrane; b) required reinforcement

The computation sequence for the simulation of the crown heading was analogous to the analyses simulating the sidewall adit heading (see Fig. 5.55).

The analysis results show that the stability of the crown heading can be proved if the tunnel face is supported by advance anchoring and the support is closed soon at the invert. As in the analyses described before, the tunnel face anchors were accounted for by a support of the tunnel face with p = 0.04 MN/m^2 (see Fig. 5.61). It can be proven that the subsidence due to the heading can be kept small in this way. The computed loading of the shotcrete membrane

of the crown due to bending and normal thrust (Fig. 5.62a) reveals a high bending compression loading at the transition to the temporary invert. The reason for this is the small radius of curvature of the shotcrete membrane of only 2 m. For reasons inherent to the construction process it is often attempted to keep the radius of curvature as small as possible. For statical reasons, on the other hand, the radius of curvature should not be less than 2 m. Supplementary reinforcement cannot be dispensed with in this case, however, although the membrane is rounded according to this requirement (Fig. 5.62b).

5.3.6 Construction

The Niedernhausen Tunnel was excavated between the northern tunnel portal at chainage km 141+499 and chainage km 141+771.5 by sidewall adit heading. The mapping during tunneling showed that the layer boundary talus material / slate is located in the crown area of the tunnel's cross-section (Fig. 5.63).

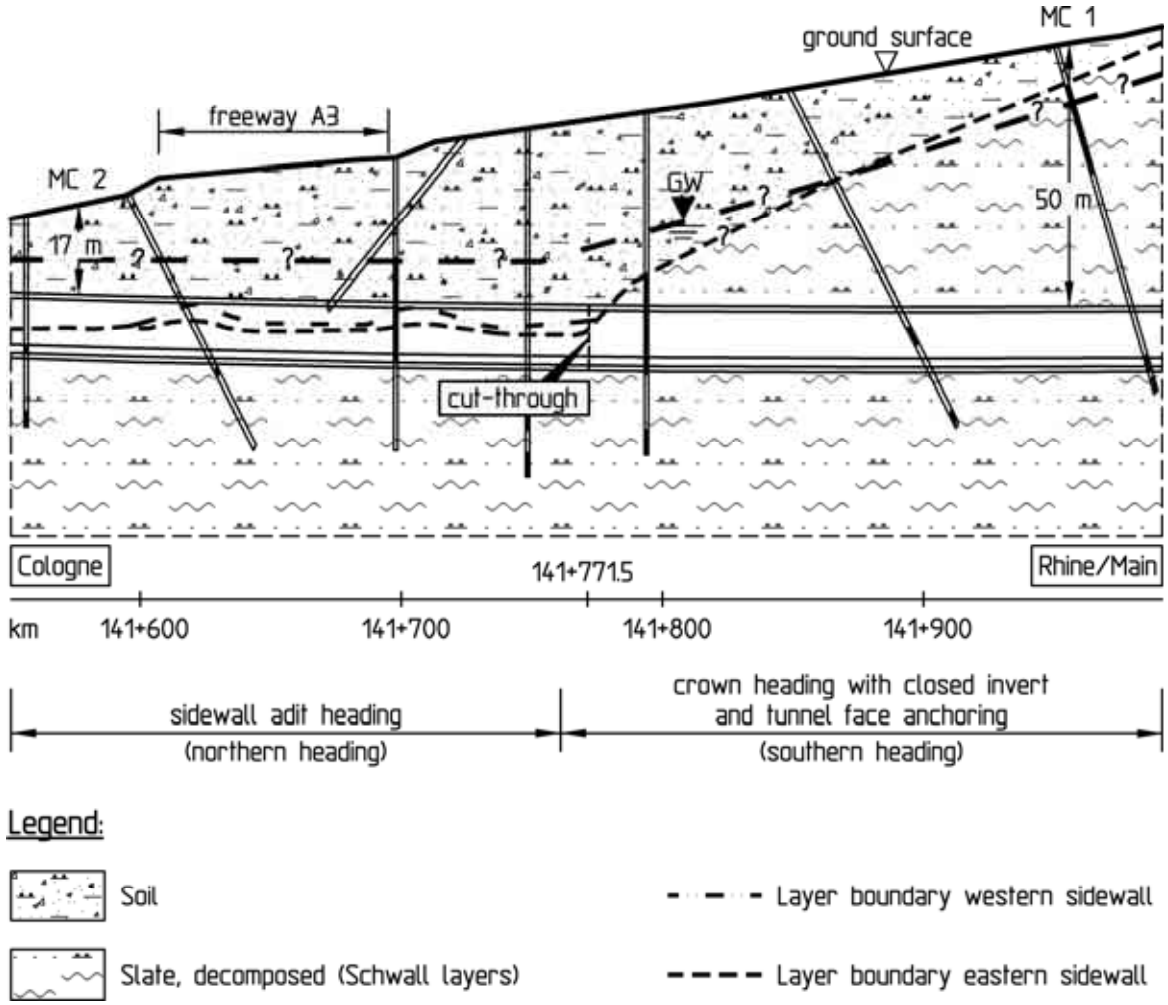

Fig. 5.63: Construction, northern section

The excavation work proved very difficult mainly because of the high groundwater level. As the closing of the invert was delayed due to the inflow of water, large subsidence resulted at the ground surface (Wittke and Sternath, 2000). To stabilize the tunnel face it was necessary to drain the ground in advance and also to support the tunnel face using shotcrete and anchors (Fig. 5.64 and 5.65). The heading performance was correspondingly low with approx. 1 m/day in the sidewall adits.

Fig. 5.64: Tunnel face support of the sidewall adit, crown

Fig. 5.65: Tunnel face support of the sidewall adit, crown and bench

Fig. 5.66 depicts the support measures during the sidewall adit heading in cross- and longitudinal section. It shows that excavation class 7A-U-1 was modified as follows with respect to the original design (see Fig. 5.49):

- Supplementary reinforcement in the sidewall adit roofs,

- support of the temporary crown inverts of the sidewall adits,
- tunnel face anchoring in the crown area of the sidewall adits,
- closed inverts in the sidewall adits at ≤ 8 m behind the crown excavation.

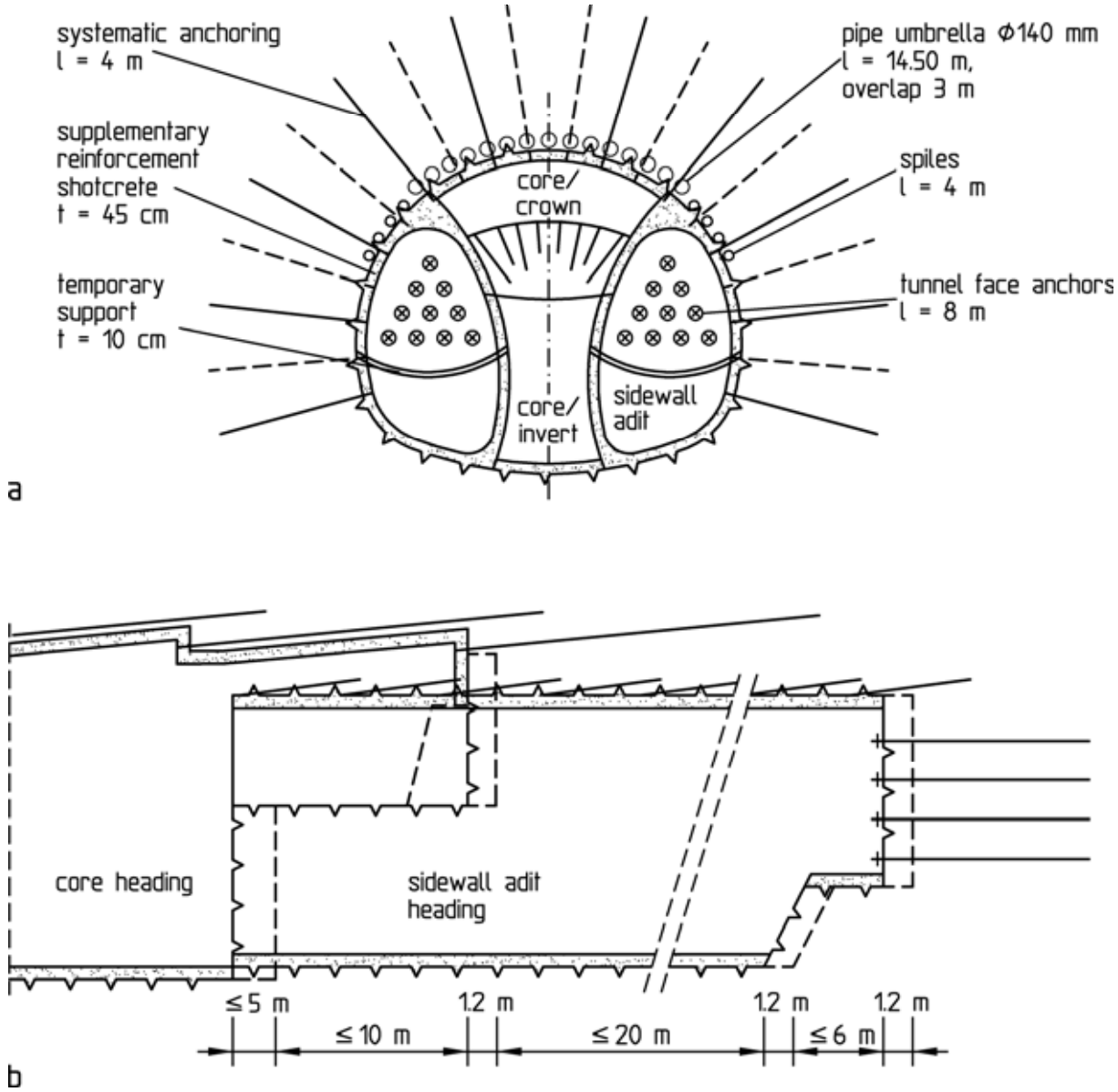

Fig. 5.66: Construction, sidewall adit heading: a) Cross-section; b) longitudinal section

Pipe umbrellas (see Fig. 5.50) were only carried out in the core area of the tunnel's cross-section during the undercrossing of the freeway A3.

For the advance drainage of the ground, at first up to 50 m long horizontal vacuum wells were constructed from the starting wall (see Fig. 5.47). In addition, vacuum lances were installed from the tunnel face during the heading. The effectiveness of the vacuum lances remained limited, however. The outflow of water in the tunnel face area could only be reduced but not be prevented in this way. The ensuing mud formation interfered considerably with the excavation.

As a consequence, the groundwater was lowered using deep vacuum wells drilled from the ground surface in advance of the excavation down to below the tunnel's invert. In the ground drained in advance it was possible to increase the heading performance markedly afterwards.

Fig. 5.67 is a photograph of the northern heading during the excavation of the core.

Fig. 5.67: Excavation of the core

From the south the tunnel was driven up to chainage km 141+771.5 by crown heading. In the section where the tunnel cross-section was located in the decomposed slate the crown was excavated up to

the cut-through with a closed invert and tunnel face anchoring (Fig. 5.63). The basis for this were the results of the FE-analyses described in Chapter 5.3.5.

Fig. 5.68 depicts the support measures carried out during the crown heading in cross- and longitudinal section. The round lengths and the excavation sequence are shown in the longitudinal section as well.

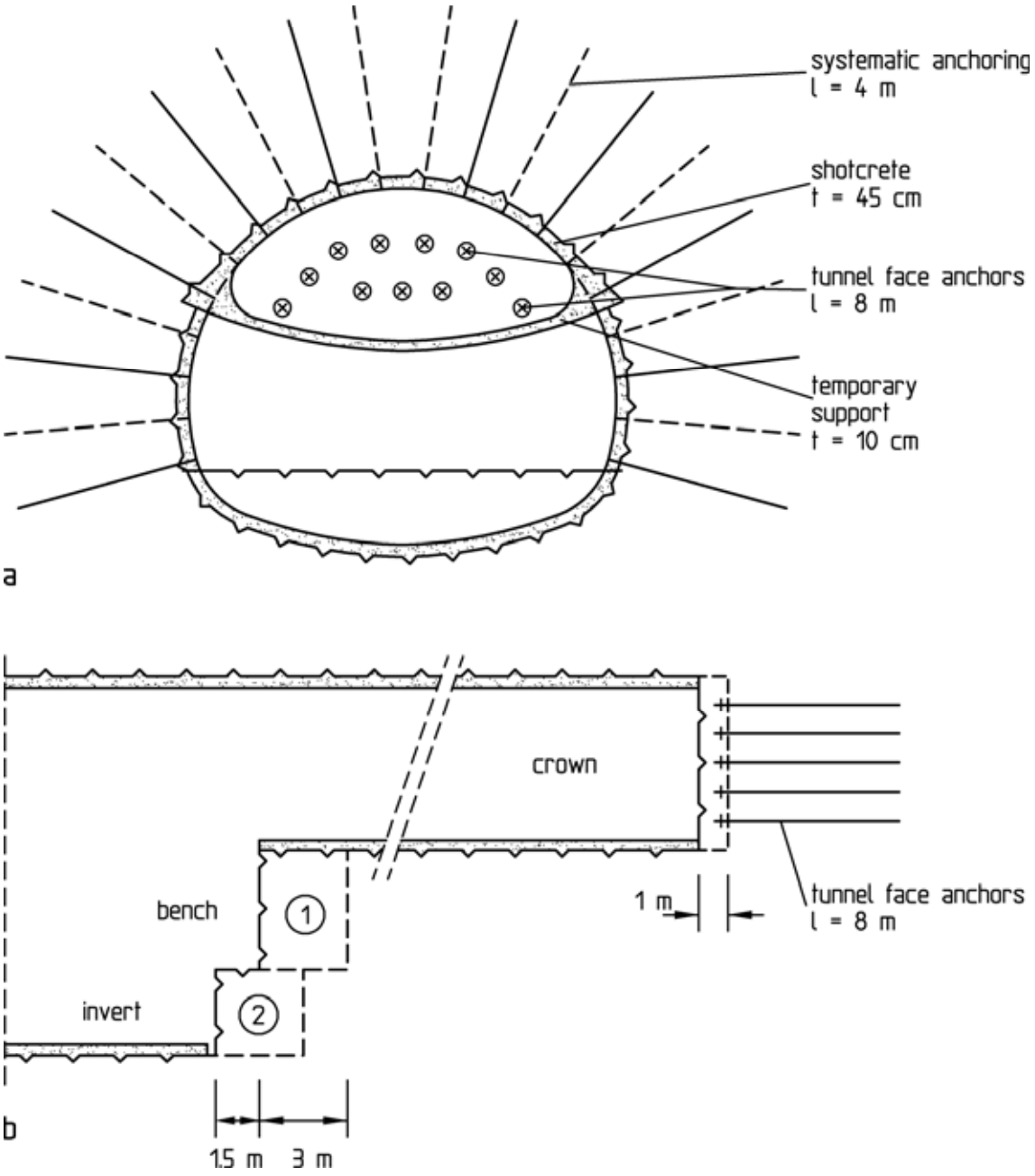

Fig. 5.68: Construction, crown heading with closed invert and tunnel face anchoring: a) Cross-section; b) longitudinal section

The computed displacements were well confirmed by the results of surface leveling and convergency measurements in the tunnel. The heading performance in the crown amounted to almost 2 m/day (Wittke and Pierau, 2000).

5.3.7 Conclusions

The Niedernhausen Tunnel was excavated over a length of approx. 350 m in the completely weathered and decomposed slates of the groundwater-bearing Schwall layers, which have a low strength and a high deformability. In this ground the freeway A3 had to be undercrossed with an overburden of 20 m to 30 m.

A sidewall adit heading with short round lengths was carried out. To stabilize the tunnel face the rock had to be drained in advance and the tunnel face had to be supported by shotcrete and anchors. The results of three-dimensional FE-analyses showed that additional measures were required to support the work space at the tunnel face, such as e. g. the support of the temporary crown invert of the two sidewall adits and the installation of spiles. Because of the extensive support measures a very low heading performance could only be achieved.

It could be proven by further three-dimensional analyses that in sections with higher overburden also a crown heading with closed invert and systematic tunnel face anchoring could be carried out in a stable way in these unfavorable ground conditions. As a consequence, the Niedernhausen Tunnel was successfully excavated by crown heading outside of the sphere of influence of freeway A3. Almost twice the heading performance of the sidewall adit heading was achieved here.

The experience gained with the excavation of the Niedernhausen Tunnel should also lead to economic solutions for future tunnel structures in comparable ground conditions. It should be possible in many cases to replace an expensive sidewall adit excavation by a crown heading with closed invert and tunnel face anchoring.